

JEFFUS DANA A., M.S. Alterations in Critical Cellular Pathways During Lytic Epstein-Barr Virus Infection (2018)

Directed by Dr. Amy L. Adamson. 97pp.

Epstein-Barr Virus (EBV) is a human herpesvirus that infects approximately 90% of the global human population. Infection with EBV is associated with several diseases, such as Burkitt's Lymphoma, nasopharyngeal carcinoma, and gastric carcinoma. In both latent and lytic states, EBV produces gene products that interfere with normal host cell signaling mechanisms. Promoter regions within the EBV genome contain binding sites for a variety of cellular transcription factors. EBV also lacks the machinery necessary for synthesis of viral proteins, and therefore must exploit major cell signaling pathways for cap-dependent translation. The PI3K–Akt–mTOR and MAPK pathways stimulate downstream targets to promote biogenesis. EBV interaction with proteins in these pathways can result in uncontrolled cell growth, proliferation, and apoptosis resistance, potentially leading to carcinogenesis. Previous research shows that under rapamycin-induced inhibition of mTORC1, a major component of PI3K–Akt–mTOR pathway, EBV lytic protein production varies in a cell-type specific manner, suggesting that EBV utilizes these pathways differently among B cells and epithelial cells. For this study, I investigated the molecular targets of EBV within these pathways to gain further insight into the mechanisms involved in synthesis of EBV lytic gene products. The results show that EBV activates variable levels of proteins within the PI3K–Akt–mTOR and MAPK pathways in different cell types during lytic replication, the MAPK pathways are used as a major alternative pathway when mTORC1 is inhibited, and inhibition of the mTOR and MAPK pathways utilized by EBV does not attenuate viral replication.

ALTERATIONS IN CRITICAL CELLULAR PATHWAYS DURING LYTIC  
EPSTEIN-BARR VIRUS INFECTION

by

Dana A. Jeffus

A Thesis Submitted to  
the Faculty of The Graduate School at  
The University of North Carolina at Greensboro  
in Partial Fulfillment  
of the Requirements for the Degree  
Master of Science

Greensboro  
2018

Approved by

---

Committee Chair

Dedicated to my sweet husband, Matthew, and wonderful sister, Jessica, for their unwavering love and support through all my endeavors.

APPROVAL PAGE

This thesis written by Dana A. Jeffus has been approved by the following committee of the Faculty of The Graduate School at The University of North Carolina at Greensboro.

Committee Chair \_\_\_\_\_  
Amy L Adamson

Committee Members \_\_\_\_\_  
Karen Katula

\_\_\_\_\_  
Paul Steimle

\_\_\_\_\_  
Date of Acceptance by Committee

\_\_\_\_\_  
Date of Final Oral Examination

## ACKNOWLEDGEMENTS

I would like to thank my advisor, Dr. Amy L. Adamson and committee members Dr. Karen Katula and Dr. Paul Steimle for their support and guidance. I would like to thank my fellow lab members Ana Tognasoli, Katelyn Miller, and Steven Moran for their assistance and support. I would like to thank Jessica Chavez and Jonah Nikouyeh for their feedback and support. I would also like to thank the UNCG biology department for funding to support this research.

## TABLE OF CONTENTS

	Page
LIST OF TABLES .....	vii
LIST OF FIGURES .....	viii
CHAPTER	
I. INTRODUCTION .....	1
Viruses and Cancer .....	1
Epstein-Barr Virus (EBV) Overview and Disease Associations .....	2
EBV Structure and Genome.....	3
EBV Entry and Replication .....	5
EBV Dependence on Host Translational Machinery .....	8
Raf Kinase Inhibitor Protein (RKIP) .....	13
Aims of Study .....	15
II. MATERIALS AND METHODS.....	16
Cell Culture and Inhibitor Treatment.....	16
Cell Fixation and Flow Cytometric Analysis.....	17
Protein Extraction, SDS-PAGE, and Immunoblot.....	17
Data Analysis .....	18
III. RESULTS .....	23
Levels of Phosphorylated AKT in mTORC1 Inhibited Conditions.....	24
Levels of Phosphorylated AMPK in mTORC1 Inhibited Conditions .....	28
Levels of Phosphorylated TSC2 in mTORC1 Inhibited Conditions .....	32
Levels of Phosphorylated mTOR in mTORC1 Inhibited Conditions .....	36
Levels of Phosphorylated P70S6K in mTORC1 Inhibited Conditions .....	40
Levels of Phosphorylated 4EBP1 in mTORC1 Inhibited Conditions .....	44

Levels of Phosphorylated p38 in mTORC1 Inhibited Conditions.....	48
Levels of Phosphorylated ERK in mTORC1 Inhibited Conditions.....	52
Levels of Phosphorylated Mnk1/2 in mTORC1 Inhibited Conditions .....	56
Levels of Phosphorylated eIF4E in mTORC1 Inhibited Conditions .....	60
Levels of RKIP and Phosphorylated RKIP in mTORC1 Inhibited Conditions.....	64
Levels of Z Protein and Phosphorylated TSC2 in mTORC1, MEK, and p38 Inhibited Conditions .....	68
Levels of Z Protein and Phosphorylated mTOR in mTORC1, MEK, and p38 Inhibited Conditions .....	72
Levels of Z Protein and Phosphorylated ERK in mTORC1, MEK, and p38 Inhibited Conditions .....	76
Levels of Z Protein and Phosphorylated Mnk1/2 in mTORC1, MEK, and p38 Inhibited Conditions .....	80
Levels of Z Protein and Phosphorylated eIF4E in mTORC1, MEK, and p38 Inhibited Conditions .....	84
IV. DISCUSSION.....	88
REFERENCES .....	95

## LIST OF TABLES

	Page
Table 1. Treatment Conditions for mTORC1 Inhibition Experiments .....	20
Table 2. Treatment Conditions for mTORC1, P38, and MEK Inhibition Experiments.....	21
Table 3. List of Antibodies Used for Flow Cytometric Analysis and Immunoblotting.....	22

## LIST OF FIGURES

	Page
Figure 1. Epstein-Barr Virion Structure, Linear Viral Genome, and Circularized Episome .....	4
Figure 2. Promoter Regions for BZLF1 and BRLF1 .....	7
Figure 3. The Phosphatidylinositol 3'-Kinase–Akt–Mechanistic Target of Rapamycin (PI3K–Akt–mTOR) Pathway.....	10
Figure 4. The Mitogen Activated Protein Kinase (MAPK) Pathways.....	12
Figure 5. Raf Kinase Inhibitor Protein (RKIP) Pathway Interactions .....	14
Figure 6. Levels of Z Protein and phospho-AKT in Epithelial Cells Across Treatment Conditions for mTORC1 Inhibition .....	26
Figure 7. Levels of Z Protein and phospho-AKT in B Cells Across Treatment Conditions for mTORC1 Inhibition .....	27
Figure 8. Levels of Z Protein and phospho-AMPK in Epithelial Cells Across Treatment Conditions for mTORC1 Inhibition .....	30
Figure 9. Levels of Z Protein and phospho-AMPK in B Cells Across Treatment Conditions for mTORC1 Inhibition .....	31
Figure 10. Levels of Z Protein and phospho-TSC2 in Epithelial Cells Across Treatment Conditions for mTORC1 Inhibition .....	34
Figure 11. Levels of Z Protein and phospho-TSC2 in B Cells Across Treatment Conditions for mTORC1 Inhibition .....	35
Figure 12. Levels of Z Protein and phospho-mTOR in Epithelial Cells Across Treatment Conditions for mTORC1 Inhibition .....	38
Figure 13. Levels of Z Protein and phospho-mTOR in B Cells Across Treatment Conditions for mTORC1 Inhibition .....	39
Figure 14. Levels of Z Protein and phospho-p70S6K in Epithelial Cells Across Treatment Conditions for mTORC1 Inhibition .....	42

Figure 15. Levels of Z Protein and phospho-p70S6K in B Cells Across Treatment Conditions for mTORC1 Inhibition .....	43
Figure 16. Levels of Z Protein and phospho-4EBP1 in Epithelial Cells Across Treatment Conditions for mTORC1 Inhibition .....	46
Figure 17. Levels of Z Protein and phospho-4EBP1 in B Cells Across Treatment Conditions for mTORC1 Inhibition .....	47
Figure 18. Levels of Z Protein and phospho-p38 in Epithelial Cells Across Treatment Conditions for mTORC1 Inhibition .....	50
Figure 19. Levels of Z Protein and phospho-p38 in B Cells Across Treatment Conditions for mTORC1 Inhibition .....	51
Figure 20. Levels of Z Protein and phospho-ERK in Epithelial Cells Across Treatment Conditions for mTORC1 Inhibition .....	54
Figure 21. Levels of Z Protein and phospho-ERK in B Cells Across Treatment Conditions for mTORC1 Inhibition .....	55
Figure 22. Levels of Z Protein and phospho-Mnk1/2 in Epithelial Cells Across Treatment Conditions for mTORC1 Inhibition .....	58
Figure 23. Levels of Z Protein and phospho-Mnk1/2 in B Cells Across Treatment Conditions for mTORC1 Inhibition .....	59
Figure 24. Levels of Z Protein and phospho-eIF4E in Epithelial Cells Across Treatment Conditions for mTORC1 Inhibition .....	62
Figure 25. Levels of Z Protein and phospho-eIF4E in B Cells Across Treatment Conditions for mTORC1 Inhibition .....	63
Figure 26. Western Blot Analysis for phospho-RKIP, RKIP and Z Protein Levels in Epithelial Cells Across Conditions for mTORC1 Inhibition.....	66
Figure 27. Western Blot Analysis for phospho-RKIP, RKIP and Z Protein Levels in B Cells Across Conditions for mTORC1 Inhibition.....	67
Figure 28. Levels of Z Protein and phospho-TSC2 in Epithelial Cells Across Treatment Conditions for mTORC1, p38, and MEK Inhibition.....	70
Figure 29. Levels of Z Protein and phospho-TSC2 in B Cells Across Treatment Conditions for mTORC1, p38, and MEK Inhibition.....	71

Figure 30. Levels of Z Protein and phospho-mTORC in Epithelial Cells Across Treatment Conditions for mTORC1, p38, and MEK Inhibition.....	74
Figure 31. Levels of Z Protein and phospho-mTOR in B Cells Across Treatment Conditions for mTORC1, p38, and MEK Inhibition.....	75
Figure 32. Levels of Z Protein and phospho-ERK in Epithelial Cells Across Treatment Conditions for mTORC1, p38, and MEK Inhibition.....	78
Figure 33. Levels of Z Protein and phospho-ERK in B Cells Across Treatment Conditions for mTORC1, p38, and MEK Inhibition.....	79
Figure 34. Levels of Z Protein and phospho-Mnk1/2 in Epithelial Cells Across Treatment Conditions for mTORC1, p38, and MEK Inhibition.....	82
Figure 35. Levels of Z Protein and phospho-Mnk1/2 in B Cells Across Treatment Conditions for mTORC1, p38, and MEK Inhibition.....	83
Figure 36. Levels of Z Protein and phospho-eIF4E in Epithelial Cells Across Treatment Conditions for mTORC1, p38, and MEK Inhibition.....	86
Figure 37. Levels of Z Protein and phospho-eIF4E in B Cells Across Treatment Conditions for mTORC1, p38, and MEK Inhibition.....	87
Figure 38. Proposed Predominant Pathways Utilized by EBV in B Cells and Epithelial Cells .....	94

## CHAPTER I

### INTRODUCTION

#### *Viruses and Cancer*

There are certain viruses capable of infecting particular host cell-types for the lifetime of the host. These sustained infections are achieved by the virus either by the production of viral proteins, which ensure retention of the viral genome in normal cellular mitotic divisions, or by integration of the viral genome into the host cell genome. In either case, the mechanisms involved in viral persistency require a distinct host-virus interaction to evade host immune responses and cell death. Oncovirus-infected host cells are at risk of developing genomic instability, alterations in DNA repair mechanisms, aberrant protein expression and activation, apoptosis resistance, and increased growth and proliferation<sup>1</sup>. Such influences on host cellular pathways contribute significantly to carcinogenesis. In fact, tumors associated with viral infection account for approximately 20% of all human cancers<sup>1</sup>. Oncoviruses accountable for this approximation include Hepatitis B and C virus (HBV and HCV, respectively), Human Papillomavirus (HPV), Human T-lymphotropic virus (HTLV), Merkel cell polyomavirus (MVC), Kaposi's sarcoma-associated herpes-virus (KSHV), and Epstein-Barr virus (EBV)<sup>2</sup>. Elucidation of virus-host interactions and mechanisms of virus survival can lend insight into novel ways to treat the cancers with which each oncovirus is associated.

### *Epstein-Barr Virus (EBV) Overview and Disease Associations*

Epstein-Barr virus (EBV, HHV-4) is a ubiquitous herpesvirus, persistently infecting approximately 90% of the global human population. EBV is most frequently acquired via salivary exchange and the initial infection is the causative agent of infectious mononucleosis (IM). Virus entry into epithelial and B cells causes the classic symptoms of IM, which typically occur approximately 5 weeks into infection. Symptoms of IM include fatigue, fever, lymphocytosis, and adenopathy<sup>3</sup>. During the initial infection period, EBV is in a lytic state where new virions are actively reproduced. Over time, lytic infection drops off and the virus enters a latent state. During latency, specific viral proteins are produced to ensure retention of the viral genome into newly synthesized mitotic daughter cells. At any point during the host's lifetime, the virus can switch from latency to reactivation of lytic reproduction<sup>3</sup>. In either phase, EBV can produce viral proteins encoded by the EBV genome that can interact with cellular proteins and alter host-cell protein expression, potentially inducing apoptosis resistance, translocation events, cell immortalization, proliferation, and alterations in DNA damage repair pathways<sup>3</sup>. These cellular responses to EBV are just a few examples of the characteristic properties necessary for carcinogenesis. In fact, EBV's discovery in 1964 was from Burkitt's lymphoma (BL) tissue<sup>3</sup>. Since then, an increasing number of associations between EBV and various malignancies have been identified. EBV is not only associated with BL, but several diseases as well, such as nasopharyngeal carcinoma (NPC), gastric carcinoma, and other cancers and autoimmune disorders<sup>3</sup>. While the precise underlying molecular mechanisms leading to cancer remain to be elucidated, EBV's role as a potent

oncovirus is evident. Because EBV resides permanently in epithelial cells and B cells for the lifespan of the host, the study of viral and host protein interactions is essential for disease intervention.

### *EBV Structure and Genome*

The EBV virion (Figure 1 A) is approximately 200nm in diameter. Linear double stranded DNA is enclosed in an icosahedral nucleocapsid that is surrounded by tegument proteins and a lipid envelope. Projecting from the envelope are finger-like projections, called glycoproteins, which assist in viral attachment and entry. Some essential glycoproteins include BMRF-2, gp350, gp220, gp42, and gH/gL<sup>4</sup>. The EBV genome is approximately 172 KBP long, and codes for approximately 85 genes<sup>4</sup>. For entry and lytic replication, the genome is linear in form (Figure 1 B). During latency in the host cell, the DNA forms a circular episome in which the ends of the linear DNA are covalently linked (Figure 1 C). Some important gene products encoded in the viral DNA include latent membrane proteins (LMP1/2), nuclear antigens (EBNAs), small nuclear RNAs (EBERs), and lytic proteins (BZLF1 or Z, and BRLF1 or R)<sup>4</sup>.

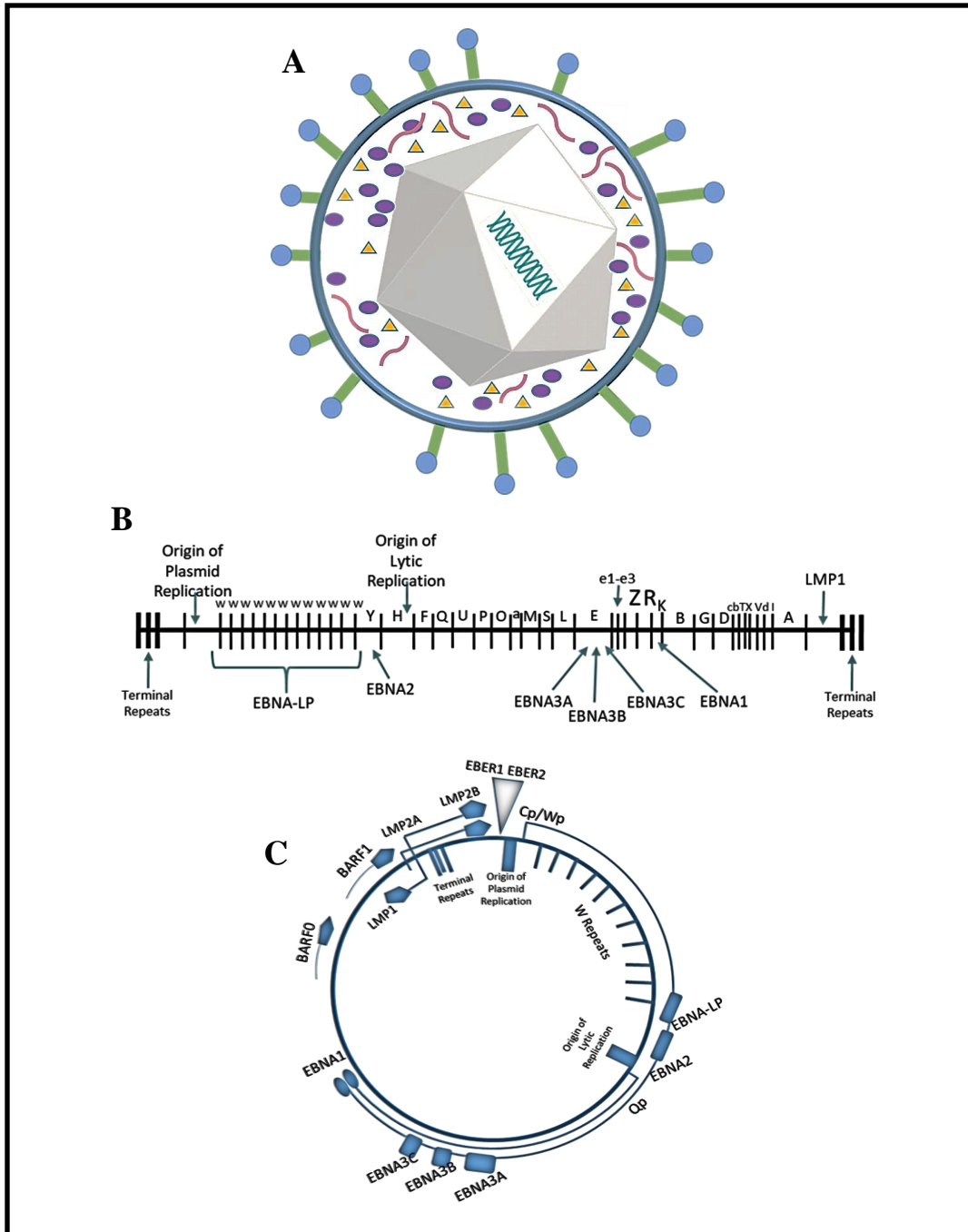


**Figure 1. Epstein-Barr Virion Structure, Linear Viral Genome, and Circularized Episome.** A) Virion. B) Linear genome. C) Episome. Images B and C adapted from Fields virology. Fields, B. N., Knipe, D. M., & Howley, P. M. (2013)

### *EBV Entry and Replication*

Epithelial cell attachment and entry occurs via viral glycoprotein BMRF-2 interaction with cellular  $\beta$ 1 integrins. Viral glycoproteins gH/gL trigger fusion with the host cell membrane, allowing nucleocapsid entry and nuclear transport of the viral genome. For B cell attachment, viral glycoproteins gp350 and gp220 bind to cellular receptor CD21. Viral protein gp42, complexed with gH/gL, interacts with cellular human leukocyte antigen (HLA) class II proteins, allowing viral envelope fusion with the cellular membrane and nucleocapsid entry to the cell<sup>5</sup>. Nuclear pores allow EBV genome entry into the cell nucleus. Should the virus become latent, the linear DNA circularizes into the episome and becomes tethered to host DNA via EBNA-1 proteins<sup>5</sup>. Lytic replication requires linear viral DNA, and waves of transcription of essential genes must occur to complete a replication cycle. Immediate early genes, BZLF1 (Z) and BRLF1 (R) encode proteins that serve as transactivators of virus replication, turning on the cascade of early and late genes required for virus replication<sup>6</sup>. Expression of Z protein not only enhances expression of R, but also upregulates its own expression, consequently amplifying the signals necessary for expression of early and late genes<sup>5</sup>. In the absence of Z and R gene products, subsequent steps of viral replication cannot occur. Upon synergistic activation via Z and R proteins, early genes initiate viral genome replication and subsequent late gene expression. Late genes produce capsid proteins, as well as proteins involved with assembly and budding of progeny virions<sup>5</sup>. Because Z protein expression can trigger expression of R protein and succeeding early and late genes, the Z gene must be tightly regulated in the latency program. Silencing of the Z

gene is accomplished using both cellular proteins and viral regulatory elements, such as cellular histone deacetylases and viral gene methylation sites<sup>5,6</sup>. Histone acetylation is crucial for Z gene activation, and Z protein preferentially binds methylated response elements of lytic cycle gene promoters<sup>4,7</sup>. EBV can alternate between latent and lytic states at any point during the host life span, and lytic activation can occur via a variety of stimuli, such as oxidative stress, inflammation, or hypoxia<sup>6</sup>. Latently infected EBV cells can also be chemically induced into lytic replication in vitro using a variety of chemical agents. Histone deacetylase inhibitors, such as sodium butyrate, can stimulate Z gene activation<sup>4</sup>. Also, 12-O-tetradecanoylphorbol-13-acetate (TPA) can stimulate Z protein's full transactivation functionality by inducing phosphorylation of Z protein's SER186 via protein kinase C (PKC)<sup>6</sup>.

The promoter regions for both Z and R genes contain binding sites for a variety of cellular transcription factors. Such interactions not only stimulate the switch from viral latency to lytic reproduction, but can also alter cellular protein activity and consequently stimulate various cell signaling pathways. The Z promoter (Figure 2 A) contains regions of binding sites for the abundant cellular transcription factors Sp1/Sp3, myocyte enhancer factor 2D (MEF2D), cAMP Response Element-Binding protein (CREB), SMADs, activating transcription factors (ATFs), and the dual-functioning activator/repressor protein, Yin Yang 1 (YY1)<sup>4,8,9</sup>. The R promoter (Figure 2 B) contains binding sites for the ubiquitous cellular transcription factors nuclear factor 1 (NF1), early growth response protein 1 (EGR-1), Sp1/Sp3, B-lymphocyte-induced maturation protein (BMP1), and activator/repressor protein, Yin Yang 1 (YY1)<sup>4,8,9</sup>. These transcription factors that bind Z

and R promoters are downstream proteins of several major cell signaling cascades, such as the protein kinase C (PKC), mitogen activated protein kinase (MAPK), transforming growth factor (TGF- $\beta$ ), phosphatidylinositol-3-kinase (PI3K), and ataxia telangiectasia mutated (ATM) pathways<sup>4,8,9,10</sup>. EBV lytic-reproduction-induced aberrant protein activity in these pathways can potentially promote genomic instability, cell growth, and cell cycle progression, all of which can contribute to carcinogenesis<sup>9,10</sup>.

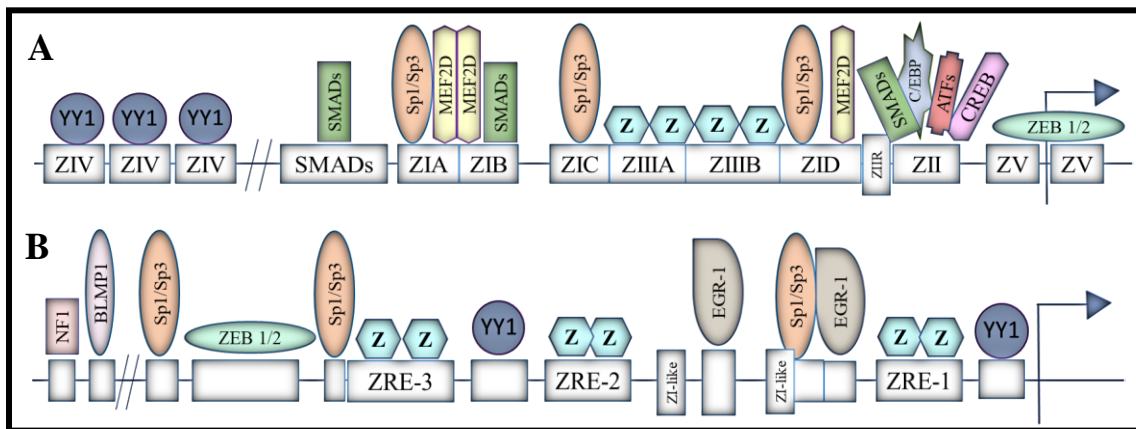


**Figure 2. Promoter Regions for BZLF1 and BRLF1.**

A) BZLF1. B) BRLF1. Schematic images highlight binding sites for key cellular transcription factors. Images not to scale.

(A) Image adapted from Fields virology. Fields, B. N., Knipe, D. M., & Howley, P. M. (2013). (B) Image adapted from Kenney, S. C., & Mertz, J. E. (2014, June). Regulation of the latent-lytic switch in Epstein–Barr virus. In *Seminars in cancer biology* (Vol. 26, pp. 60-68). Academic Press.

### *EBV Dependence on Host Translational Machinery*

Like all viruses, EBV lacks the critical apparatus for synthesis of viral proteins. For survival, evolution, reproduction, and ability to spread to new hosts, viruses must exploit host cellular translational machinery for production of vital gene products<sup>11</sup>. EBV and all other mammalian DNA viruses must maintain cap-dependent translation and are therefore reliant on major cell signaling pathways that stimulate key proteins that bind the 5'-end of mRNA molecules<sup>12</sup>. The phosphatidylinositol 3'-kinase–Akt–mechanistic target of rapamycin (PI3K–Akt–mTOR) is a major cell signaling pathway that activates key proteins involved in macromolecule synthesis, making it a common target pathway for viruses to manipulate.

The PI3K–Akt–mTOR pathway (Figure 3) is continuously used by cells to integrate a diverse array of nutritional and environmental signals to promote cell growth, metabolism, proliferation, protein synthesis, and cell survival<sup>13</sup>. The pathway is activated through a variety of stimuli, such as cytokines, growth factors, integrins, and hormones. Receptor-mediated activation occurs when receptor tyrosine kinases (RTKs) receive a signal which triggers dimerization and autophosphorylation<sup>12</sup>. Insulin receptor substrate 1 (IRS1), an adaptor protein, binds phosphotyrosine and activates PI3K. PI3K then phosphorylates phosphatidylinositol-4,5-bisphosphate (PIP2), converting it to phosphatidylinositol-3,4,5-triphosphate (PIP3)<sup>12</sup>. This conversion recruits Akt and PDK1 to the membrane, positioning Akt for phosphorylation by PDK1<sup>12</sup>. Akt can phosphorylate and activate a variety of targets<sup>14</sup>. In the PI3K–Akt–mTOR pathway, Akt phosphorylates tuberous sclerosis 1 and 2 (TSC1/2) which is a complex that negatively

regulates Rheb-GTP by stimulating cellular GTPases<sup>12</sup>. TSC1/2 loses inhibitory function upon phosphorylation via Akt, and Rheb-GTP activates the mTORC1 complex<sup>12</sup>. mTORC1 and mTORC2 are the two functionally discrete complexes at the heart of this pathway. Each complex contains a unique set of subunits along with the catalytic subunit, mTOR, a serine threonine kinase that phosphorylates a variety of targets. The mTORC2 complex is the minor player in this pathway, and less is known about its functionality. It is known that mTORC2 regulates insulin signaling via IRS1 and promotes cell survival via activation of Akt<sup>15</sup>. mTORC1 is a positive regulator of protein synthesis via phosphorylation of downstream effectors<sup>13</sup>. Major targets of mTORC1 are p70S6K and the eIF4E binding protein (4EBP1). Upon phosphorylation, p70S6K phosphorylates targets that promote cap-dependent translation, ribosome production, and translation elongation<sup>16</sup>. In its unphosphorylated state, 4EBP1 is bound to and inhibits eukaryotic translation initiation factor (eIF4E). Phosphorylation of 4EBP1 via mTORC1 prevents binding to eIF4E, thereby enabling eIF4E to participate in cap-dependent translation<sup>16</sup>.

Because the PI3K-Akt-mTOR pathway promotes protein synthesis, cell growth, metabolism, survival, and proliferation, it is commonly implicated in cancer. Recent studies show increased levels of phosphorylated mTOR in gastric carcinoma, increased levels of phosphorylated Akt in undifferentiated versus differentiated non-keratinizing nasopharyngeal carcinoma, and increased phosphorylated p70S6K in lymphoma cells<sup>17,18,19</sup>. Moreover, recent genomic profiling of nasopharyngeal carcinoma (NPC)

links expression of EBV viral genes and upregulated mTOR pathway activity to the enhancement of malignant properties of NPC<sup>20</sup>.

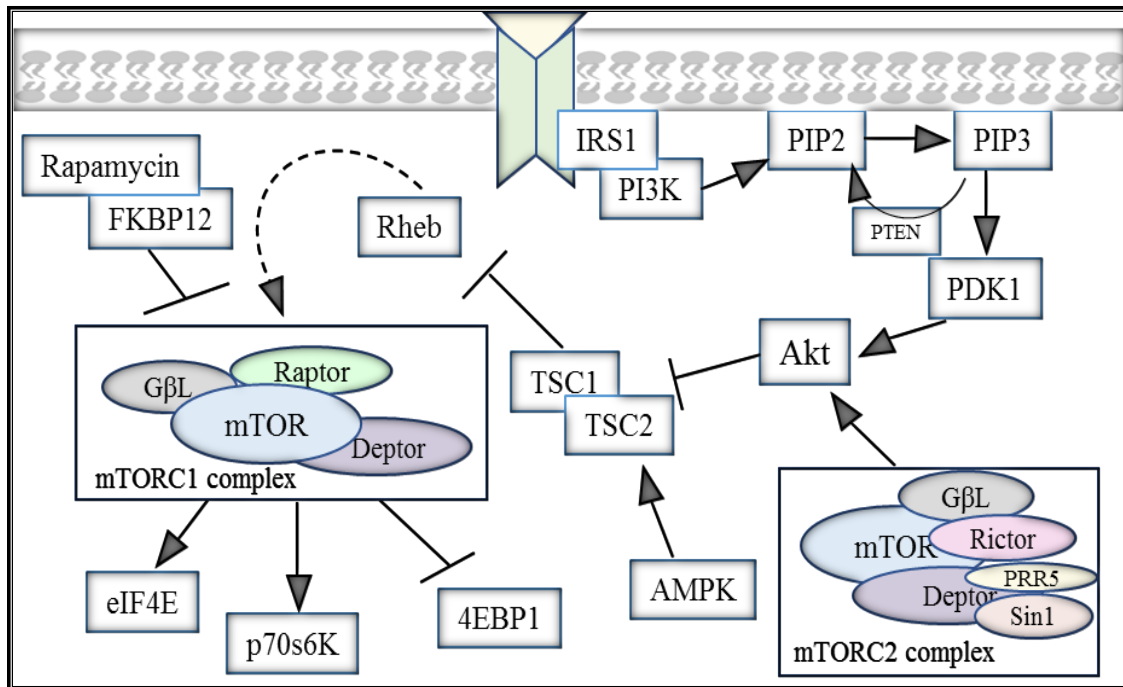


**Figure 3. The Phosphatidylinositol 3'-Kinase-AKT-Mechanistic Target of Rapamycin (PI3K-Akt-mTOR) Pathway.**

Therapeutic intervention through inhibition of the PI3K–Akt–mTOR signaling pathway could prove to be a promising strategy in the treatment of certain cancers. Rapamycin is a well-known macrolide compound that selectively inhibits mTORC1. The compound is an antifungal metabolite produced by the soil bacterium *Streptomyces hygroscopicus* in the soil of Rapa Nui. Rapamycin specifically inhibits mTORC1 by complexing with the 12 kDa FK506-binding protein (FKBP12) and acting as an allosteric inhibitor of mTOR in the mTORC1 complex, thereby preventing phosphorylation of downstream targets<sup>21</sup>. Recent studies have shown suppression of

invasion protein MMP-2 in nasopharyngeal cancer stem cells, as well as improved antitumor effects of ionizing radiation when treating NPC<sup>22,23</sup>. Another recent study found that rapamycin treatment significantly inhibited tumor development and splenomegaly in a transgenic murine model of EBV-related Burkitt's lymphoma<sup>24</sup>. While these studies sound promising, rapamycin treatment for cancer and EBV-associated diseases has disadvantages. For example, the compound is a potent immunosuppressant by inhibiting B and T cell proliferation<sup>21</sup>. Additionally, studies in our lab have shown that rapamycin attenuates EBV lytic protein translation in a cell-type specific manner. Rapamycin decreases EBV lytic replication in B cells, but *increases* EBV lytic gene expression in epithelial cells<sup>25</sup>.

EBV's ability to persistently produce lytic gene products and even *increase* viral protein synthesis in the absence of a fully functional PI3K–Akt–mTOR pathway despite mandatory necessity for cap-dependent translation is suggestive of another cellular signaling pathway at play. Parallel to the PI3K–Akt–mTOR pathway are the Mitogen activated protein kinase (MAPK) pathways (Figure 4). Similar to the PI3K–Akt–mTOR pathway, the MAPK pathways are comprised of kinases responsible for protein synthesis, metabolism, cell growth, survival, and proliferation<sup>26</sup>. Key MAPK proteins include Ras, a small GTP-binding protein, extracellular signal-regulated kinase 1/2 (ERK 1/2), p38, and MAPK-interacting kinases (Mnk1/2)<sup>27</sup>. Mnk1 and Mnk2 each exist as two isoforms, Mnk1a and 1b, and Mnk2a and 2b<sup>27</sup>. These isoforms are produced via alternative splicing. Mnk1a and Mnk2a contain binding sites for MAPK proteins and are generally localized in the cytoplasm, while Mnk1b and Mnk2b are dispersed in the nucleus and

cytoplasm<sup>27</sup>. Mnk2a has a greater affinity for ERK and also has a high basal activity. Mnk1b and Mnk2b lack MAPK binding sites and also do not contain nuclear export sequences<sup>28</sup>. The Mnks are key downstream targets of the MAPK proteins p38 and ERK and play an important role in regulation of eIF4E. Phosphorylation of eIF4E via the Mnk kinases enables cap-dependent translation<sup>28</sup>. Because eIF4E is a common target of the PI3K–Akt–mTOR and MAPK pathways, it is likely for viruses reliant on cap-dependent translation to stimulate either pathway.

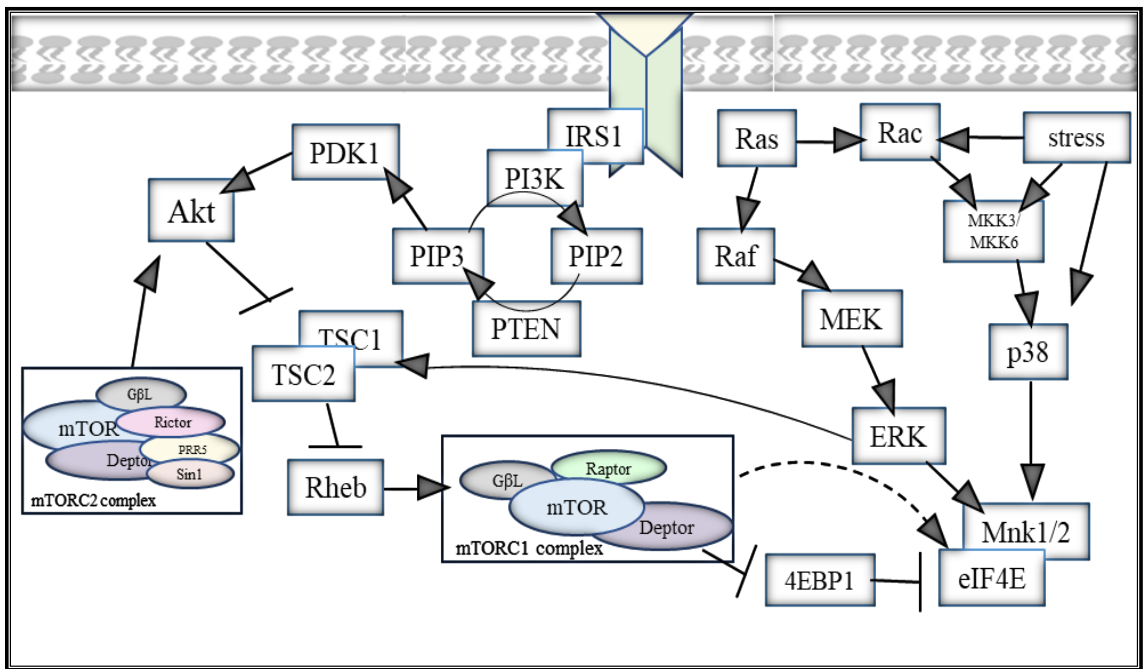


**Figure 4. The Mitogen Activated Protein Kinase (MAPK) Pathways.**

### *Raf Kinase Inhibitor Protein (RKIP)*

A negative regulator of the MAPK pathway Raf/MEK/ERK is the metastasis suppressor Raf kinase inhibitor protein (RKIP, Figure 5). RKIP is a 23 kDa cytosolic protein that binds specifically to Raf. RKIP-Raf binding is an event which dissociates the Raf/MEK complex, competitively inhibiting MEK phosphorylation, thereby decreasing downstream activation of Mnk1/2 and eIF4E<sup>29</sup>. RKIP is highly abundant in cells and has additional target pathways. Several key targets influenced by RKIP include NF- $\kappa$ B, GPCR, and GSK3 $\beta$ <sup>30</sup>. In the NF- $\kappa$ B pathway, RKIP interferes with I $\kappa$ B kinase (IKK), an upstream regulator of IKB. This interaction prevents dissociation and ubiquitination of IKB from NF- $\kappa$ B, thus preventing NF- $\kappa$ B from nuclear translocation and activation of target genes<sup>29</sup>. RKIP can also be phosphorylated via protein kinase C (PKC), which deactivates RKIP as a Raf inhibitor and allows phosphorylated RKIP to inhibit G-protein-coupled-receptor kinase 2 (GRK2), a modulator of G-protein coupled receptors (GPCRs)<sup>30</sup>. GPCRs are known to stimulate signal transducers and activators (STATs). RKIP also inhibits p38 activation of glycogen synthase kinase 3 $\beta$  (GSK3 $\beta$ )<sup>31</sup>. GSK3 $\beta$  is a kinase involved in several pathways that regulate proliferation, apoptosis, and glucose regulation<sup>31</sup>. Being a metastasis suppressor, RKIP is a multifunctional modulator of many pathways that lead to transcription, translation, biogenesis, and cell survival. However, RKIP's role in cancer is not well known and clearly defined. Studies have shown that downregulated RKIP and increased phosphorylated-RKIP are both common in metastatic tissues<sup>29,30,31</sup>. Few studies have been conducted to evaluate RKIP and

phosphorylated-RKIP levels in relation to EBV latent and lytic states or EBV associated cancers.

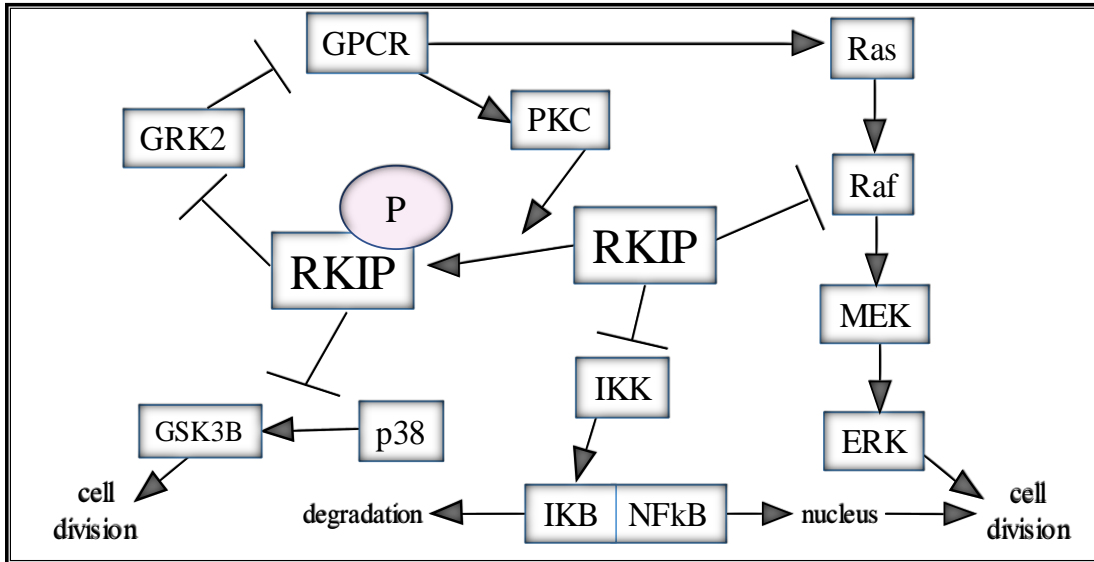


**Figure 5. Raf Kinase Inhibitor Protein (RKIP) Pathway Interactions.**

Image adapted from Ling, H. H., Mendoza-Viveros, L., Mehta, N., & Cheng, H. Y. M. (2014). Raf kinase inhibitory protein (RKIP): functional pleiotropy in the mammalian brain. *Critical Reviews™ in Oncogenesis*, 19(6).

### *Aims of Study*

Previous studies in our lab have shown that inhibition of the mTORC1 complex of the PI3K-Akt-mTOR cell signaling pathway has differential effects on EBV lytic protein production amongst infected B cells and epithelial cells, suggestive of a cell-type-specific and multiple-pathway approach to translation of key lytic viral proteins. It is well established that EBV is associated with several diseases where aberrant protein activity is a contributing factor. Identification of the major cell signaling pathways and specific proteins being modulated for viral self-survival and replication can lead to a greater understanding of the mechanisms involved in EBV-induced diseases, potential attenuation of viral protein production, and the development of targeted therapies. The goals of this study are as follows: in depth investigation of protein activation within the PI3K-Akt-mTOR and MAPK pathways with and without mTORC1 inhibition when EBV is lytic; use of MEK and p38 inhibitors in combination with mTORC1 inhibition to further investigate protein activation within the PI3K-Akt-mTOR and MAPK pathways and evaluate the possibility of attenuation of lytic protein production; and investigate what role, if any, RKIP and phosphorylated RKIP may have in the production of EBV viral proteins when mTORC1 is inhibited. Flow cytometric analysis and immunoblotting techniques will be used to complete these aims of study.

## CHAPTER II

### MATERIALS AND METHODS

#### *Cell Culture and Inhibitor Treatment*

Raji, an EBV positive Burkitt's lymphoma cell line was grown in Thermo Scientific's RPMI liquid media. AGS-BDNeo, and EBV positive adenocarcinoma cell line was grown in Thermo Scientific's Ham's F-12 liquid media. To maintain cellular retention of the viral episome in the epithelial cells, 500 $\mu$ g/mL of neomycin (G418) obtained from MP Biomedicals, LLC was added to the liquid media. Both RPMI and F-12 media was enriched with 10% fetal bovine serum (Gibco; Thermo Scientific), as well as 10 $\mu$ L/mL of fungicide, penicillin, and streptomycin. Cell culture was maintained at 37 degrees Celcius with 5% CO<sub>2</sub>. EBV lytic replication was induced with the HDAC inhibitor, 12-O-tetradecanoylphorbol-13-acetate (TPA), and sodium butyrate (NaB). Raji cells were treated with 20ng/mL of TPA and 3 mM NaB. Due to sensitivity to HDAC inhibitor treatment, AGS-BDNeo cells were treated with 5ng/mL TPA and 0.75mM NaB. For inhibition of mTORC1, cells were treated with 5nM rapamycin (Sigma Aldrich) 24 hours prior to induction. For inhibition of p38 and MEK, cells were treated 30 minutes prior to induction with 10 $\mu$ M SB203580 and 10 $\mu$ M UO126, respectively (Cell Signaling). Experimental conditions with mTORC1, p38, and MEK inhibitor treatments listed in Tables 1 and 2.

### *Cell Fixation and Flow Cytometric Analysis*

Harvested cells from biological triplicates were washed in 1x phosphate-buffered saline (PBS) and fixed in 60% acetone at 4 degrees Celsius for 10 minutes. Following fixation, cells were washed with 0.3% bovine serum albumin (BSA) (Fisher Scientific) dissolved in 1x PBS. Subsequently, cells were resuspended in 100 $\mu$ L primary antibody (Table 3) diluted 1:200 in 1x PBS, 0.3% BSA, 5% donkey serum, and 0.10% Triton-X (incubation mix) and incubated for one hour at 23 degrees Celsius. Afterwards, cells were washed with the PBS+BSA mixture and resuspended in 100 $\mu$ L secondary antibody (Table 3) diluted 1:400 in incubation mix. After one-hour incubation period at 23 degrees Celsius, cells were washed again in PBS+BSA and resuspended in 500 $\mu$ L PBS. Z protein was detected using secondary antibody Alexa 488 fluorophore (Jackson Immunoresearch). Phosphorylated proteins of interest within cell signaling pathways were detected using secondary antibody CY5 fluorophore (Jackson Immunoresearch). Sample protein expression was quantified using the inCyte module for the Guava easyCyte 6-2L benchtop flow cytometer.

### *Protein Extraction, SDS-PAGE, and Immunoblot*

Cells from biological triplicates were harvested and suspended in lysis buffer containing 150mM NaCl, 5mM EDTA, 0.1% NP-40, 50mM pH 7 HEPES, and Thermo Scientific's protease/phosphatase inhibitor (1:100 dilution). After two freeze-thaw cycles at -80 degrees Celsius and 37 degrees Celsius, suspension was centrifuged at 4 degrees Celsius for 10 minutes to remove cellular debris. Extract protein concentration was determined via Bradford assay and approximately 20-40 $\mu$ g were loaded. Proteins were

separated on a 10% SDS-PAGE gel at 200V. Upon completion, proteins were transferred to a Millipore Immobilon-PDVF membrane overnight at 100mA. Once complete, membranes were blocked with 0.25% milk block/PBS containing 0.1% Fisher Scientific Tween 20. Blots underwent washes and detection reactions in a Millipore SNAP i.d. 2.0 Protein Detection System. Blots were incubated with appropriate antibodies (Table 3), washed 4x in western wash containing 1x PBS and 0.1% Tween 20, and incubated with the appropriate secondary antibody (Table 3) for 10 minutes. Blots were washed 4x with western wash and exposed to an enhanced chemiluminescent (ECL) substrate (Advansta) for 5 minutes. Chemiluminescent imaging was completed using LI-COR Biosciences c-digit blot scanner.

#### *Data Analysis*

Each flow cytometric and immunoblot experiment was performed in biological triplicate. Western blot protein bands were quantified using Image Studio Digits software. Flow cytometric sample analyses were conducted at 1000 events. Flow cytometric output was gated on histogram and scatterplot (red CY5 versus green 488) regions at the end of background signal; any signal beyond background was recorded as positive for proteins of interest in percent of total cells. Double positive percent of cells are red and green fluorescent cells present in the 1<sup>st</sup> scatterplot quadrant. Cells positive for phosphorylated cellular proteins of interest are red fluorescent cells present in the 2<sup>nd</sup> scatterplot quadrant. Cells positive for Z protein are green fluorescent cells present in the 4<sup>th</sup> scatterplot quadrant. All data represent means  $\pm$  SD from biological triplicates.

Statistical significance of results was determined by two-tailed student T-test with a significant p-value  $<0.05$ .

**Table 1. Treatment Conditions for mTORC1 Inhibition Experiments.**

<b>Condition</b>	<b>Uninduced</b>	<b>Induced with HDAC inhibitors</b>	<b>5nM rapamycin treatment</b>
<b>1</b>	•		
<b>2</b>	•		•
<b>3</b>		•	
<b>4</b>		•	•

**Table 2. Treatment Conditions for mTORC1, P38, and MEK Inhibition Experiments.**

Condition	Uninduced	Induced with HDAC inhibitors	5nM rapamycin treatment	10 $\mu$ M p38 inhibitor	10 $\mu$ M MEK inhibitor
1	•				
2	•		•		
3	•			•	
4	•				•
5	•			•	•
6	•		•	•	
7	•		•		•
8	•		•	•	•
9		•			
10		•	•		
11		•		•	
12		•			•
13		•		•	•
14		•	•	•	
15		•	•		•
16		•	•	•	•

**Table 3. List of Antibodies Used for Flow Cytometric Analysis and Immunoblotting.**

<u>Antibody</u>	<u>Source</u>	<u>Primary/Secondary?</u>	<u>Use</u>
EBV Zebra (BZ1) (mouse)	Santa Cruz	Primary	Flow cytometry, Immunoblotting
Goat-anti-mouse HRP	Jackson ImmunoResearch	Secondary	Immunoblotting
Goat-anti-rabbit HRP	Jackson ImmunoResearch	Secondary	Immunoblotting
$\alpha$ -tubulin (mouse)	Santa Cruz	Primary	Immunoblotting
RKIP (rabbit)	Cell Signaling	Primary	Flow cytometry, Immunoblotting
p-RKIP (rabbit)	Santa Cruz	Primary	Flow cytometry, Immunoblotting
p-mTORC1 (rabbit)	Cell Signaling	Primary	Flow cytometry
p-MEK (rabbit)	Cell Signaling	Primary	Flow cytometry
p-Mnk1/2	Cell Signaling	Primary	Flow Cytometry
p-ERK (rabbit)	Cell Signaling	Primary	Flow cytometry
p-AMPK (rabbit)	Cell Signaling	Primary	Flow cytometry
p-p38 (rabbit)	Cell Signaling	Primary	Flow cytometry
p-TSC2 (rabbit)	Cell Signaling	Primary	Flow cytometry
p-4EBP1 (rabbit)	Cell Signaling	Primary	Flow cytometry
p-eIF4E (rabbit)	Cell Signaling	Primary	Flow cytometry
p-p70S6K (rabbit)	Cell Signaling	Primary	Flow cytometry
p-AKT1/2/3 (mouse)	Santa Cruz	Primary	Flow cytometry
Donkey-anti-mouse 488	Jackson ImmunoResearch	Secondary	Flow cytometry
Donkey-anti-rabbit cy5	Jackson ImmunoResearch	Secondary	Flow cytometry
Donkey-anti-mouse cy5	Jackson ImmunoResearch	Secondary	Flow cytometry

## CHAPTER III

### RESULTS

Previous studies in our lab have shown that inhibition of the mTORC1 complex with rapamycin inhibits EBV lytic replication in a cell type specific manner<sup>25</sup>. This study aims to investigate levels of activated phosphorylated proteins in the PI3K-Akt-mTOR and MAPK pathways; investigate RKIP and phosphorylated RKIP levels during mTORC1 inhibition and lytic replication in epithelial cells and B cells; and determine the effects of inhibition of select proteins within those pathways using mTORC1, MEK, and p38 inhibitors.

To investigate levels of phosphorylated activated proteins in the PI3K-Akt-mTOR and MAPK pathways, evaluate cell-type specific lytic replication mechanisms, and assess levels of RKIP and phosphorylated RKIP in EBV infected epithelial cells and B cells, AGS-BDNeo and Raji cells were treated under the conditions listed in Table 1. Cells were then harvested and prepared for flow cytometric analysis or immunoblot analysis. Table 3 shows complete list of primary and secondary antibodies used for all experiment. To investigate levels of phosphorylated activated proteins downstream of MEK and p38 in the MAPK pathways, evaluate cell-type specific lytic replication mechanisms, and assess whether EBV lytic proteins can be attenuated by blocking the pathways that lead to cap-dependent translation, epithelial cells and B cells were treated under the conditions

listed in Table 2. Cells were then harvested and prepared for flow cytometric analysis.

Table 3 shows complete list of primary and secondary antibodies used.

#### *Levels of Phosphorylated AKT in mTORC1 Inhibited Conditions*

Levels of phosphorylated AKT and Z protein were measured using flow cytometric analysis. Phosphorylated AKT phosphorylates TSC1/2 which activates mTORC1 downstream. Measuring phosphorylated AKT in relation to Z protein expression provides insight into the pathways being utilized by EBV for protein translation and lytic replication.

Significant increases in total relative Z protein levels were observed in epithelial cells for conditions 3 and 4 relative to conditions 1 and 2 ( $p < 0.05$ ) (Figure 6 A). No significant differences were observed in total phosphorylated AKT levels across treatment conditions for epithelial cells (Figure 6 A). Figure 6 B shows the percent totals of epithelial cells positive for phosphorylated AKT, Z protein, or both proteins simultaneous (double positive). Conditions 3 and 4 show significant increases in percent of epithelial cells positive for Z protein alone relative to conditions 1 and 2 ( $p < 0.05$ ) (Figure 6 B). No significant differences in percent of epithelial cells positive for phosphorylated AKT alone or double positive epithelial cells were observed (Figure 6 B). Lytic rapamycin treated epithelial cells positive for phosphorylated AKT without Z protein only account for approximately 0.2% of cells. Double positive epithelial cells only account for approximately 7% of total lytic rapamycin treated cells. While Z protein in epithelial cells increases with rapamycin treatment, it does not appear to be related to phosphorylated AKT levels.

Significant increases in total relative Z protein levels were observed in B cells for conditions 3 and 4 relative to conditions 1 and 2 ( $p < 0.05$ ) (Figure 7 A). The general trends of decrease in Z protein levels are observed in lytic cells with rapamycin treatment as with other trials. No significant differences were observed in phosphorylated AKT levels across treatment conditions for B cells; however, while Z protein decreases in induced cells with rapamycin treatment, phosphorylated AKT levels remain constant (Figure 7 A). Figure 7 B shows the percent of B cells positive for phosphorylated AKT, Z protein, or both proteins simultaneous (double positive). Condition 4 (Figure 7 B) shows the general trend of decrease in lytic B cells with rapamycin treatment, however, many of the cells that remain lytic despite rapamycin treatment are double positive for phosphorylated AKT and Z protein. In fact, nearly 50% of remaining lytic cells after rapamycin treatment are positive for phosphorylated AKT. Rapamycin treated B cells positive for phosphorylated AKT alone account for less than .10% of total lytic cells. These observations suggest that phosphorylated AKT levels correspond to Z protein levels in B cells that remain lytic after rapamycin treatment.

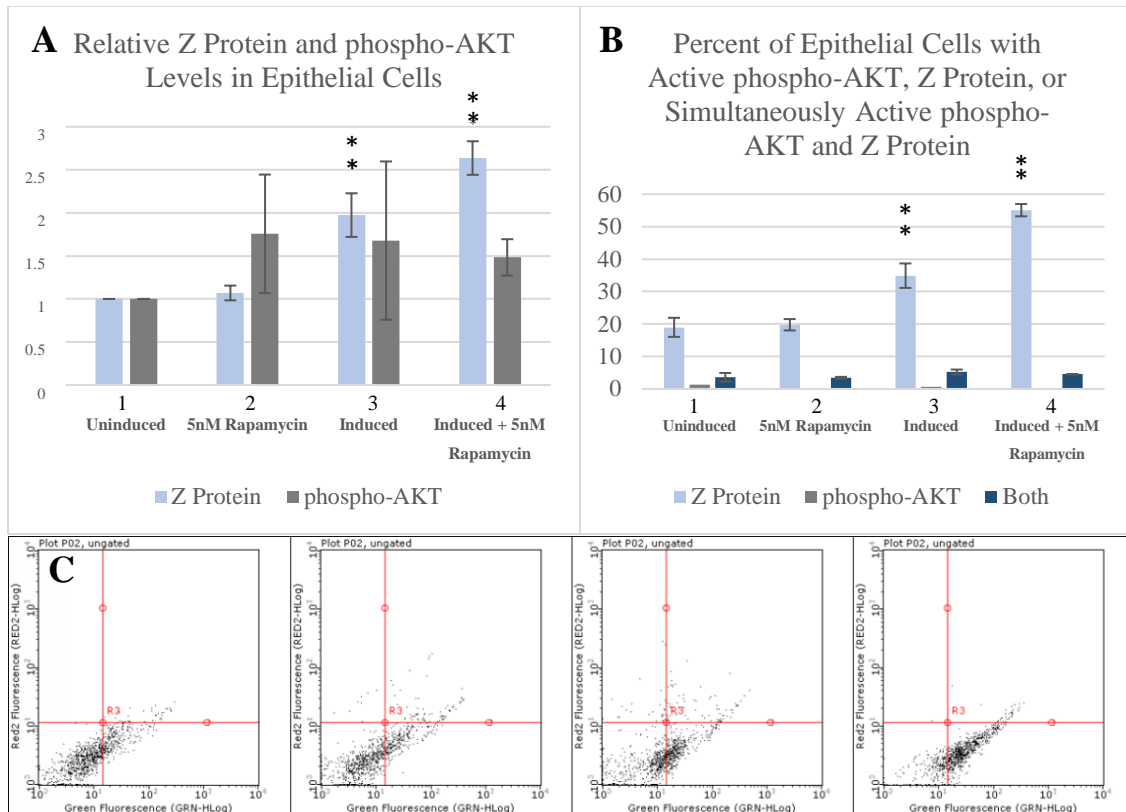


**Figure 6. Levels of Z Protein and phospho-AKT in Epithelial Cells Across Treatment Conditions for mTORC1 Inhibition. A.** Relative epithelial cell Z and phospho-AKT levels; Z protein levels significant for conditions 3 and 4 relative to conditions 1 and 2 ( $p < 0.05$ ). **B.** Percent of epithelial cells positive for Z, phospho-AKT, and double positive for Z and phospho-AKT; cells positive for Z protein significant for conditions 3 and 4 relative to conditions 1 and 2 ( $p < 0.05$ ). **C.** Scatterplots showing percent of cells positive for Z, phospho-AKT, or double positive. All data represent means  $\pm$  SD from biological triplicates.

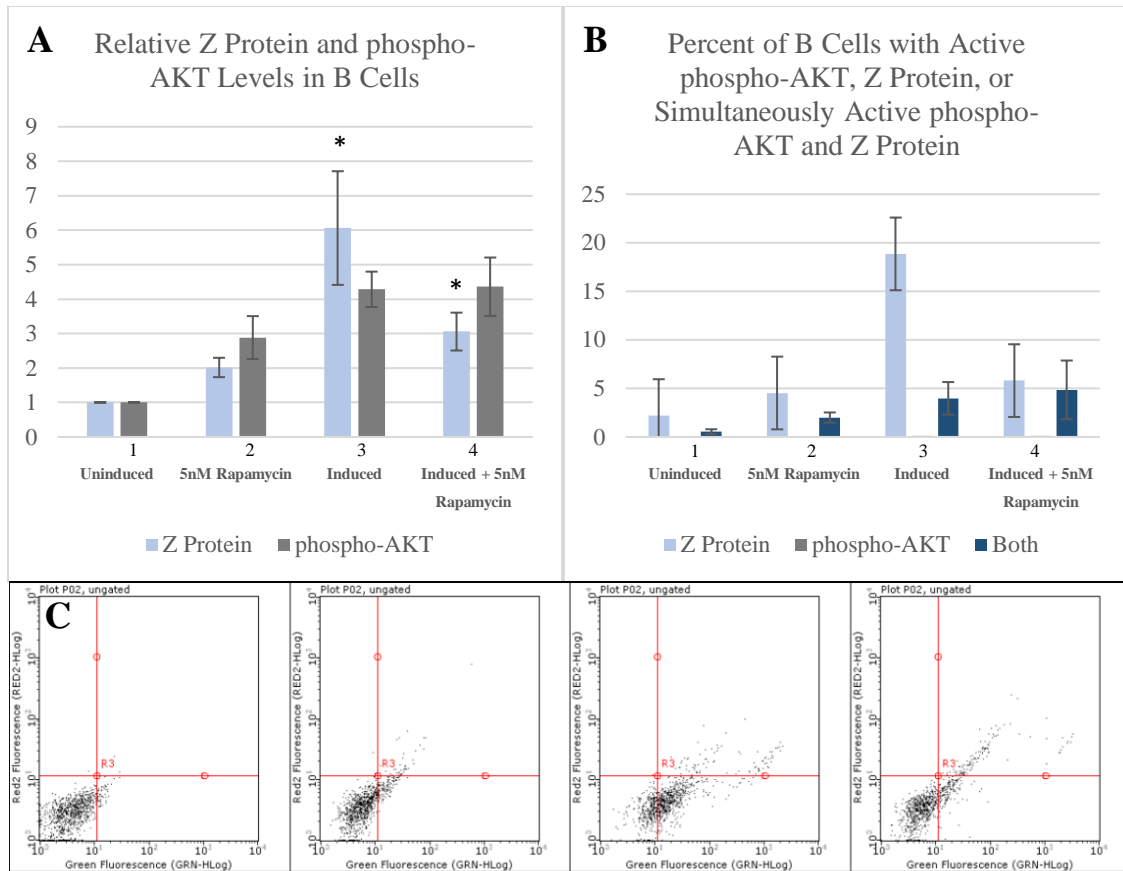


**Figure 7. Levels of Z Protein and phospho-AKT in B Cells Across Treatment Conditions for mTORC1 Inhibition.** **A.** Relative B cell Z and phospho-AKT levels; Z protein levels significant for conditions 3 and 4 relative to conditions 1 and 2 ( $p < 0.05$ ). **B.** Percent of B cells positive for Z, phospho-AKT, and double positive for Z and phospho-AKT. **C.** Scatterplots showing percent of cells positive for Z, phospho-AKT, or double positive. All data represent means  $\pm$  SD from biological triplicates.

### *Levels of Phosphorylated AMPK in mTORC1 Inhibited Conditions*

Levels of phosphorylated AMPK and Z protein were measured using flow cytometric analysis. AMPK is phosphorylated under stress conditions to inhibit mTORC1. Measuring phosphorylated AMPK in relation to Z protein expression provides insight into the pathways being utilized by EBV for protein translation and lytic replication.

Significant increases in total relative Z protein levels were observed in epithelial cells for conditions 3 and 4 relative to condition 1 ( $p < 0.05$ ) (Figure 8 A). No significant differences were observed in total relative phosphorylated AMPK levels across treatment conditions for epithelial cells (Figure 8 A). Figure 8 B shows the percent totals of epithelial cells positive for phosphorylated AMPK, Z protein, or both proteins simultaneous (double positive). Conditions 3 and 4 show significant increases in percent of epithelial cells positive for Z protein alone relative to condition 1 ( $p < 0.05$ ) (Figure 8 B). No significant differences in percent of epithelial cells positive for phosphorylated AMPK alone or double positive epithelial cells were observed (Figure 8 B). It appears that phosphorylated AMPK levels are invariable in epithelial cells during lytic replication and rapamycin treatment. While Z protein in epithelial cells increases with rapamycin treatment, it does not appear to be related to phosphorylated AMPK levels.

Significant increases in total relative Z protein levels were observed in B cells for condition 3 relative to condition 1 ( $p < 0.05$ ) (Figure 9 A). The general trend of decrease in Z protein levels are observed in lytic cells with rapamycin treatment as with other

trials. No significant differences were observed in phosphorylated AMPK levels across treatment conditions for B cells; however, while Z protein decreases in lytic cells with rapamycin treatment, phosphorylated AMPK levels show trends of increase (Figure 9 A). Figure 9 B shows the percent totals of B cells positive for phosphorylated AMPK, Z protein, or both proteins simultaneous (double positive). Condition 4 (Figure 9 B) shows the general trend of decrease in lytic B cells with rapamycin treatment. Approximately 70% of B cells that remain lytic are double positive for phosphorylated AMPK and Z protein (Figure 9 B). Considering the trends of decrease in Z protein and increase in phosphorylated AMPK in rapamycin treated lytic B cells (Figure 9 A, B) and given that phosphorylated AMPK is antagonistic of the mTOR pathway, AMPK levels might correspond with decreases in Z protein levels when lytic B cells are rapamycin treated.

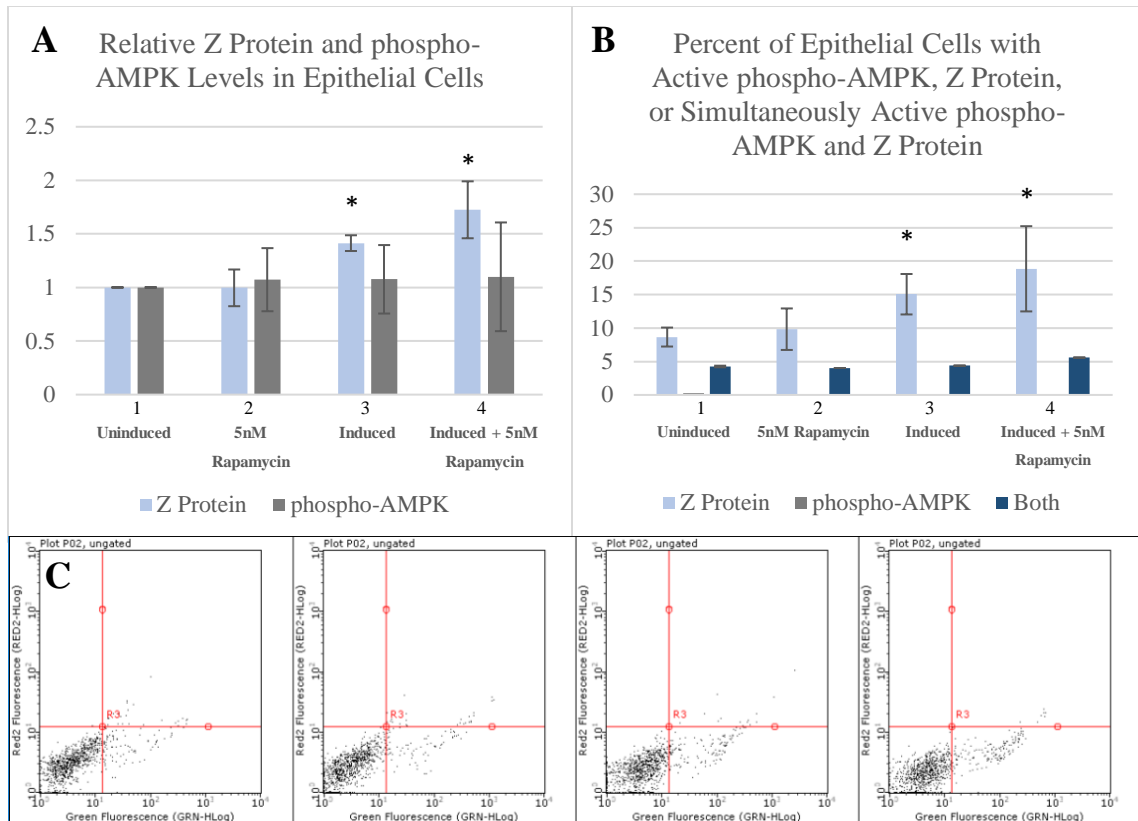


**Figure 8. Levels of Z Protein and phospho-AMPK in Epithelial Cells Across Treatment Conditions for mTORC1 Inhibitor.** **A.** Relative epithelial cell Z and phospho-AMPK levels; Z protein levels significant for conditions 3 and 4 relative to condition 1 ( $p < 0.05$ ). **B.** Percent of epithelial cells positive for Z, phospho-AMPK, and double positive for Z and phospho-AMPK; cells positive for Z protein significant for conditions 3 and 4 relative to condition 1 ( $p < 0.05$ ). **C.** Scatterplots showing percent of cells positive for Z, phospho-AMPK, or double positive. All data represent means  $\pm$  SD from biological triplicates.

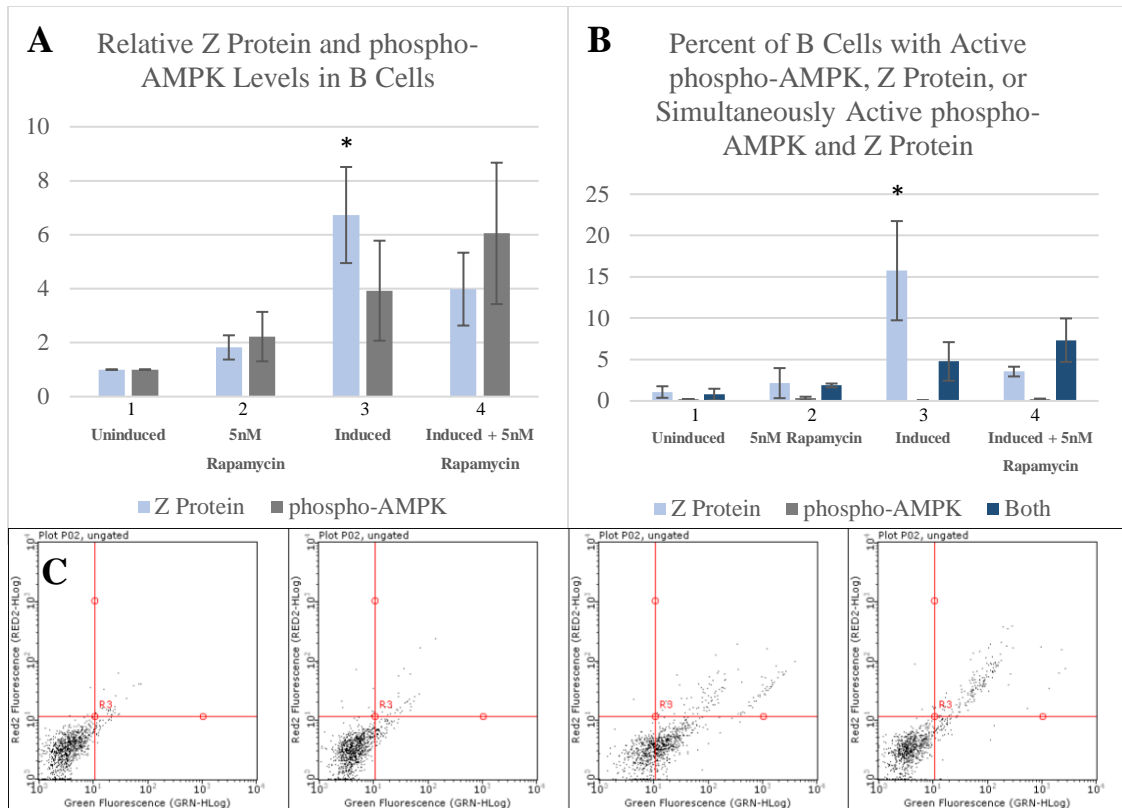


**Figure 9. Levels of Z Protein and phospho-AMPK in B Cells Across Treatment Conditions for mTORC1 Inhibition.** **A.** Relative B cell Z and phospho-AMPK levels; Z protein levels significant for condition 3 relative to condition 1 ( $p < 0.05$ ). **B.** Percent of B cells positive for Z, phospho-AMPK, and double positive for Z and phospho-AMPK; cells positive for Z protein significant for condition 3 relative to condition 1 ( $p < 0.05$ ). **C.** Scatterplots showing percent of cells positive for Z, phospho-AMPK, or double positive. All data represent means  $\pm$  SD from biological triplicates.

### *Levels of Phosphorylated TSC2 in mTORC1 Inhibited Conditions*

Levels of phosphorylated TSC2 and Z protein were measured using flow cytometric analysis. Upon phosphorylation, TSC2 loses its inhibitory function over Rheb-GTP, thereby allowing activation of mTORC1 downstream. Measuring phosphorylated TSC2 in relation to Z protein expression provides insight into the pathways being utilized by EBV for protein translation and lytic replication.

No significant increases in total relative Z protein levels were observed in epithelial cells across treatment conditions in these trials, however, the same general trends of increase in Z protein levels during rapamycin treatment are observed as in other trials (Figure 10 A). No significant differences were observed in phosphorylated TSC2 levels across treatment conditions for epithelial cells (Figure 10 A). Figure 10 B shows the percent totals of epithelial cells positive for phosphorylated TSC2, Z protein, or both proteins simultaneous (double positive). Conditions 3 and 4 show trends of increase in percent of epithelial cells positive for Z protein alone (Figure 10 B). No significant differences in percent of epithelial cells positive for phosphorylated TSC2 alone or double positive epithelial cells were observed (Figure 10 B). While the majority of phosphorylated TSC2 positive cells are double positive, it appears that phosphorylated TSC2 levels are invariable in epithelial cells during lytic replication and rapamycin treatment. While Z protein in epithelial cells increases with rapamycin treatment, it does not appear to be related to phosphorylated TSC2 levels.

Significant increase in total relative Z protein levels in B cells is observed in condition 3 relative to conditions 1 and 2 ( $p < 0.05$ ) (Figure 11 A). Trends of decrease in Z protein levels during rapamycin treatment are observed in lytic B cells (Figure 11A). Phosphorylated TSC2 levels show trends of increase in B cells, despite rapamycin treatment and decrease in Z protein levels (Figure 11A). Figure 11 B shows the percent totals of B cells positive for phosphorylated TSC2, Z protein, or both proteins simultaneous (double positive). Condition 4 (Figure 11 B) shows the general trend of decrease in lytic B cells with rapamycin treatment, however, many of the cells that remain lytic despite rapamycin treatment are double positive for phosphorylated TSC2 and Z protein. Conditions 3 and 4 for percent of double positive cells are significant relative to condition 1 ( $p < 0.05$ ). Nearly 75% of remaining lytic cells after rapamycin treatment are double positive for phosphorylated TSC2 and Z protein (Figure 11 B). Rapamycin treated B cells positive for phosphorylated TSC2 alone account for less than .10% of total lytic cells (Figure 11 B). These results suggest that phosphorylated TSC2 levels correspond to Z protein levels in B cells that remain lytic after rapamycin treatment.

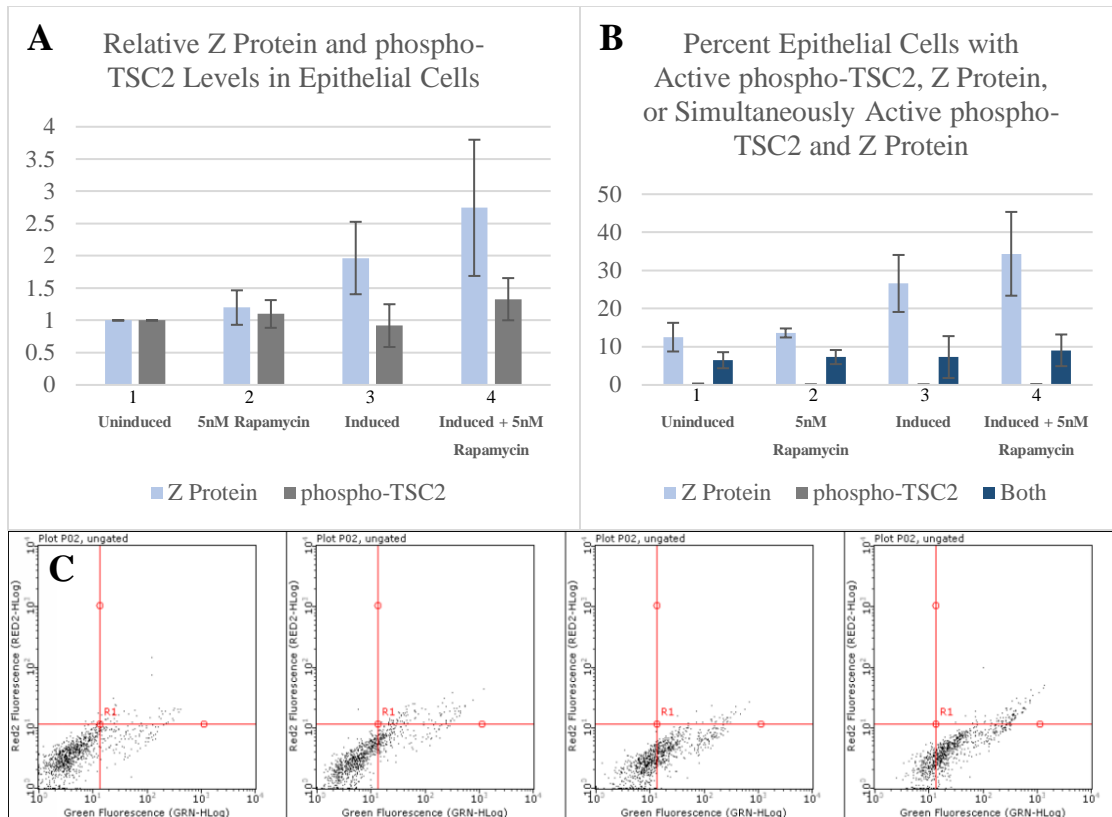


**Figure 10. Levels of Z Protein and phospho-TSC2 in Epithelial Cells Across Treatment Conditions for mTORC1 Inhibition.** **A.** Relative epithelial cell Z and phospho-TSC2 levels. **B.** Percent of epithelial cells positive for Z, phospho-TSC2, and double positive for Z and phospho-TSC2. **C.** Scatterplots showing percent of cells positive for Z, phospho-TSC2, or double positive. All data represent means  $\pm$  SD from biological triplicates.

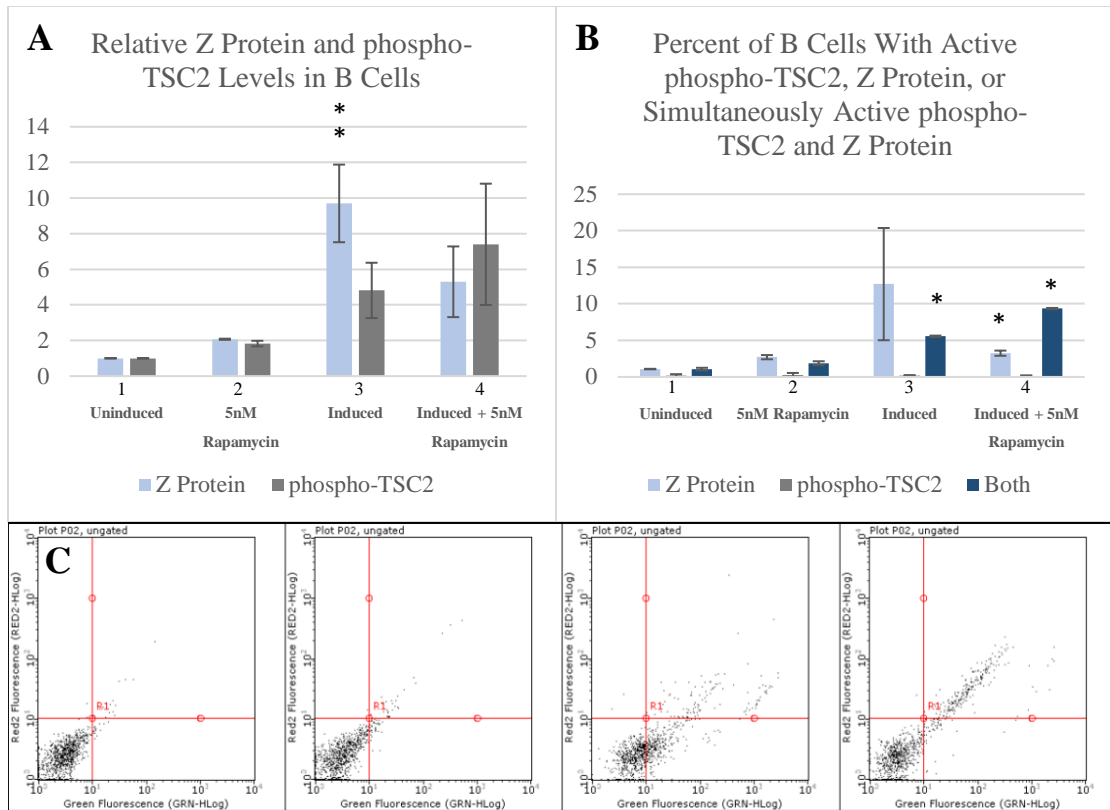


**Figure 11. Levels of Z Protein and phospho-TSC2 in B Cells Across Treatment Conditions for mTORC1 Inhibition.** **A.** B cell Z and phospho-TSC2 levels; Z protein values significant for condition 3 relative to conditions 1 and 2 ( $p < 0.05$ ). **B.** Percent of B cells positive for Z, phospho-TSC2, and double positive for Z and phospho-TSC2; double positive conditions 3 and 4 significant relative to condition 1 ( $p < 0.05$ ). **C.** Scatterplots showing percent of cells positive for Z, phospho-TSC2, or double positive. All data represent means  $\pm$  SD from biological triplicates.

### *Levels of Phosphorylated mTOR in mTORC1 Inhibited Conditions*

Levels of phosphorylated mTOR and Z protein were measured using flow cytometric analysis. Upon phosphorylation, mTOR phosphorylates downstream targets p70S6K and 4EBP1, thereby activating protein synthesis. Rapamycin does not inhibit phosphorylation of mTOR, but instead binds to FKBP12 and prevents phosphorylation of downstream targets by mTOR. Measuring phosphorylated mTOR in relation to Z protein expression provides insight into the pathways being utilized by EBV for protein translation and lytic replication.

Significant increases in total relative Z protein levels were observed in epithelial cells in conditions 2, 3, and 4 relative to condition 1 ( $p < 0.05$ ) (Figure 12 A). Figure 12 B shows the percent totals of epithelial cells positive for phosphorylated mTOR, Z protein, or both proteins simultaneous (double positive). Condition 4 shows significant increase in Z protein levels relative to condition 1 ( $p < 0.05$ ) (Figure 12 B). Double positive epithelial cells for mTOR and Z protein account for approximately 40% of total lytic cells in the induced condition (Figure 12 B). Double positive epithelial cells for mTOR and Z protein account for approximately 30% of all lytic epithelial cells during rapamycin treatment (Figure 12 B). Z protein in epithelial cells increases with rapamycin treatment, and it appears it may be related to phosphorylated mTOR levels.

Significant increases in total relative Z protein levels were observed in B cells in condition 3 relative to conditions 1 and 2 ( $p < 0.05$ ) (Figure 13 A). The same general trends of decrease in Z protein levels under rapamycin treated and induced conditions in

B cells are observed as in other trials (Figure 13 A). Despite decreases in Z protein levels in condition 4, significant increases in phosphorylated mTOR were observed in B cells in conditions 3 and 4 relative to conditions 1 and 2 ( $p < 0.05$ ) (Figure 13 A). Figure 13 B shows the percent totals of B cells positive for phosphorylated mTOR, Z protein, or both proteins simultaneous (double positive). Significant increases were observed in double positive cells in conditions 3 and 4 relative to conditions 1 and 2 ( $p < 0.05$ ) (Figure 13 B). In fact, approximately 61% of remaining lytic cells after rapamycin treatment are double positive for phosphorylated mTOR and Z protein (Figure 13 B). Rapamycin treated B cells positive for phosphorylated mTOR alone account for less than .10% of total lytic cells (Figure 13 B). These observations suggest that phosphorylated mTOR levels correspond to Z protein levels in B cells that remain lytic after rapamycin treatment.

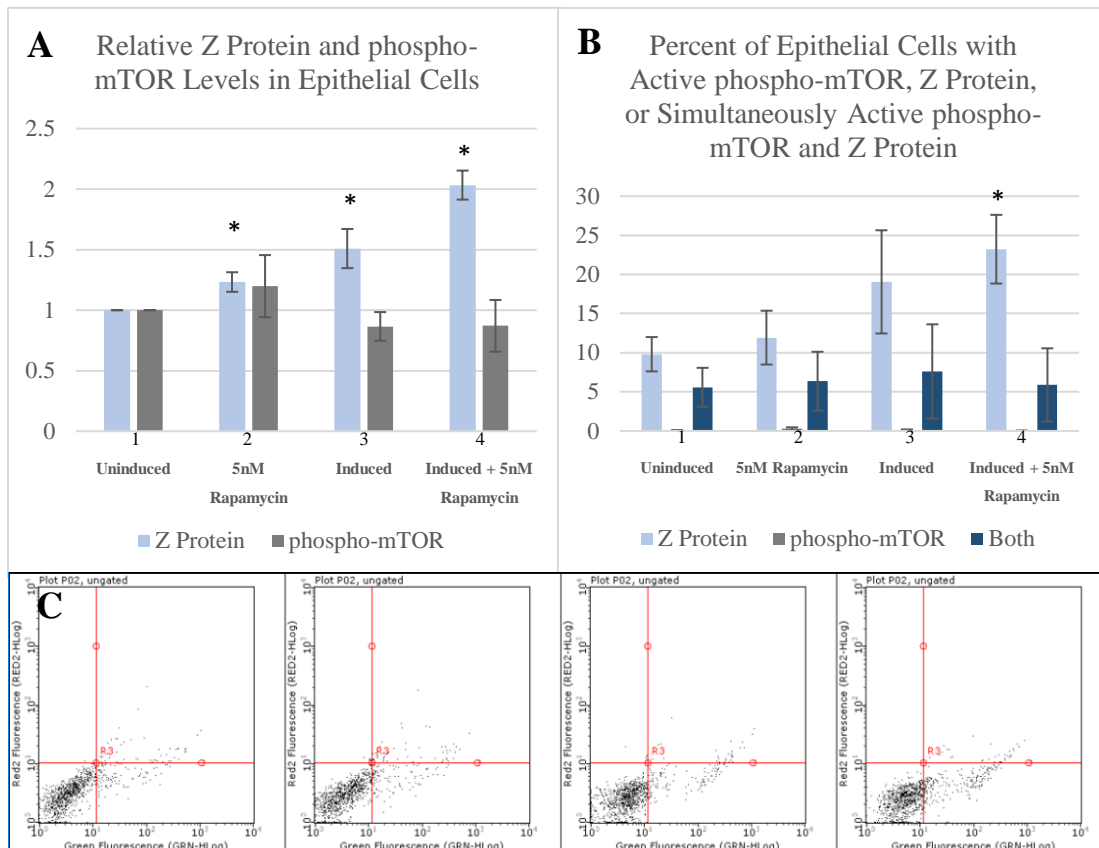


**Figure 12. Levels of Z Protein and phospho-mTOR in Epithelial Cells Across Treatment Conditions for mTORC1 Inhibition.** **A.** Relative epithelial cell Z and phospho-mTOR levels; conditions 2, 3, and 4 significant relative to condition 1. **B.** Percent of epithelial cells positive for Z, phospho-mTOR, and double positive for Z and phospho-mTOR; condition 4 Z protein significant relative to condition 1 ( $p < 0.05$ ). **C.** Scatterplots showing percent of cells positive for Z, phospho-mTOR, or double positive. All data represent means  $\pm$  SD from biological triplicates.

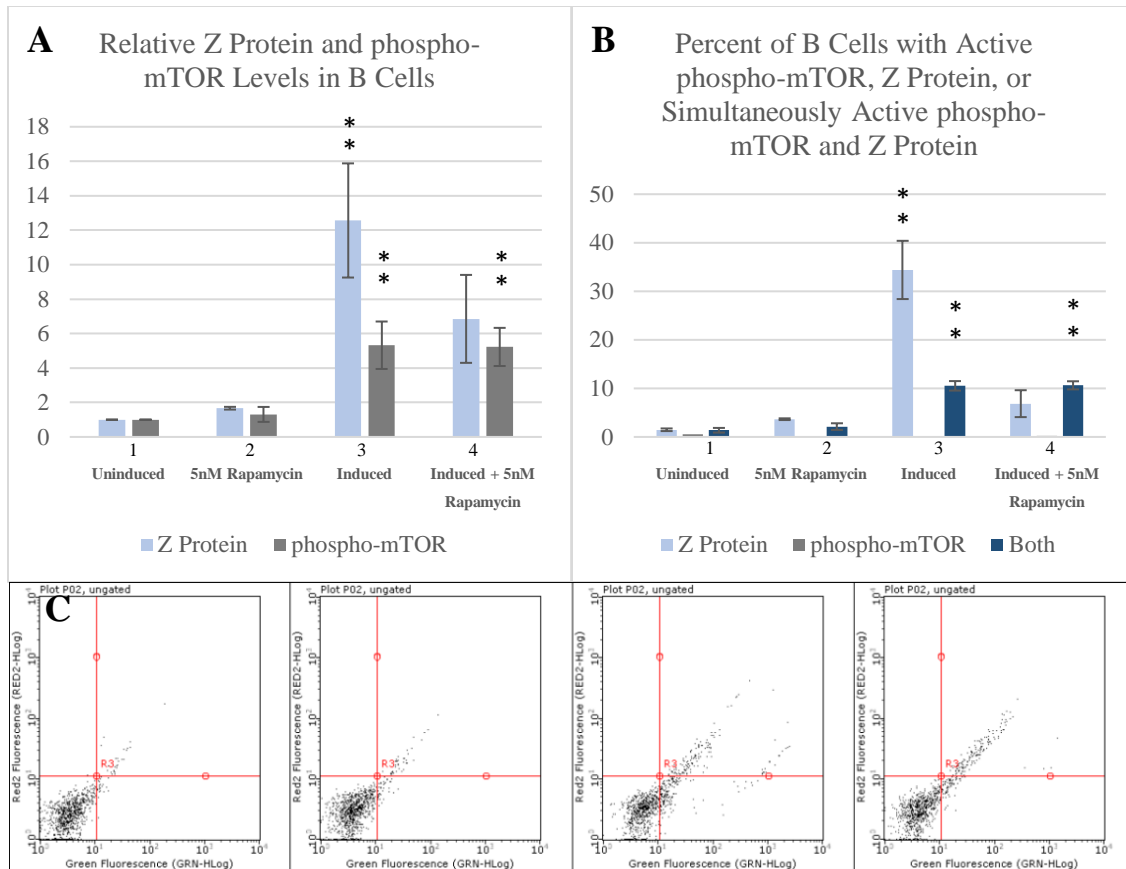


**Figure 13. Levels of Z Protein and phospho-mTOR in B Cells Across Treatment Conditions for mTORC1 Inhibition.** **A.** B cell Z and phospho-mTOR levels; Z protein values significant for condition 3 relative to conditions 1 and 2 ( $p < 0.05$ ). **B.** Percent of B cells positive for Z, phospho-mTOR, and double positive for Z and phospho-mTOR; double positive conditions 3 and 4 significant relative to conditions 1 and 2 ( $p < 0.05$ ). **C.** Scatterplots showing percent of cells positive for Z, phospho-mTOR, or double positive. All data represent means  $\pm$  SD from biological triplicates.

### *Levels of Phosphorylated p70S6K in mTORC1 Inhibited Conditions*

Levels of phosphorylated p70S6K and Z protein were measured using flow cytometric analysis. Phosphorylation of p70S6K triggers protein synthesis at the ribosome. Measuring phosphorylated p70S6K in relation to Z protein expression provides insight into the pathways being utilized by EBV for protein translation and lytic replication.

A significant increase in total relative Z protein level was observed in condition 3 relative to conditions 1 and 2 in epithelial cells ( $p < 0.05$ ) (Figure 14 A). Significant increase in phosphorylated p70S6k levels for conditions 2 and 3 relative to condition 1 were observed in epithelial cells ( $p < 0.05$ ) (Figure 14 A). Trends of increase in phosphorylated p70S6K correspond to trends of increase in Z protein (Figure 14 A, B). Figure 14 B shows the percent totals of epithelial cells positive for phosphorylated p70S6K, Z protein, or both proteins simultaneous (double positive). Significant increase in double positive epithelial cells was observed in condition 3 relative to condition 1 ( $p < 0.05$ ) (Figure 14 B). Approximately 45% of all lytic epithelial cells in condition 4 are double positive for Z protein and phosphorylated p70S6K (Figure 14 B). These observations suggest that phosphorylated p70S6K levels may correspond to Z protein levels in epithelial cells.

Significant increases in total relative Z protein levels were observed in B cells for conditions 3 and 4 relative to conditions 1 and 2 ( $p < 0.05$ ) (Figure 15 A). Trends of decrease in Z protein levels during rapamycin treatment were observed (Figure 15 A).

While no significant differences in total phosphorylated p70S6K levels were observed in B cells, trends of increase across conditions were observed (Figure 15 A). Figure 15 B shows the percent totals of B cells positive for phosphorylated p70S6K, Z protein, or both proteins simultaneous (double positive). Significant increase in double positive B cells was observed in condition 3 relative to condition 1 ( $p < 0.05$ ) (Figure 15 B).

Approximately 52% of all lytic B cells remaining after rapamycin treatment in condition 4 are double positive for Z protein and phosphorylated p70S6K (Figure 15 B). These observations suggest that phosphorylated p70S6K levels may correspond to Z protein levels in B cells that remain lytic after rapamycin treatment, despite decreases in Z protein levels.

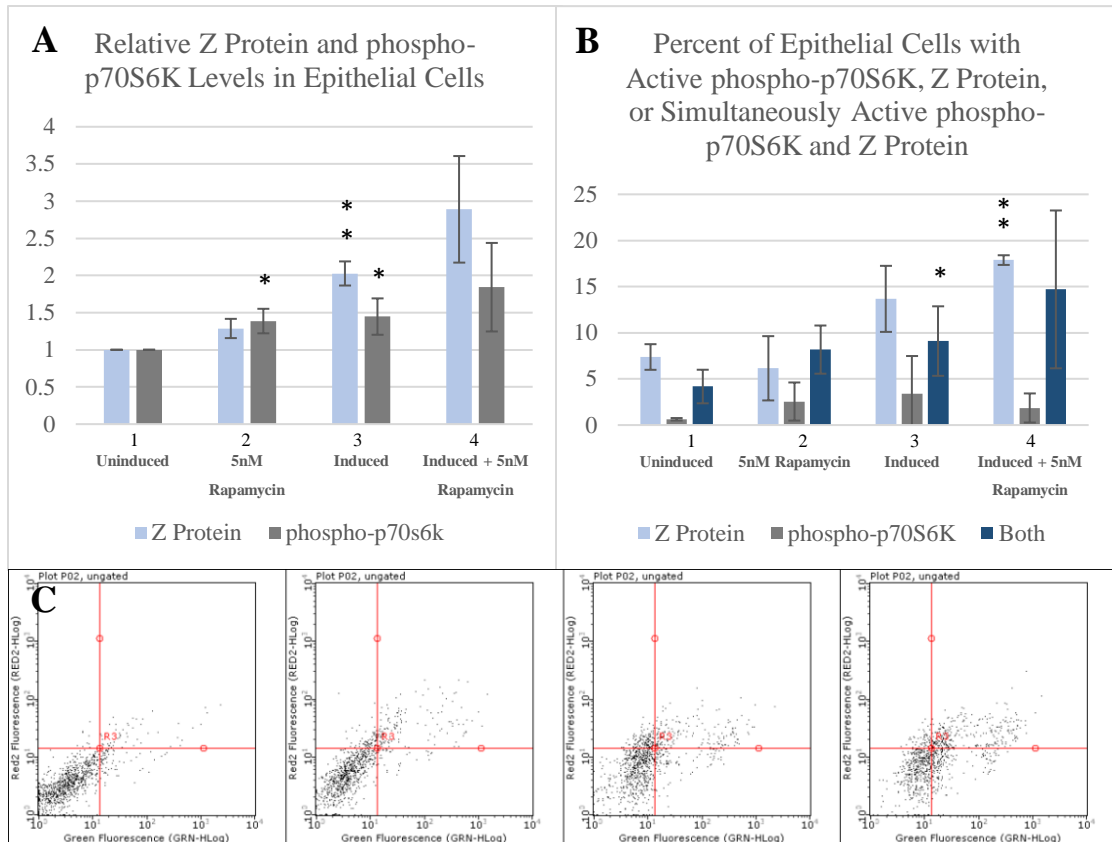


**Figure 14. Levels of Z Protein and phospho-p70S6K in Epithelial Cells Across Treatment Conditions for mTORC1 Inhibition.** **A.** Relative epithelial cell Z and phospho-p70S6K levels; Z protein values significant in condition 3 relative to conditions 1 and 2; conditions 2 and 3 total relative phospho-p70S6K levels significant relative to condition 1 ( $p < 0.05$ ). **B.** Percent of epithelial cells positive for Z, phospho-p70S6K, and double positive for Z and phospho-p70S6K; condition 4 Z protein significant relative to conditions 1 and 2, condition 3 double positive significant relative to condition 1 ( $p < 0.05$ ). **C.** Scatterplots showing percent of cells positive for Z, phospho-p70S6K, or double positive. All data represent means  $\pm$  SD from biological triplicates.

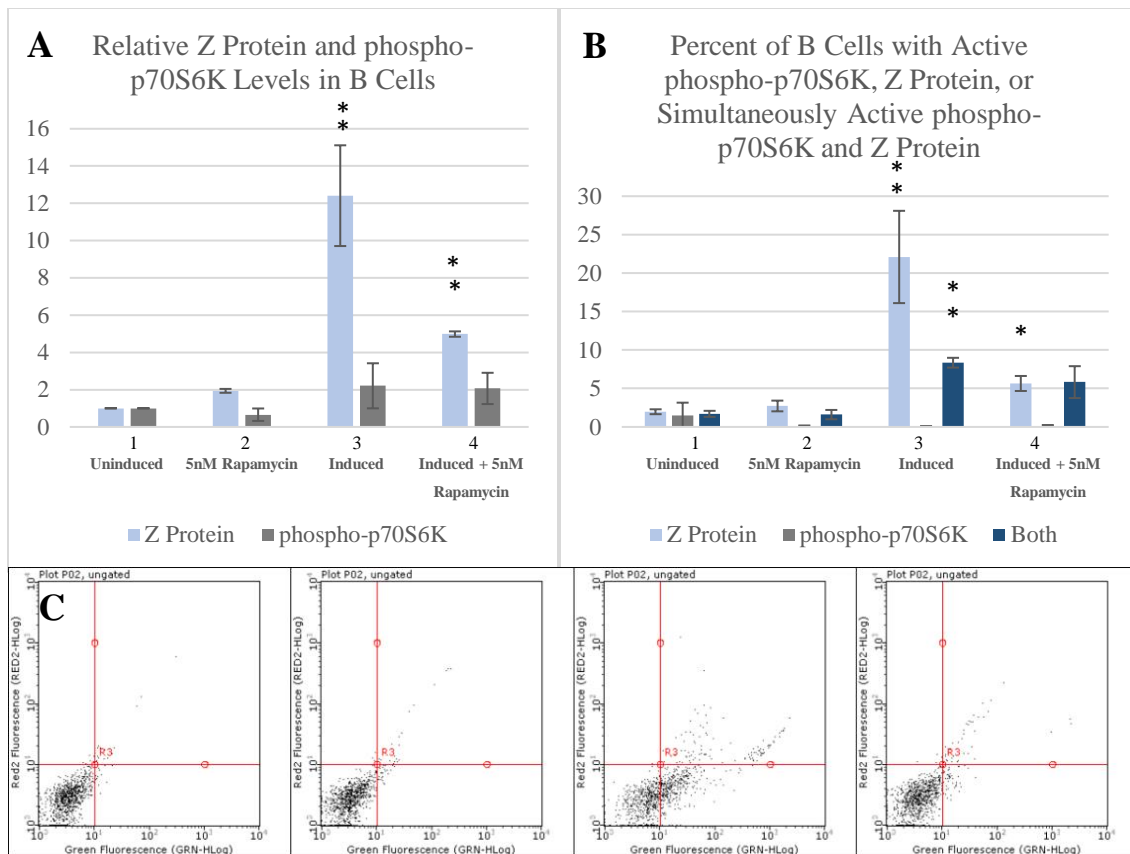


**Figure 15. Levels of Z Protein and phospho-p70S6K in B Cells Across Treatment Conditions for mTORC1 Inhibition.** **A.** B cell Z and phospho-p70S6K levels; Z protein levels significant for conditions 3 and 4 relative to conditions 1 and 2 ( $p < 0.05$ ). **B.** Percent of B cells positive for Z, phospho-p70S6K, and double positive for Z and phospho-p70S6K; condition 3 double positive significant relative to condition 1, conditions 3 and 4 Z protein only significant to conditions 1 and 2 ( $p < 0.05$ ). **C.** Scatterplots showing percent of B cells positive for Z, phospho-p70S6K, or double positive. All data represent means  $\pm$  SD from biological triplicates.

### *Levels of Phosphorylated 4EBP1 in mTORC1 Inhibited Conditions*

Levels of phosphorylated 4EBP1 and Z protein were measured using flow cytometric analysis. 4EBP1 inhibits eIF4E, a protein that binds 5' cap of mRNA. Upon phosphorylation, 4EBP1 will release eIF4E, thereby activating cap dependent translation. Measuring phosphorylated 4EBP1 in relation to Z protein expression provides insight into the pathways being utilized by EBV for protein translation and lytic replication.

Significant increase was observed in total relative Z protein levels in epithelial cells in conditions 3 and 4 relative to conditions 1 and 2 ( $p < 0.05$ ) (Figure 16 A). Significant decrease in phosphorylated 4EBP1 level was observed in epithelial cells in condition 3 relative to condition 1 ( $p < 0.05$ ) (Figure 16 A). Figure 16 B shows the percent totals of epithelial cells positive for phosphorylated 4EBP1, Z protein, or both proteins simultaneous (double positive). Trends of increase in Z protein was observed in conditions 3 and 4 in epithelial cells (Figure 16 B). Only approximately 10% of all lytic epithelial cells in conditions 3 and 4 are double positive for Z protein and phosphorylated 4EBP1 (Figure 16 B). These observations suggest that phosphorylated 4EBP1 levels may not correspond to Z protein levels in epithelial cells.

A significant increase in total relative Z protein levels was observed in condition 3 relative to condition 2 in B cells ( $p < 0.05$ ) (Figure 17 A). A significant increase in phosphorylated 4EBP1 levels were observed in B cells for conditions 3 and 4 relative to conditions 1 and 2 ( $p < 0.05$ ) (Figure 17 A). The same trends of decrease in Z protein production in lytic B cells treated with rapamycin are observed as in other trials (Figure

17 A). Figure 17 B shows the percent totals of B cells positive for phosphorylated 4EBP1, Z protein, or both proteins simultaneous (double positive). Trends of decrease in percent of cells with active Z protein was observed on condition 4 (Figure 17 B). Double positive B cells for phosphorylated 4EBP1 and Z protein were significantly increased in conditions 3 and 4 relative to conditions 1 and 2 ( $p < 0.05$ ) (Figure 17 B). Nearly all cells positive for phosphorylated 4EBP1 are also Z positive, and approximately 64% of all remaining lytic B cells under rapamycin conditions are double positive (Figure 17 B). These trends suggest phosphorylated 4EBP1 may correlate with Z protein production in remaining lytic B cells with rapamycin treatment, despite overall decrease in Z protein levels.

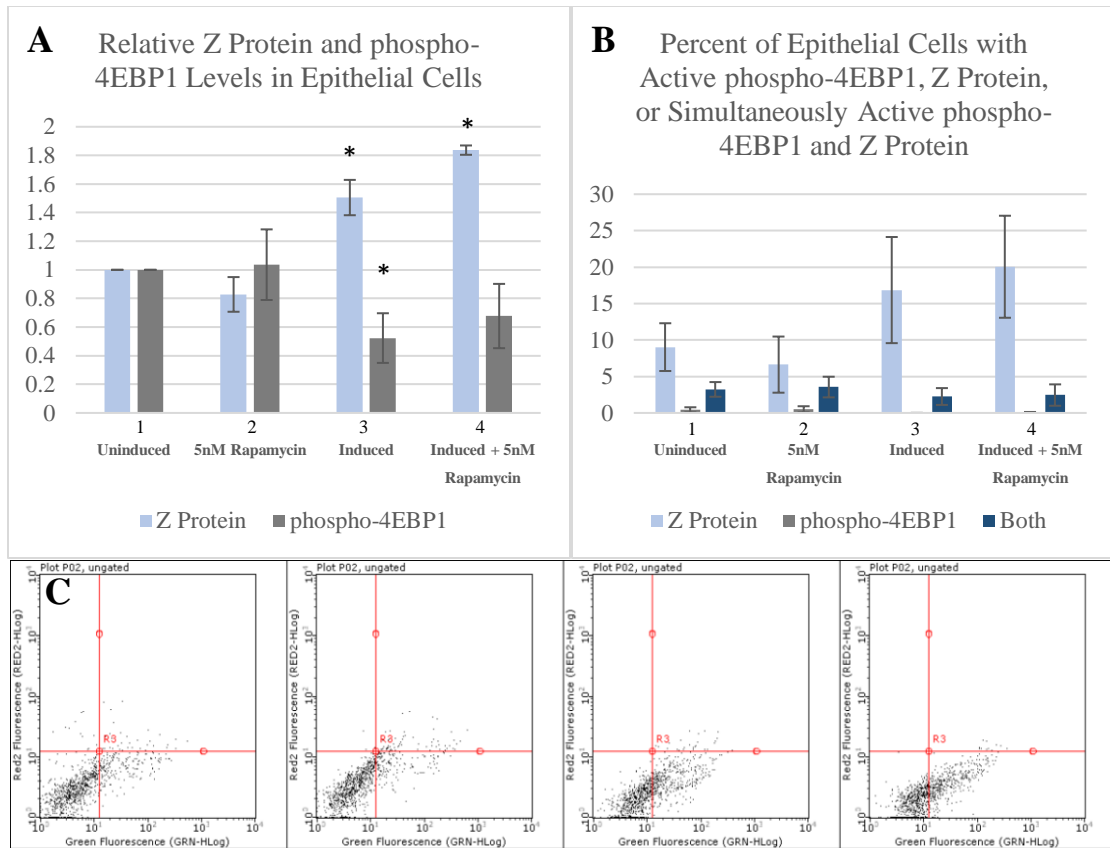


**Figure 16. Levels of Z Protein and phospho-4EBP1 in Epithelial Cells Across Treatment Conditions for mTORC1 Inhibition. A.** Epithelial cell Z and phospho-4EBP1 levels; Z protein level values significant for conditions 3 and 4 relative to conditions 1 and 2; phospho-4EBP1 level values significant for condition 3 relative to 1 ( $p < 0.05$ ). **B.** Percent of epithelial cells positive for Z, phospho-4EBP1, and double positive for Z and phospho-4EBP1. **C.** Scatterplots showing percent of cells positive for Z, phospho-4EBP1, or double positive. All data represent means  $\pm$  SD from biological triplicates.

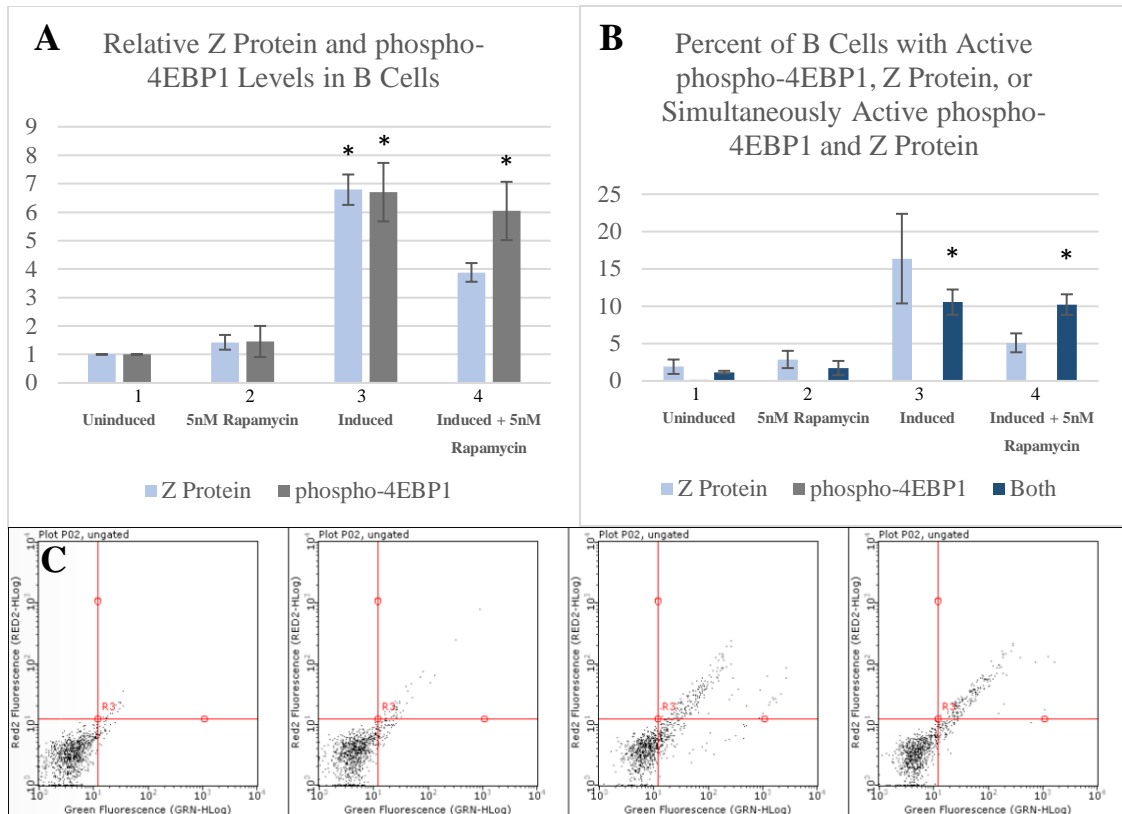


**Figure 17. Levels of Z Protein and phospho-4EBP1 in B Cells Across Treatment Conditions for mTORC1 Inhibition.** **A.** B cell Z and phospho-4EBP1 levels; Z protein level values significant for condition 3 relative to condition 2; phospho-4EBP1 level values significant for conditions 3 and 4 relative to conditions 1 and 2 ( $p < 0.05$ ). **B.** Percent of B cells positive for Z, phospho-4EBP1, and double positive for Z and phospho-4EBP1; double positive conditions 3 and 4 significant relative to conditions 1 and 2 ( $p < 0.05$ ). **C.** Scatterplots showing percent of cells positive for Z, phospho-4EBP1, or double positive. All data represent means  $\pm$  SD from biological triplicates.

### *Levels of Phosphorylated p38 in mTORC1 Inhibited Conditions*

Levels of phosphorylated p38 and Z protein were measured using flow cytometric analysis. P38 is a MAPK protein that becomes activated during cell stress conditions. Upon phosphorylation, p38 phosphorylates Mnk1/2, which in turn activates eIF4E, a protein that binds 5' caps of mRNA and aids in translation. Measuring phosphorylated p38 in relation to Z protein expression provides insight into the pathways being utilized by EBV for protein translation and lytic replication.

Significant differences were observed in total relative Z protein levels in epithelial cell in conditions 3 and 4 relative to conditions 1 and 2 ( $p < 0.05$ ) (Figure 18 A). Trends of increase in Z protein levels are observed in rapamycin treated and induced cells as in other trials (Figure 18 A). A trend of increase is observed for phosphorylated p38 levels in relation to Z protein levels. Figure 18 B shows the percent totals of epithelial cells positive for phosphorylated p38, Z protein, or both proteins simultaneous (double positive). Significant increases in percent of cells positive for Z protein was observed in conditions 3 and 4 relative to conditions 1 and 2 in epithelial cells ( $p < 0.06$ ) (Figure 18 B). Approximately 30% of all lytic epithelial cells in conditions 3 and 4 are double positive for Z protein and phosphorylated p38 (Figure 18 B). These observations suggest that phosphorylated p38 levels may correspond to Z protein levels in epithelial cells.

Significant increases in Z protein levels in B cells were observed in conditions 3 and 4 relative to conditions 1 and 2 ( $p < 0.05$ ) (Figure 19 A). The same general trends of decrease in Z protein levels with rapamycin treatment are observed as in other trials.

While no significant changes were observed in total relative p38 levels in B cells, there appears to be a trend of increase in p38 in conditions 3 and 4, despite rapamycin treatment and decrease in Z protein levels (Figure 19 A). Figure 19 B shows the percent totals of B cells positive for phosphorylated p38, Z protein, or both proteins simultaneous (double positive). Significant increase in percent of cells positive for Z protein was observed in condition 3 relative to condition 1 ( $p < 0.05$ ) (Figure 19 B). While the percent of double positive cells for phosphorylated p38 and Z protein are not statistically significant, there are trends of increase. Nearly all the phosphorylated p38 positive cells are positive for Z protein as well. Also, approximately 66% of all remaining lytic cells after rapamycin treatment are double positive for Z protein and phosphorylated p38. These results suggest that phosphorylated p38 levels may correspond to Z protein levels in B cells, and most of the cells that remain lytic after rapamycin treatment are also phosphorylated p38 positive.

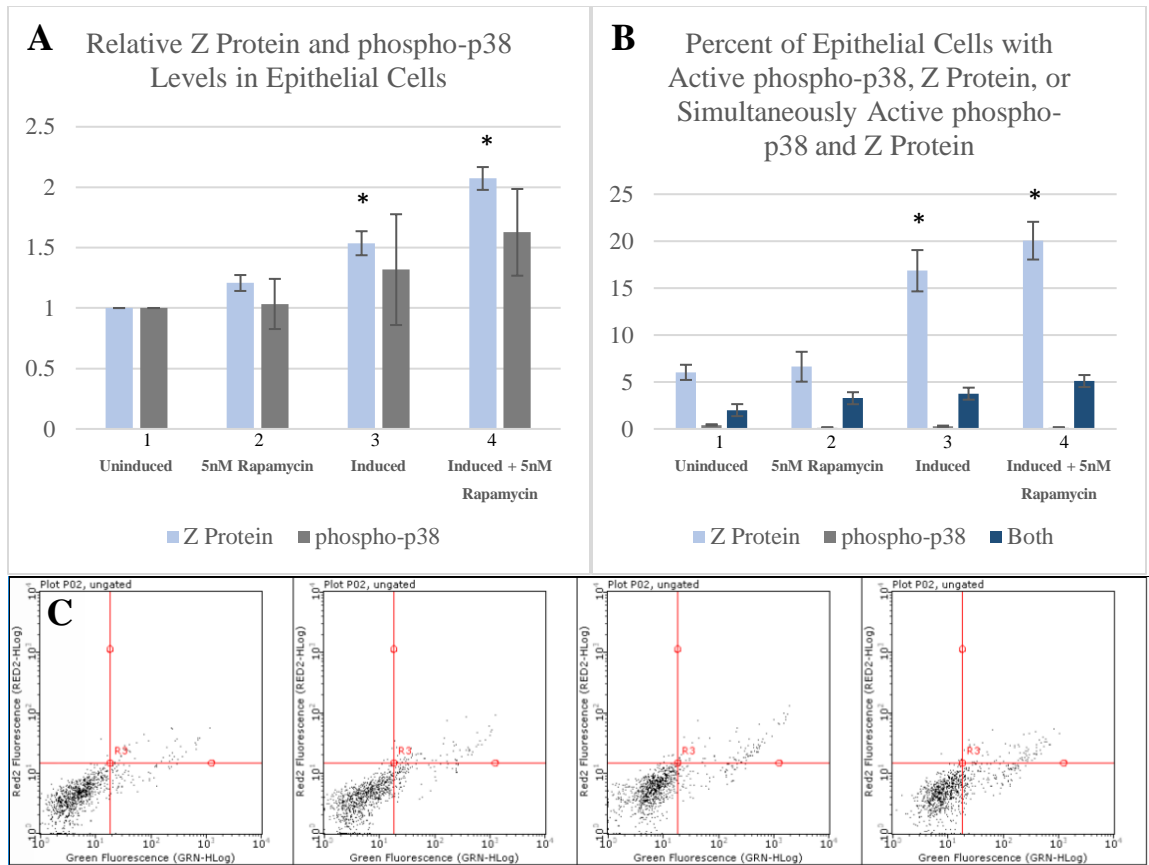


**Figure 18. Levels of Z Protein and phospho-p38 in Epithelial Cells Across Treatment Conditions for mTORC1 Inhibition.** **A.** Epithelial cell Z and phospho-p38 levels; Z protein level values significant for conditions 3 and 4 relative to 1, and condition 3 relative to condition 2 ( $p < 0.05$ ). **B.** Percent of epithelial cells positive for Z, phospho-p38, and double positive for Z and phospho-p38; conditions 3 and 4 for Z protein significant relative to conditions 1 and 2 ( $p < 0.05$ ). **C.** Scatterplots showing percent of cells positive for Z, phospho-p38, or double positive. All data represent means  $\pm$  SD from biological triplicates.

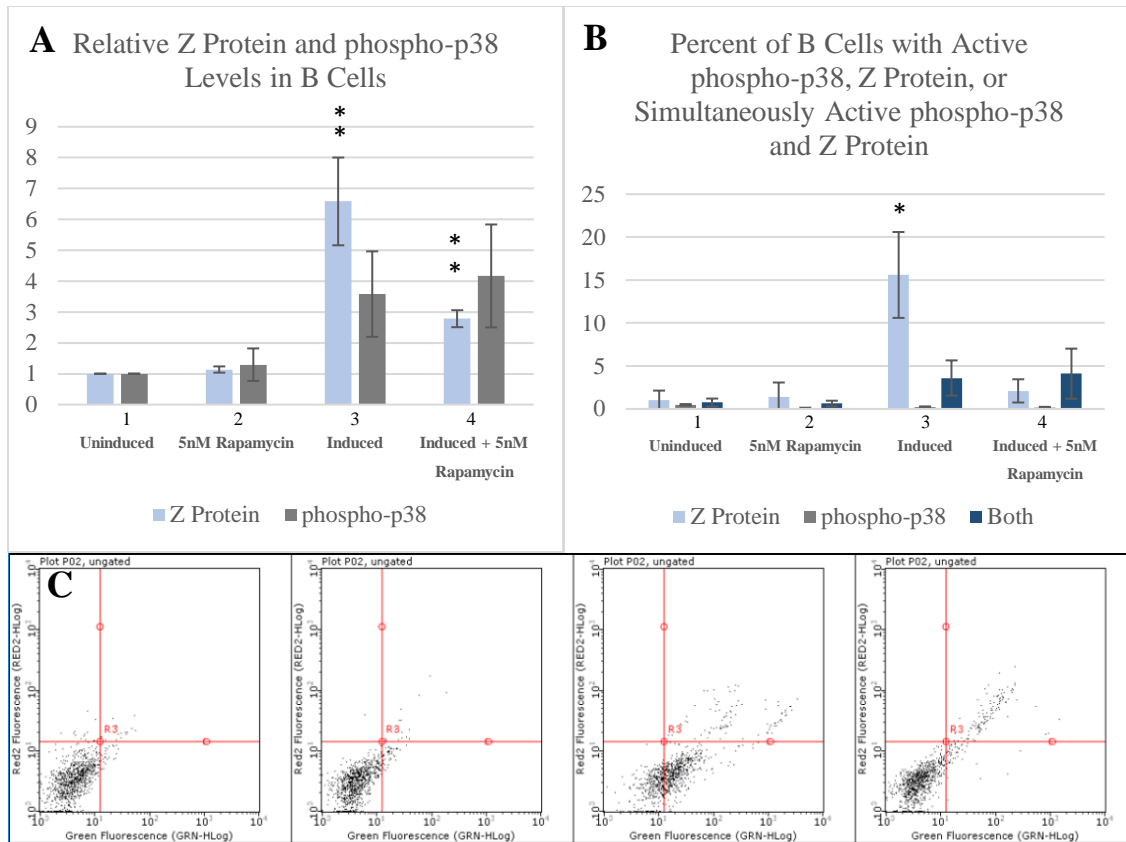


**Figure 19. Levels of Z Protein and phospho-p38 in B Cells Across Treatment Conditions for mTORC1 Inhibition. A.** B cell Z and phospho-p38 levels; Z protein level values significant for conditions 3 and 4 relative to condition 1 ( $p < 0.05$ ). **B.** Percent of B cells positive for Z, phospho-p38, and double positive for Z and phospho-p38; Z positive condition 3 significant relative to condition 1 ( $p < 0.05$ ). **C.** Scatterplots showing percent of cells positive for Z, phospho-p38, or double positive. All data represent means  $\pm$  SD from biological triplicates.

### *Levels of Phosphorylated ERK in mTORC1 Inhibited Conditions*

Levels of phosphorylated ERK and Z protein were measured using flow cytometric analysis. ERK is a MAPK protein that becomes activated upon phosphorylation via MEK. Upon phosphorylation, ERK phosphorylates Mnk1/2 and TSC1/2, which in turn activates eIF4E, a protein that binds 5' caps of mRNA and aids in translation. Measuring phosphorylated ERK in relation to Z protein expression provides insight into the pathways being utilized by EBV for protein translation and lytic replication.

No significant differences in total relative Z protein levels across treatment conditions were observed for epithelial cells, although the same trends of increase in Z protein are observed as with other trials (Figure 20 A). Significant increase in phosphorylated ERK levels were observed in epithelial cells in for condition 4 relative to condition 1 ( $p < 0.05$ ) (Figure 20 A). Figure 20 B shows the percent totals of epithelial cells positive for phosphorylated ERK, Z protein, or both proteins simultaneous (double positive). No significant increases in percent of cells positive for Z protein was observed; however, the general trends of increase in Z protein expression in rapamycin treated induced cells are observed as in other trials (Figure 20 B). The percent of double positive cells for conditions 3 and 4 are significantly increased in relation to condition 1 ( $p < 0.05$ ) (Figure 20 B). Approximately 40% of all lytic cells in conditions 3 and 4 are double positive for phosphorylated ERK and Z protein (Figure 20 B). These observations

suggest that phosphorylated ERK levels may correspond to increased Z protein levels in epithelial cells during mTORC1 inhibition.

No significant differences in total relative Z protein levels were observed in B cells for treatment conditions, observed are the same general trends of decrease in Z protein expression with rapamycin treatment is observed as in other trials (Figure 21 A). No significant differences in phosphorylated ERK were observed across treatment conditions for B cells (Figure 21 A). However, despite decreases in Z protein levels with rapamycin treatment in induced cells, phosphorylated ERK levels increase. Figure 21 B shows the percent totals of B cells positive for phosphorylated ERK, Z protein, or both proteins simultaneous (double positive). No significant changes in percent of cells positive for Z protein was observed; however, the general trends of decrease in Z protein expression in rapamycin treated induced cells are observed as in other trials (Figure 20 B). The percent of double positive cells for condition 4 are significantly increased in relation to conditions 1 and 2 ( $p < 0.05$ ) (Figure 21 B). Approximately 80% of remaining lytic cells in rapamycin treated condition 4 are double positive for phosphorylated ERK and Z protein (Figure 21 B). These observations suggest that phosphorylated ERK may correspond with Z protein levels in lytic B cells that are rapamycin treated, despite decreases in Z protein levels.

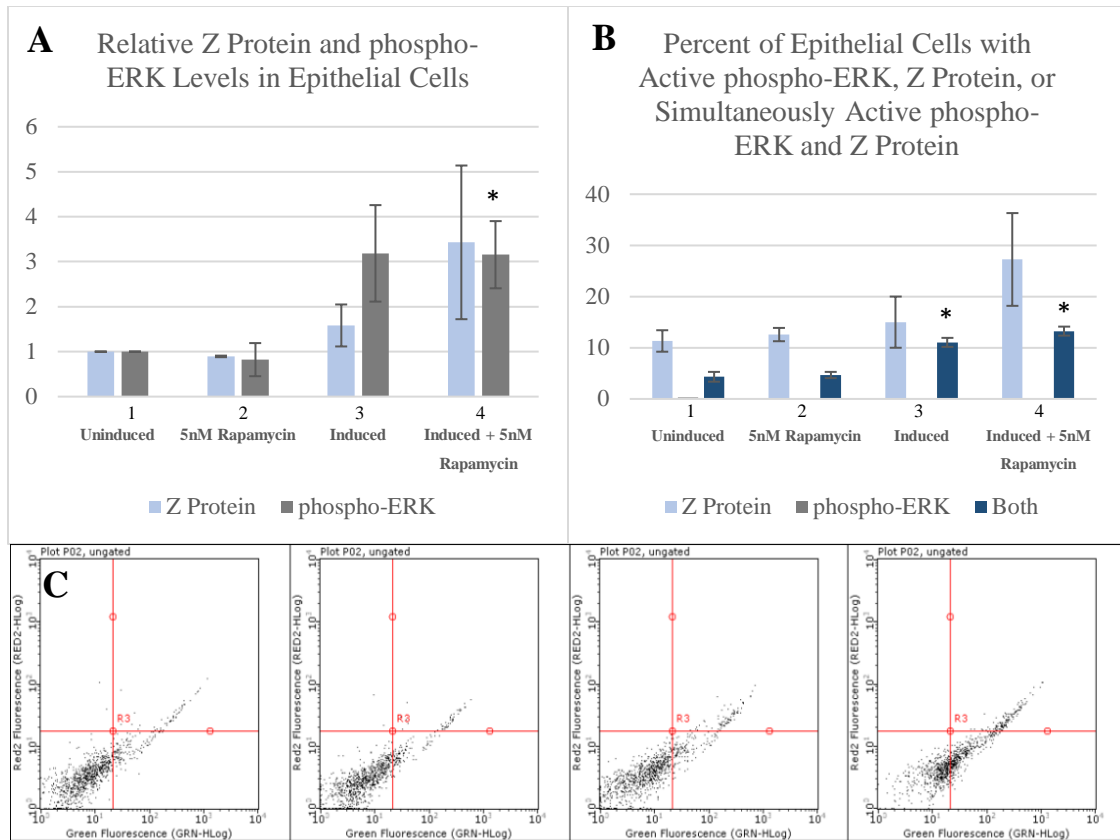


**Figure 20. Levels of Z Protein and phospho-ERK in Epithelial Cells Across Treatment Conditions for mTORC1 Inhibition.** **A.** Epithelial cell Z and phospho-ERK levels; phosphorylated ERK level value significant for condition 4 relative to conditions 1 and 2 ( $p < 0.05$ ). **B.** Percent of epithelial cells positive for Z, phospho-ERK, and double positive for Z and phospho-ERK; double positive conditions 3 and 4 significant relative to condition 1 ( $p < 0.05$ ). **C.** Scatterplots showing percent of cells positive for Z, phospho-ERK, or double positive. All data represent means  $\pm$  SD from biological triplicates.

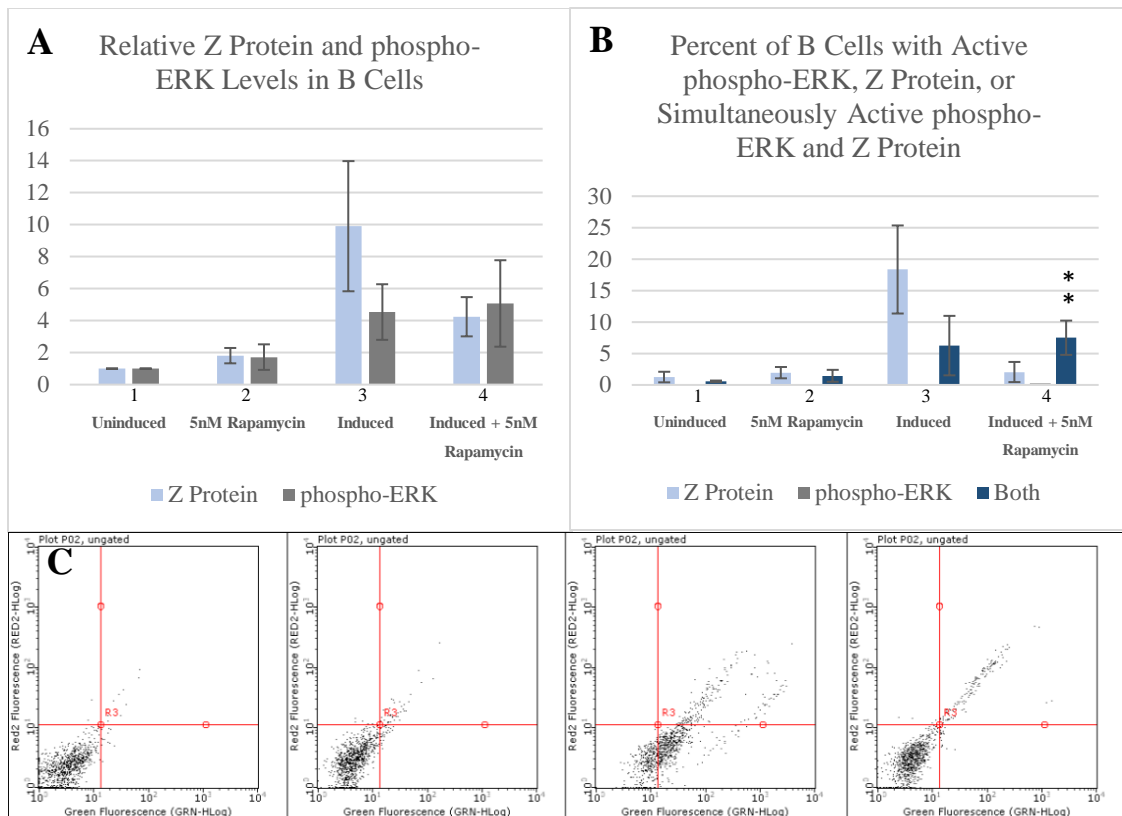


**Figure 21. Levels of Z Protein and phospho-ERK in B Cells Across Treatment Conditions for mTORC1 Inhibition.** **A.** B cell Z and phospho-ERK levels. **B.** Percent of B cells positive for Z, phospho-ERK, and double positive for Z and phospho-ERK; double positive condition 4 significant relative to conditions 1 and 2 ( $p < 0.05$ ). **C.** Scatterplots showing percent of cells positive for Z, phospho-ERK, or double positive. All data represent means  $\pm$  SD from biological triplicates.

### *Levels of Phosphorylated Mnk1/2 in mTORC1 Inhibited Conditions*

Levels of phosphorylated Mnk1/2 and Z protein were measured using flow cytometric analysis. Mnk1/2 is a MAPK protein that becomes activated upon phosphorylation via ERK and p38. Upon phosphorylation, Mnk1/2 phosphorylates eIF4E, which is a protein that binds 5' caps of mRNA and aids in translation. Measuring phosphorylated Mnk1/2 levels in relation to Z protein expression provides insight into the pathways being utilized by EBV for protein translation and lytic replication.

No significant increases in relative total Z protein levels in epithelial cells were observed; however, the general trends of increase in Z protein levels in induced rapamycin treated conditions are observed as in other trials. Significant increases of total relative phosphorylated Mnk1/2 levels in epithelial cells were observed in conditions 3 and 4 relative to condition 1 ( $p < 0.05$ ) (Figure 22 A). Figure 22 B shows the percent totals of epithelial cells positive for phosphorylated Mnk1/2, Z protein, or both proteins simultaneous (double positive). No significant increases in percent of cells positive for Z protein were observed; however, the general trends of increase in Z protein expression in rapamycin treated induced cells are observed as in other trials (Figure 22 B). The percent of double positive cells for condition 4 are significantly increased in relation to condition 1 ( $p < 0.05$ ) (Figure 22 B). Approximately 45% of all lytic cells in conditions 3 and 4 are double positive for phosphorylated Mnk1/2 and Z protein (Figure 22 B). These results suggest that phosphorylated Mnk1/2 may correlate with increases in Z protein levels in lytic epithelial cells.

Significant increase in relative total Z protein levels were observed in B cells in condition 3 relative to condition 1 ( $p < 0.05$ ) (Figure 23 A). Trends of decrease in Z protein levels during induction and rapamycin treatment are observed as in other trials (Figure 23 A). Despite decreases in Z protein levels during rapamycin treatment, phosphorylated Mnk1/2 values remain constant (Figure 23 A). Figure 23 B shows the percent totals of B cells positive for phosphorylated Mnk1/2, Z protein, or both proteins simultaneous (double positive). Significant increases in percent of cells positive for Z protein were observed in condition 3 relative to condition 1 ( $p < 0.05$ ) (Figure 23 B). The percent of double positive cells for conditions 3 and 4 are significantly increased in relation to condition 1 ( $p < 0.05$ ) (Figure 23 B). Approximately 50% of remaining lytic cells in rapamycin treated condition 4 are double positive for phosphorylated Mnk1/2 and Z protein (Figure 23 B). These observations suggest that phosphorylated Mnk1/2 may correlate with Z protein levels in B cells that remain lytic despite rapamycin treatment and overall Z protein decreases.

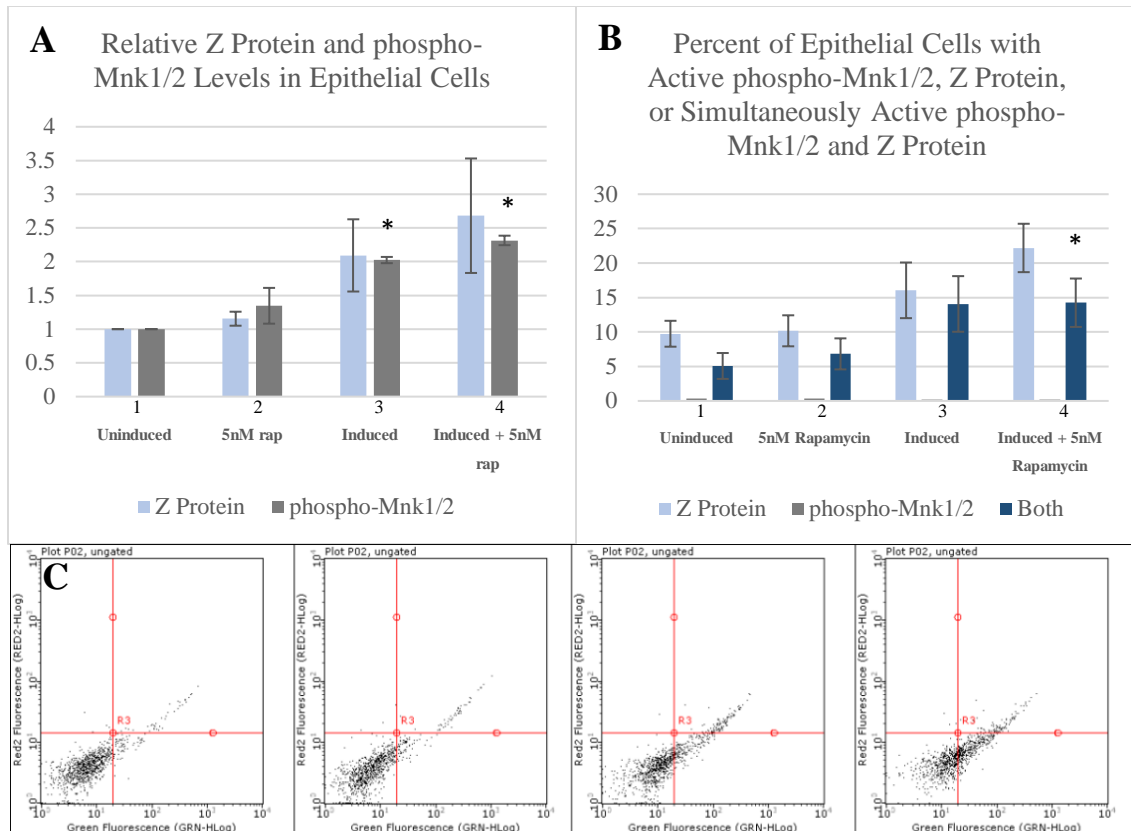


**Figure 22. Levels of Z Protein and phospho-Mnk1/2 in Epithelial Cells Across Treatment Conditions for mTORC1 Inhibition.** **A.** Epithelial cell Z and phospho-Mnk1/2 levels; phosphorylated Mnk1/2 level value significant for conditions 3 and 4 relative to conditions 1 and 2 ( $p < 0.05$ ). **B.** Percent of epithelial cells positive for Z, phospho-Mnk1/2, and double positive for Z and phospho-Mnk1/2; condition 4 double positive significant relative to condition 1 ( $p < 0.05$ ). **C.** Scatterplots showing percent of cells positive for Z, phospho-Mnk1/2, or double positive. All data represent means  $\pm$  SD from biological triplicates.

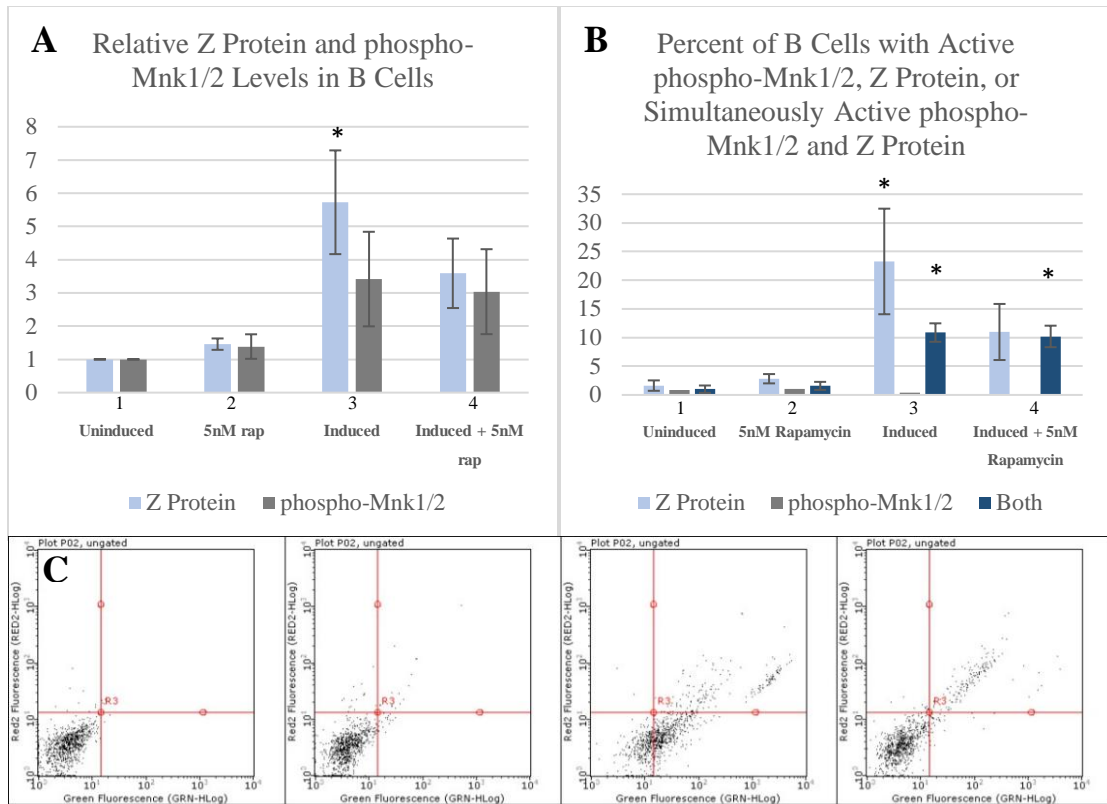


**Figure 23. Levels of Z Protein and phospho-Mnk1/2 in B Cells Across Treatment Conditions for mTORC1 Inhibition.** **A.** C cell Z and phospho-Mnk1/2 levels; Z protein level value significant for condition 3 relative to condition 1 ( $p < 0.05$ ). **B.** Percent of B cells positive for Z, phospho-Mnk1/2, and double positive for Z and phospho-Mnk1/2; conditions 3 and 4 double positive values significant relative to condition 1, percent Z protein positive cells in condition 3 significant relative to condition 1 ( $p < 0.05$ ). **C.** Scatterplots showing percent of cells positive for Z, phospho-Mnk1/2, or double positive. All data represent means  $\pm$  SD from biological triplicates.

### *Levels of Phosphorylated eIF4E in mTORC1 Inhibited Conditions*

Levels of phosphorylated eIF4E and Z protein were measured using flow cytometric analysis. eIF4E is a protein that becomes activated upon phosphorylation via Mnk1/2 and 4EBP1. Upon phosphorylation, eIF4E binds 5' caps of mRNA and aids in translation. Measuring phosphorylated eIF4E levels in relation to Z protein expression provides insight into the pathways being utilized by EBV for protein translation and lytic replication.

Significant increases in Z protein levels were observed in epithelial cells for conditions 2 and 4 relative to condition 1 ( $p < 0.05$ ) (Figure 24 A). The same general trends of increase in Z protein levels during lytic replication and rapamycin treatment are observed as in other trials. Significant increase in phosphorylated eIF4E level was observed in conditions 4 and 2 relative to condition 1 ( $p < 0.05$ ) (Figure 24 A). Figure 24 B shows the percent totals of epithelial cells positive for phosphorylated eIF4E, Z protein, or both proteins simultaneous (double positive). No significant increases in percent of cells positive for Z protein were observed but the overall trends of increase observed as with other trials are seen here (Figure 24 B). The percent of eIF4E and double positive cells appear to increase with Z protein levels. Approximately 60% of lytic cells in conditions 3 and 4 are double positive for phosphorylated eIF4E and Z protein (Figure 24 B). These observations suggest that phosphorylated eIF4E may correlate with Z protein levels in epithelial cells.

No significant levels of Z protein were observed in B cells, but the same general trends of increased Z protein under rapamycin treatment are observed as in other trials (Figure 25 A). It appears that phosphorylated eIF4E increases despite lowered levels of Z protein in condition 4 (Figure 25 A). Figure 25 B shows the percent totals of B cells positive for phosphorylated eIF4E, Z protein, or both proteins simultaneous (double positive). No significant values in percent of cells positive for Z protein were observed but the overall trends of decrease with rapamycin treatment are observed as with other trials are seen here (Figure 25 B). It appears that with decrease in Z protein phosphorylated eIF4E levels increase, particularly for cells that are double positive. In fact, approximately 71% of cells expressing Z protein are expressing phosphorylated-eIF4E as well (Figure 25 B). This suggest that phosphorylated eIF4E levels correlate to Z protein production in lytic B cells, despite rapamycin treatment and Z protein level decreases.

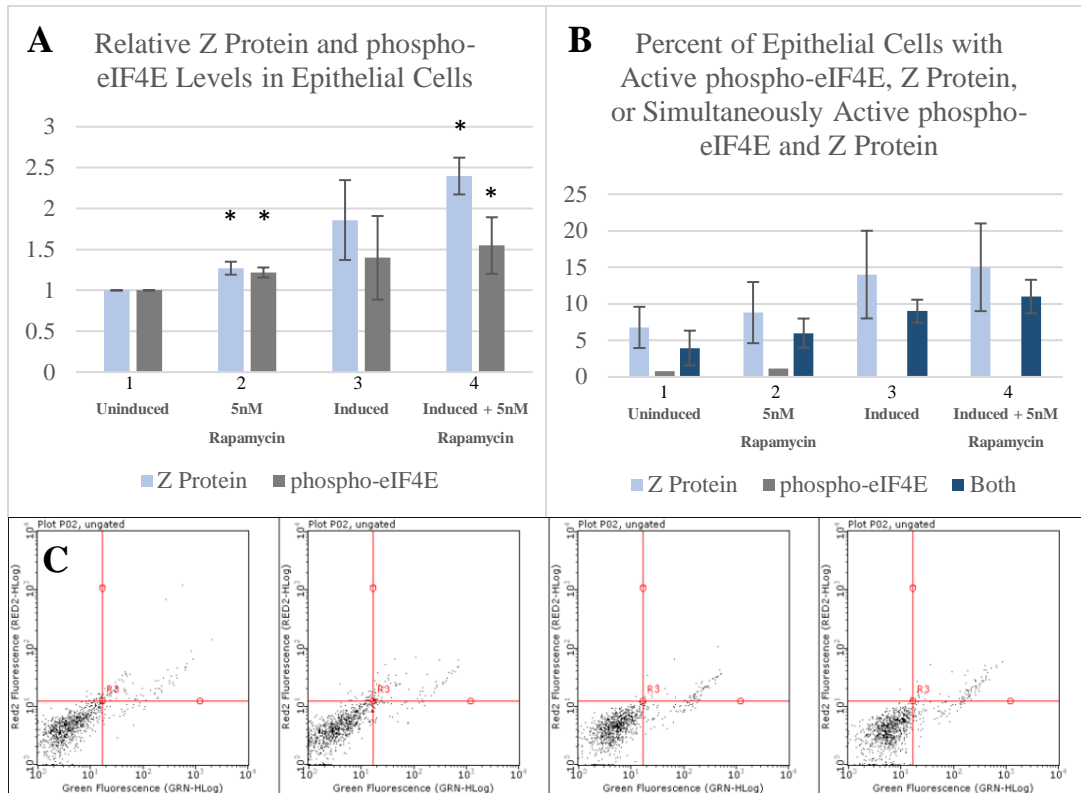


**Figure 24. Levels of Z Protein and phospho-eIF4E in Epithelial Cells Across Treatment Conditions for mTORC1 Inhibition.** **A.** Epithelial cell Z and phospho-eIF4E levels; phosphorylated eIF4E level value significant for conditions 2 and 4 relative to condition 1 ( $p < 0.05$ ). **B.** Percent of epithelial cells positive for Z, phospho-eIF4E, and double positive for Z and phospho-eIF4E. **C.** Scatterplots showing percent of cells positive for Z, phospho-eIF4E, or double positive. All data represent means  $\pm$  SD from biological triplicates.

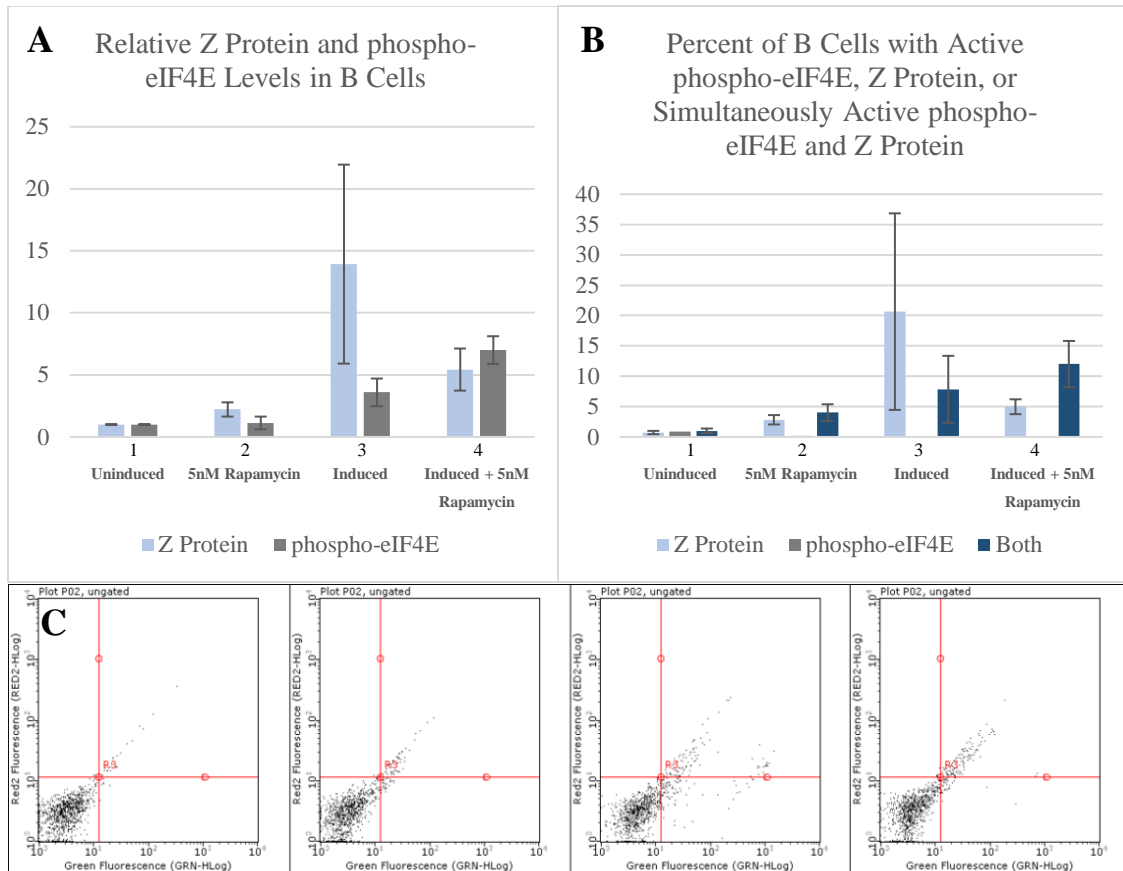


**Figure 25. Levels of Z Protein and phospho-eIF4E in B Cells Across Treatment Conditions for mTORC1 Inhibition.** **A.** B cell Z and phospho-eIF4E levels. **B.** Percent of B cells positive for Z, phospho-eIF4E, and double positive for Z and phospho-eIF4E. **C.** Scatterplots showing percent of cells positive for Z, phospho-eIF4E, or double positive. All data represent means  $\pm$  SD from biological triplicates.

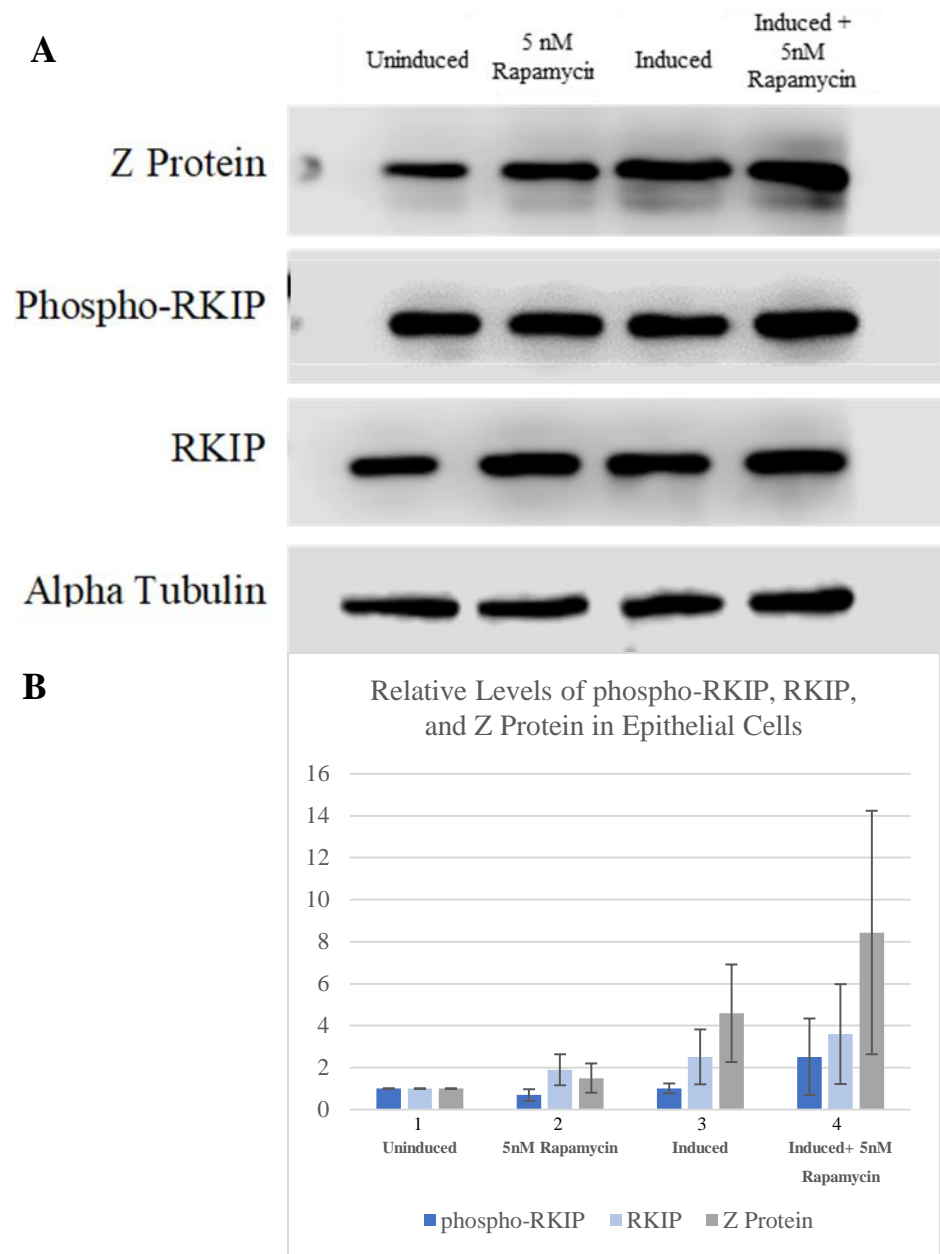
### *Levels of RKIP and Phosphorylated RKIP in mTORC1 Inhibited Conditions*

Levels of RKIP and phosphorylated RKIP along with Z protein were measured using western blot analysis. RKIP is an inhibitor of the MAPK protein ERK by binding to its upstream activator, Raf. Upon phosphorylation, RKIP loses its ability to inhibit Raf and becomes active as a modulator of other pathways such as the NF- $\kappa$ B and GPCR pathways. RKIP and phosphorylated RKIP's role in relation to EBV lytic replication is not well defined. Measuring RKIP and phosphorylated RKIP levels in relation to Z protein expression provides insight into the pathways being utilized by EBV for protein translation and lytic replication.

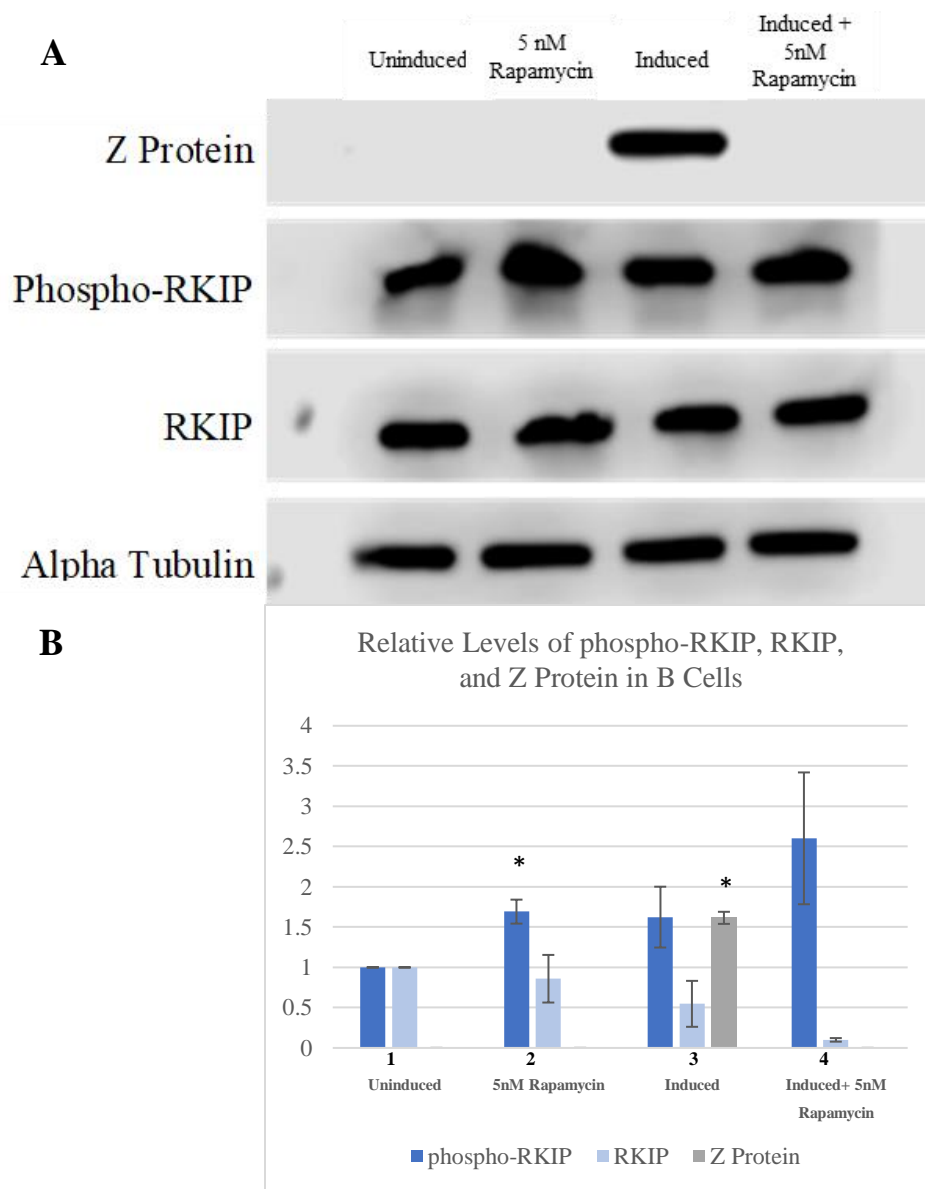
Figure 26 A shows the western blot image for phosphorylated RKIP, RKIP and Z protein in epithelial cells. There was no significant difference in observed levels of Z protein in epithelial cells amongst treatment conditions (Figure 26 B). There were trends of increased Z protein levels in lytic epithelial cells treated with rapamycin as in other trials. No significant variability in RKIP or phosphorylated RKIP was observed. It appears that RKIP and phosphorylated RKIP levels do not correspond to Z protein levels in epithelial cells, but further investigation may be necessary.

Figure 27 A shows the western blot image for phosphorylated RKIP, RKIP and Z protein in B cells. Z Protein levels were significantly increased in condition 3 relative to condition 1 ( $p < 0.05$ ) (Figure 27 B). No significant differences in RKIP were observed amongst conditions. Phosphorylated RKIP was significantly increased in condition 2 relative to condition 1 ( $p < 0.05$ ) (Figure 27 B). There are trends of increase in

phosphorylated RKIP levels in rapamycin treated condition 4. It is possible that phosphorylated RKIP plays a role in the observed response of EBV in B cells to rapamycin treatment; however, further investigation may be necessary.



**Figure 26. Western Blot Analysis for phospho-RKIP, RKIP and Z Protein Levels in Epithelial Cells Across Conditions for mTORC1 Inhibition. A.** Imaging for epithelial cell western blot analysis. **B.** Graphical representation of quantified protein bands. All data represent means  $\pm$  SD from biological triplicates.



**Figure 27. Western Blot Analysis for phospho-RKIP, RKIP, and Z Protein Levels in B Cells Across Conditions for mTORC1 Inhibition. A.** Imaging for B cell western blot analysis. **B.** Graphical representation of quantified protein bands; condition 2 phospho-RKIP values significant relative to condition 1 ( $p < 0.05$ ), condition 3 Z protein levels significant relevant to condition 1 ( $p < 0.05$ ). All data represent means  $\pm$  SD from biological triplicates.

*Levels of Z Protein and Phosphorylated TSC2 in mTORC1, MEK, and p38 Inhibited Conditions*

Levels of phosphorylated TSC2 and Z protein were measured using flow cytometric analysis. Upon phosphorylation, TSC2 loses its inhibitory function over Rheb-GTP, thereby allowing activation of mTORC1 downstream. TSC2 can be phosphorylated by AKT and ERK. Measuring phosphorylated TSC2 in relation to Z protein expression during mTORC1 and MAPK protein inhibition provides insight into the pathways being utilized by EBV for protein translation and lytic replication.

In epithelial cell trials for Z protein and phosphorylated TSC2 levels during mTORC1, MEK, and p38 inhibited conditions, significant decrease in Z protein level was observed in condition 5 relative to condition 1 and condition 11 relative to condition 10 ( $p < 0.05$ ) (Figure 28). While levels of Z protein and phosphorylated TSC2 levels showed trends of decrease in conditions 3 and 6 relative to condition 1, these trends were not statistically significant. Levels of Z protein and phosphorylated TSC2 increased across all other conditions with significant p-values ( $p < 0.05$ ) for conditions 8, 9, 10, 12, 13, 14, 15, and 16 relative to condition 1 ( $p < 0.05$ ) (Figure 28). In general, epithelial cell conditions treated with rapamycin increase in Z protein levels and phosphorylated TSC2 levels. It also appears that even though attenuation of EBV lytic replication is not possible with the use of the inhibitors, p38 seems to be the inhibitor treatment that provides the most drastic decrease in Z protein and phosphorylated TSC2 levels in

epithelial cells. This suggests EBV utilizes the p38 MAPK pathway in addition to the mTOR pathway in epithelial cells for translation of viral proteins.

In B cell trials for Z protein and phosphorylated TSC2 levels during mTORC1, MEK, and p38 inhibited conditions, significant decrease in Z protein level was observed in condition 3 relative to 2, and conditions 10, 11, and 12 relative to condition 9 ( $p < 0.05$ ) (Figure 29). Significant decrease in phosphorylated TSC2 level was observed in condition 5 relative to condition 1. Significant increase in Z protein levels was observed in conditions 6, 9, and 11 relative to condition 1 ( $p < 0.05$ ) (Figure 29). While not significant, trends of decrease in phosphorylated TSC2 levels were observed in conditions with MEK inhibitor, due to the inhibition of phosphorylation of TSC2. Rapamycin decreased Z protein levels just as in other trials, but the increases in phosphorylated TSC2 are observed just as in the mTORC1 inhibited trials. Combinations of multiple inhibitors in conditions 14, 15, and 16 increased Z protein levels and phosphorylated TSC2 (Figure 29). The mechanism by which EBV translates its proteins under these conditions is not known, as EBV requires cap-dependent translation for protein synthesis, and condition 16 blocks all the pathways. It appears the MEK inhibitor decreased Z protein levels in lytic B cells more than rapamycin treatment; and the MEK inhibitor treatment provided a significant decrease relative to the induced condition. This suggests that EBV uses the MAPK MEK and ERK pathway in B cells in addition to the mTORC1 pathway.

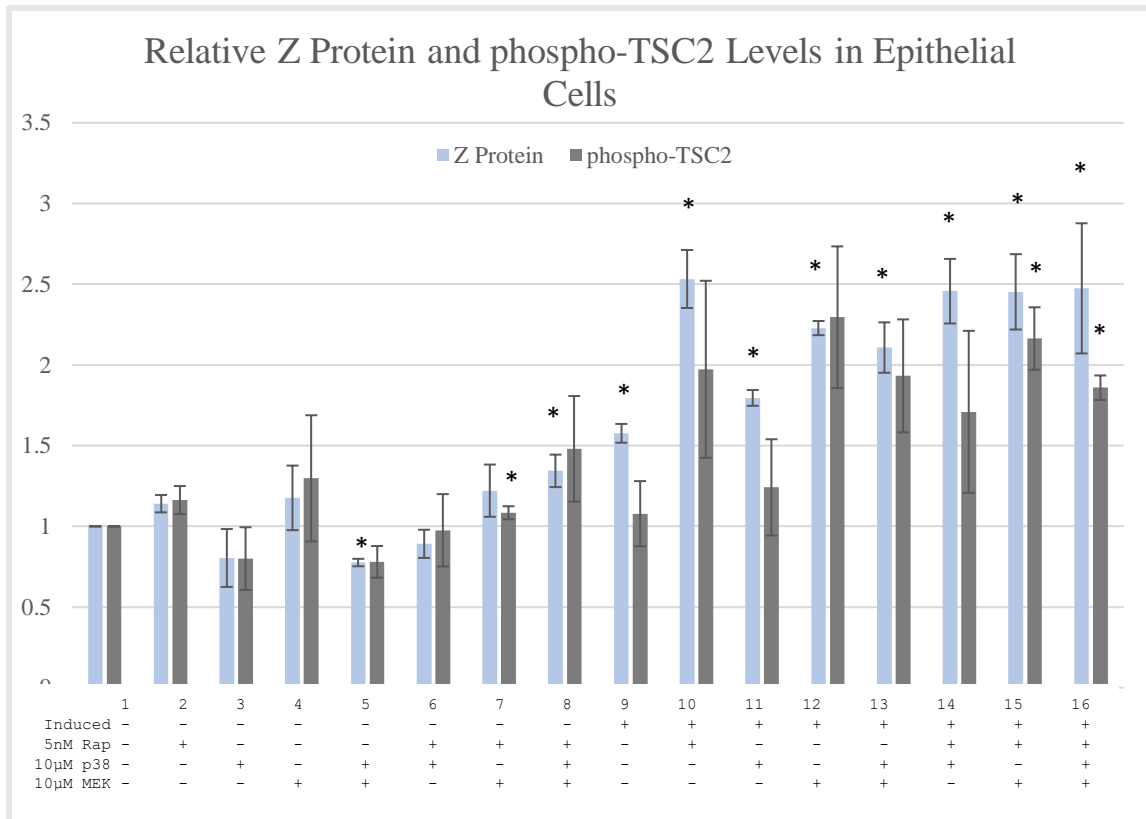


**Figure 28. Levels of Z Protein and phospho-TSC2 in Epithelial Cells Across Treatment Conditions for mTORC1, p38, and MEK Inhibition.** Epithelial cell Z and phospho-TSC2 levels. Significant decrease in Z protein levels observed in condition 5 relative to condition 1 and condition 11 relative to condition 10 ( $p < 0.05$ ). Significant increases in Z protein levels observed in conditions 8, 9, 10, 12, 13, 14, 15, and 16 relative to condition 1 ( $p < 0.05$ ). All data represent means  $\pm$  SD from biological triplicates.

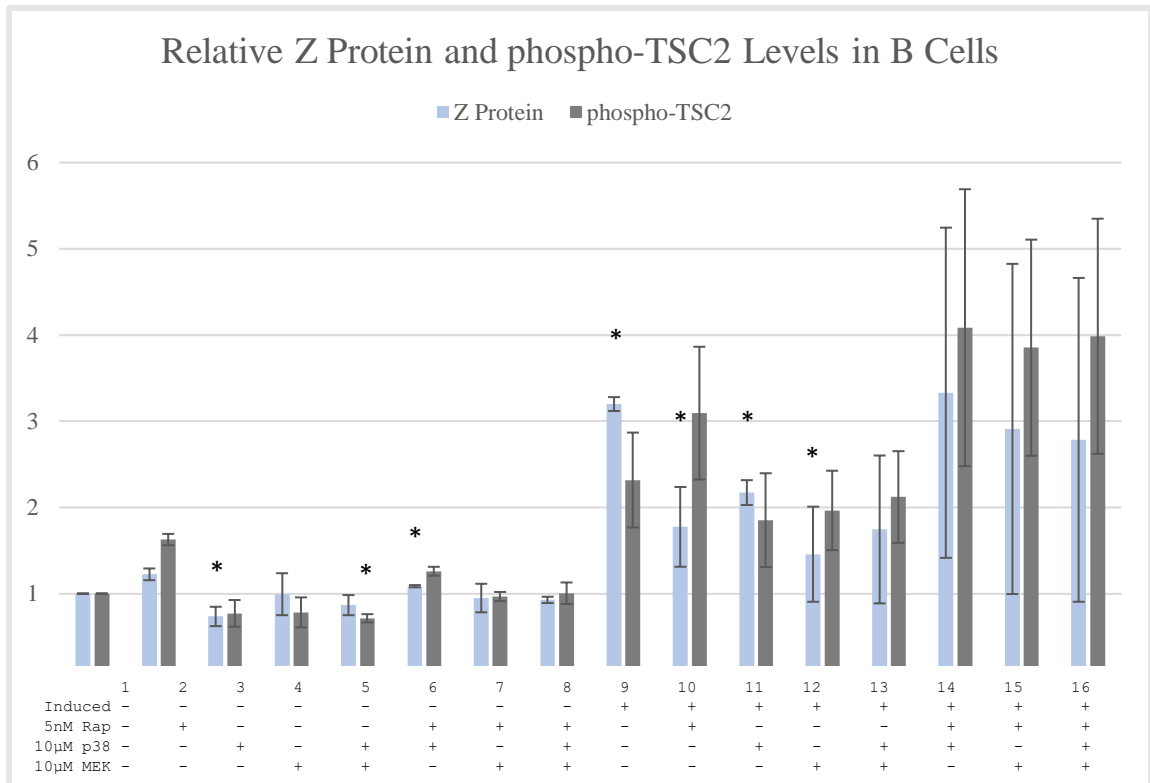


**Figure 29. Levels of Z Protein and phospho-TSC2 in B Cells Across Treatment Conditions for mTORC1, p38, and MEK Inhibition.** B cell Z and phospho-TSC2 levels. Significant decrease in Z protein levels observed in condition 3 relative to condition 2 and conditions 10, 11, and 12 relative to condition 9 ( $p < 0.05$ ). Significant increase in Z protein levels observed in conditions 6, 9, and 11 relative to condition 1 ( $p < 0.05$ ). Significant decrease in phospho-TSC2 levels observed in condition 5 relative to condition 1 ( $p < 0.05$ ). All data represent means  $\pm$  SD from biological triplicates.

*Levels of Z Protein and Phosphorylated mTOR in mTORC1, MEK, and p38 Inhibited Conditions*

Levels of phosphorylated mTOR and Z protein were measured using flow cytometric analysis. mTOR becomes activated downstream of Rheb-GTP when TSC2 becomes phosphorylated. TSC2 can be phosphorylated via Akt or ERK. Upon phosphorylation, mTOR will phosphorylate p70S6K and 4EBP1 which are involved in protein synthesis. Measuring phosphorylated mTOR in relation to Z protein expression during mTORC1 and MAPK protein inhibition provides insight into the pathways being utilized by EBV for protein translation and lytic replication.

The results for epithelial cell trials for Z protein and phosphorylated mTOR levels during mTORC1, MEK, and p38 inhibited conditions mirrors the results of phosphorylated TSC2 levels because TSC2 phosphorylates mTOR. Significant decreases in Z protein levels are observed in conditions 2 and 3 relative to condition 1, and condition 11 relative to condition 10 ( $p < 0.05$ ) (Figure 30). Significant increases in Z protein levels are observed in conditions 10, 12, 13, 14, 15, and 16 relative to condition 1 ( $p < 0.05$ ) (Figure 30). Amongst all other conditions, there were no significant observed decreases in Z protein levels. Observed levels of phosphorylated mTOR were significantly decreased in condition 2 relative to condition 1 ( $p < 0.05$ ) (Figure 30). Amongst all other conditions, there were no significantly lowered levels of phosphorylated mTOR. Inhibitor combinations in conditions 12, 13, 14, 15, and 16 triggered increased Z protein expression for reasons not understood (Figure 30). For this

data set, it appears that p38 inhibition attenuates viral lytic replication the most effectively, which suggests that EBV uses the p38 MAPK pathway in addition to the mTOR pathway for translation of viral proteins.

The results for B cell trials for Z protein and phosphorylated mTOR levels during mTORC1, MEK, and p38 inhibited conditions mirror the results for phosphorylated TSC2 trial because TSC2 phosphorylates mTOR. Statistically significant increase in Z protein levels were observed in conditions 11 and 14 relative to condition 1 ( $p < 0.05$ ) (Figure 31). Statistically significant increases in phosphorylated mTOR levels were observed in conditions 2, 6, 7, 9, 10, 11, 14, and 15 relative to condition 1 ( $p < 0.05$ ) (Figure 31). While no statistically significant decrease in Z protein level was observed, there are trends of decrease in conditions 12 and 13 (Figure 31). Rapamycin decreased Z protein levels just as in other trials, but the increases in phosphorylated mTOR are observed just as in the mTORC1 inhibited trials. Combinations of multiple inhibitors in conditions 14, 15, and 16 increased Z protein levels and phosphorylated mTOR (Figure 31). The mechanism by which EBV translates its proteins under these conditions is not known, as EBV requires cap-dependent translation for protein synthesis, and condition 16 blocks all pathways. It appears the p38 and MEK inhibitors decreased Z protein levels in lytic B cells more than rapamycin treatment; this suggests that EBV uses the MAPKs p38 and ERK pathways in addition to the mTORC1 pathway. The MEK inhibitor was most effective at attenuating Z protein in B cells, suggesting MEK may be the more predominate route of EBV for protein translation and replication in B cells.

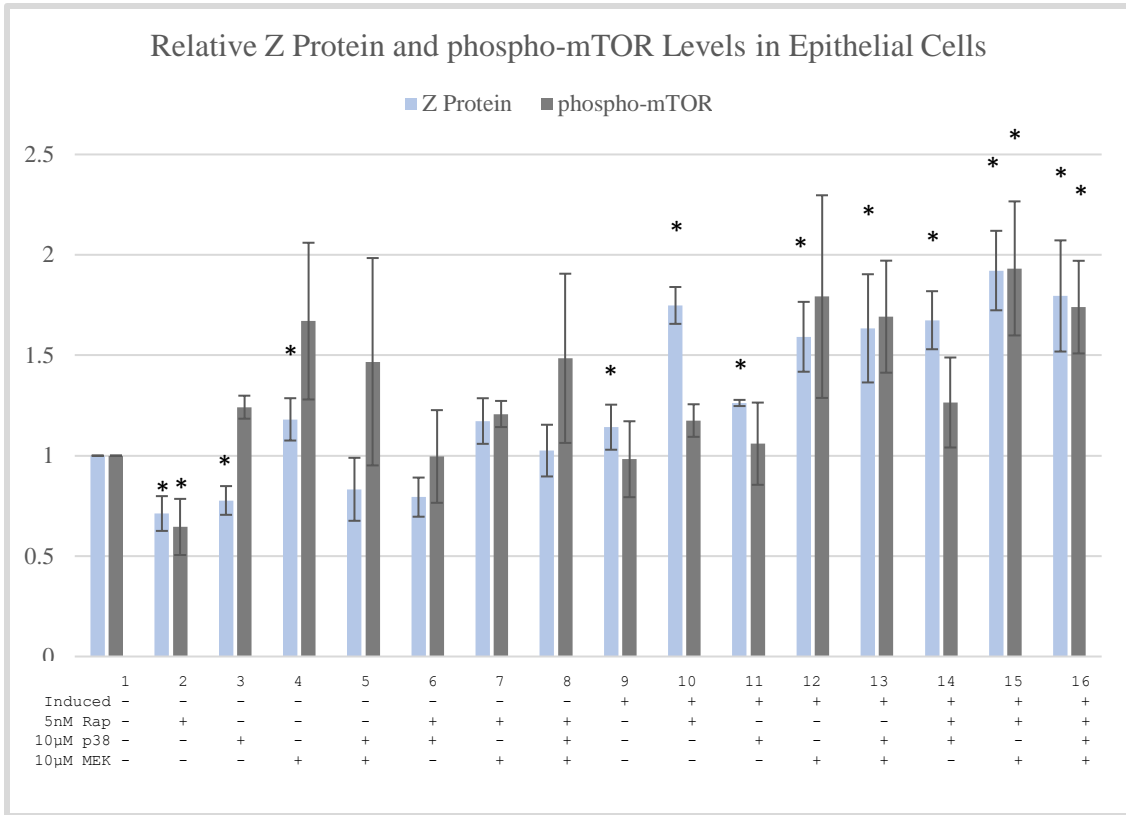


**Figure 30. Levels of Z Protein and phospho-mTOR in Epithelial Cells Across Treatment Conditions for mTORC1, p38, and MEK Inhibition.** Epithelial cell Z and phospho-mTOR levels. Significant decreases in Z protein levels observed in conditions 2 and 3 relative to condition 1 and condition 11 relative to condition 10 ( $p < 0.05$ ). Significant increases in Z protein levels observed in conditions 10, 12, 13, 14, 15, and 16 relative to condition 1 ( $p < 0.05$ ). Significant decrease in phospho-mTOR level observed in condition 2 relative to condition 1 ( $p < 0.05$ ). All data represent means  $\pm$  SD from biological triplicates.

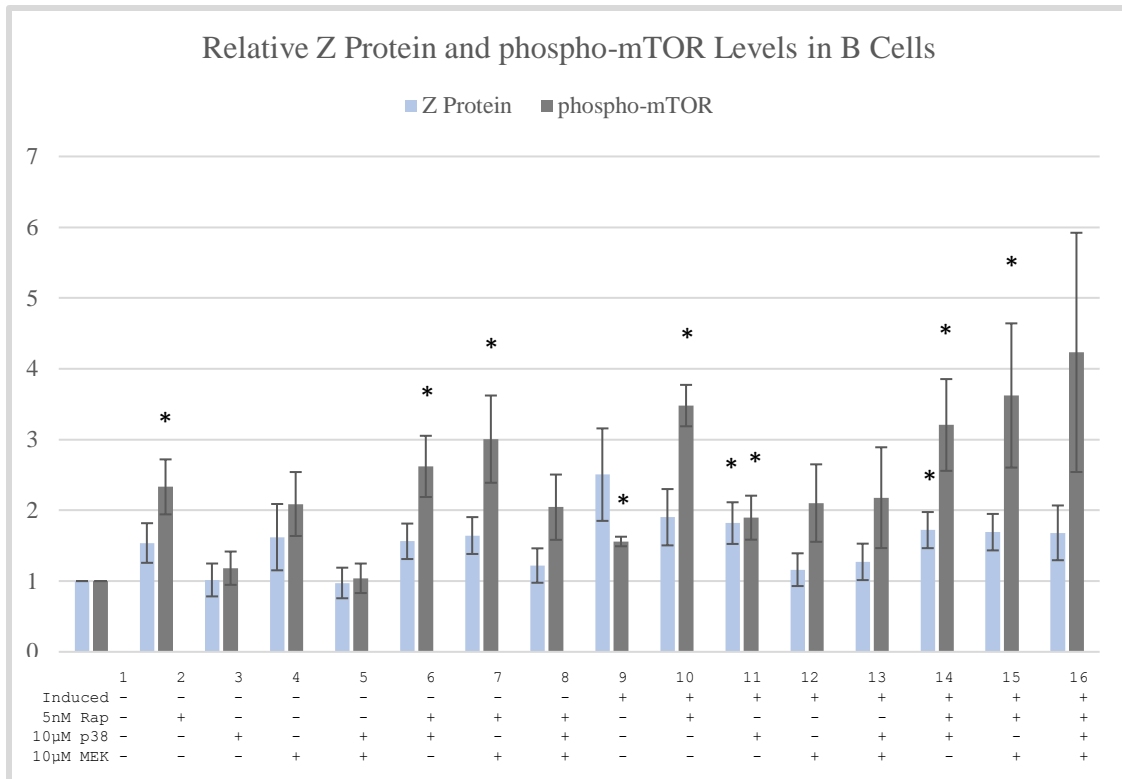


**Figure 31. Levels of Z Protein and phospho-mTOR in B Cells Across Treatment Conditions for mTORC1, p38, and MEK Inhibition.** B cell Z and phospho-mTOR levels. Significant increase in Z protein levels were observed in conditions 11 and 14 relative to condition 1 ( $p < 0.05$ ). Significant increase in phospho-mTOR levels were observed in conditions 2, 6, 7, 9, 10, 11, 14, and 15 relative to condition 1 ( $p < 0.05$ ). All data represent means  $\pm$  SD from biological triplicates.

*Levels of Z Protein and Phosphorylated ERK in mTORC1, MEK, and p38 Inhibited Conditions*

Levels of phosphorylated ERK and Z protein were measured using flow cytometric analysis. Upon phosphorylation, ERK phosphorylates TSC2 and Mnk1/2, which in turn go on to activate proteins involved in cap-dependent translation and protein synthesis. Measuring phosphorylated ERK in relation to Z protein expression during mTORC1 and MAPK protein inhibition provides insight into the pathways being utilized by EBV for protein translation and lytic replication.

In epithelial cell trials for Z protein and phosphorylated ERK levels during mTORC1, MEK, and p38 inhibited conditions, no significant decreases in Z protein levels are observed. Significant increases in Z protein levels are observed in conditions 10, 11, 12, 13, 14, 15, and 16 relative to condition 1 ( $p < 0.05$ ) (Figure 32). Decrease in Z protein levels were observed in condition 11 relative to condition 10. Levels of phosphorylated ERK were not significantly altered by use of inhibitors, but a trend of decrease was observed in the MEK inhibited condition 12. Trends of Z protein decrease were most extensive in the p38 inhibited condition 11 (Figure 32). These data suggest EBV use of p38 for Z protein production in addition to the mTOR pathway in epithelial cells.

In B cell trials for Z protein and phosphorylated ERK levels during mTORC1, MEK, and p38 inhibition, Z protein levels were not significantly decreased amongst any of the conditions. Significant increases in Z protein levels were observed in conditions 9,

10, 11, 12, 14, 15, and 16 relative to condition 1 ( $p < 0.05$ ) (Figure 33). Levels of phosphorylated ERK were not significantly decreased amongst any of the conditions, but trends of decrease were seen in conditions 11, 12, and 13 (Figure 33). The MEK inhibitor treatment in condition 12 decreased Z protein levels most drastically. This suggests the use of the MEK/ERK MAPK pathways for lytic replication in B cells.

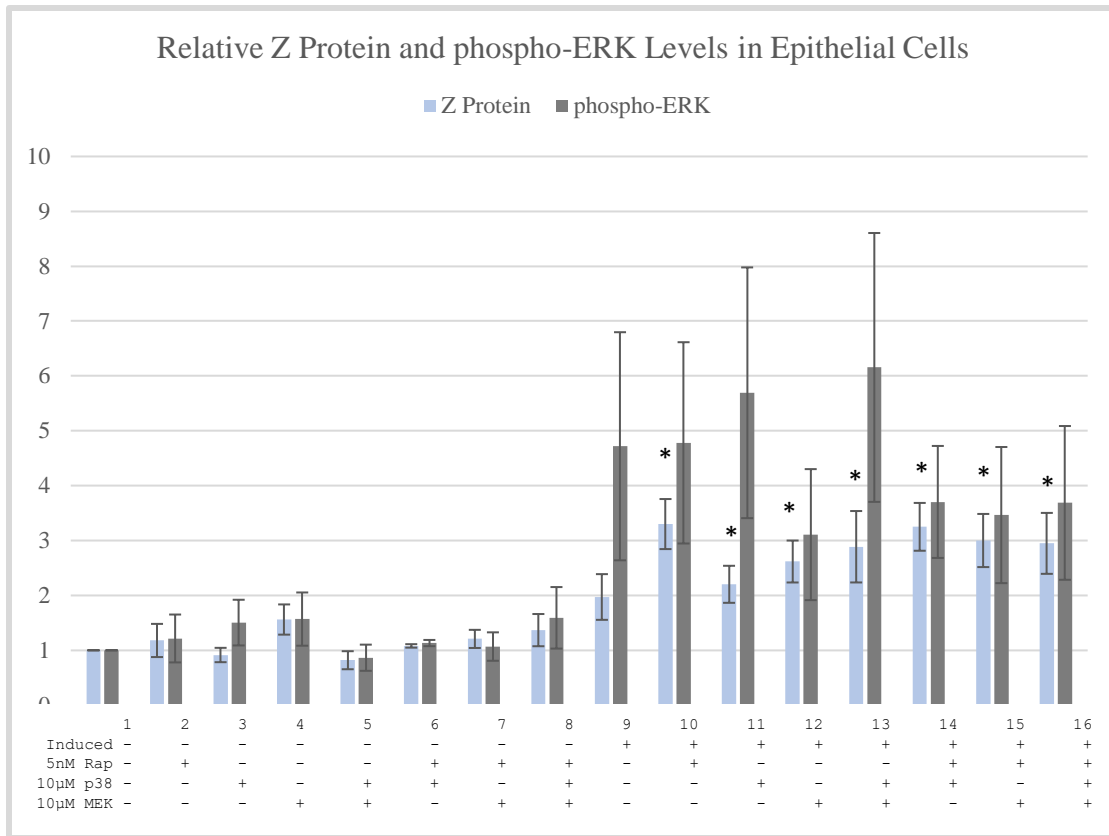


**Figure 32. Levels of Z Protein and phospho-ERK in Epithelial Cells Across Treatment Conditions for mTORC1, p38, and MEK Inhibition.** Epithelial cell Z and phospho-ERK levels. Significant increase in Z protein levels observed in conditions 10, 11, 12, 13, 14, 15, and 16 relative to condition 1 ( $p < 0.05$ ). All data represent means  $\pm$  SD from biological triplicates.

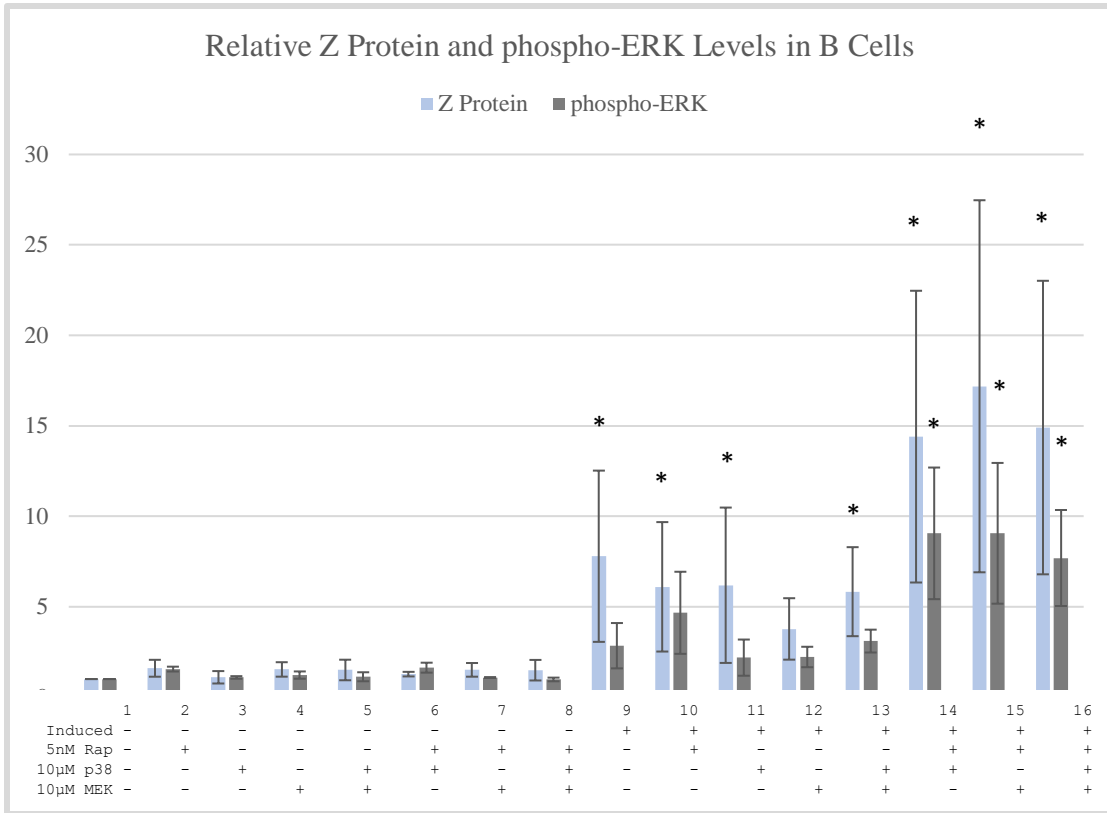


**Figure 33. Levels of Z Protein and phospho-ERK in B Cells Across Treatment Conditions for mTORC1, p38, and MEK Inhibition.** B cell Z and phospho-ERK levels. Significant increase in Z protein levels observed in conditions 9, 10, 11, 12, 14, 15, and 16 relative to condition 1 ( $p < 0.05$ ). All data represent means  $\pm$  SD from biological triplicates.

*Levels of Z Protein and Phosphorylated Mnk1/2 in mTORC1, MEK, and p38 Inhibited Conditions*

Levels of phosphorylated Mnk1/2 and Z protein were measured using flow cytometric analysis. Mnk1/2 is a MAPK protein that becomes activated upon phosphorylation via ERK and p38. Upon phosphorylation, Mnk1/2 phosphorylates eIF4E, which is a protein that binds 5' caps of mRNA and aids in translation. Measuring phosphorylated Mnk1/2 levels in relation to Z protein expression provides insight into the pathways being utilized by EBV for protein translation and lytic replication.

In epithelial cell trials for Z protein and phosphorylated Mnk1/2 levels during mTORC1, MEK, and p38 inhibited conditions, no significant decreases in Z protein levels were observed. Significant increases in Z protein levels are observed in conditions 7, 9, 10, 12, 14, 15, and 16 relative to condition 1 ( $p < 0.05$ ) (Figure 34). Significant increases in levels of phosphorylated Mnk1/2 were observed in conditions 12, 15, and a6 ( $p < 0.05$ ) (Figure 34). A trend of decrease in Z protein and phosphorylated Mnk1/2 was observed in the p38 inhibited condition 11 (Figure 34). This suggests EBV uses the p38 MAPK pathway for Z protein production in addition to the mTOR pathway in epithelial cells.

In B cell trials for Z protein and phosphorylated Mnk1/2 levels during mTORC1, MEK, and p38 inhibited conditions observed levels of Z protein were significantly decreased in condition 3 relative to condition 2, conditions 12, 13, 14, 15, and 16 relative to condition 9, and conditions 12, 13, 14, 15, and 16 relative to condition 11 ( $p < 0.05$ )

(Figure 35). Significant increase in Z protein levels were observed in conditions 6, 7, 8, 9, and 11 relative to condition 1 ( $p < 0.05$ ) (Figure 35). Levels of phosphorylated Mnk1/2 were significantly decreased in condition 13 relative to condition 10 ( $p < 0.05$ ) (Figure 35). Levels of phosphorylated Mnk1/2 were significantly increased in conditions 9, 10, 11, 12, 13, 14, 15, 16 relative to condition 1 ( $p < 0.05$ ). It appears conditions 12 and 13 with MEK and p38 inhibitors most drastically inhibits Z protein and phosphorylated Mnk1/2 levels in these trials. These data suggest EBV utilizes p38 and MEK MAPKs for protein translation and lytic replication in addition to mTOR in B cells.

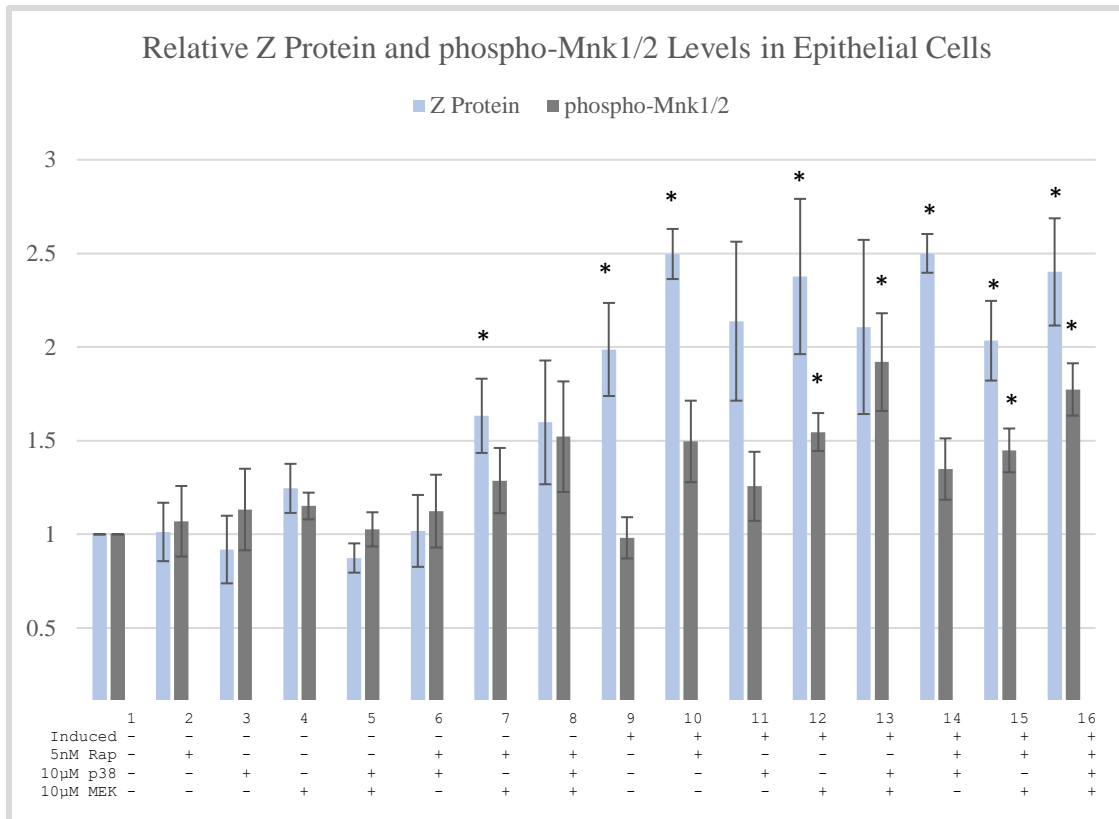


**Figure 34. Levels of Z Protein and phospho-Mnk1/2 in Epithelial Cells Across Treatment Conditions for mTORC1, p38, and MEK Inhibition.** Epithelial cell Z and phospho-Mnk1/2 levels. Significant increases in Z protein levels observed in conditions 7, 9, 10, 12, 14, 15, and 16 relative to condition 1 ( $p < 0.05$ ). Significant increase in levels of phospho-Mnk1/2 observed in conditions 12, 15, and 16 ( $p < 0.05$ ). All data represent means  $\pm$  SD from biological triplicates.

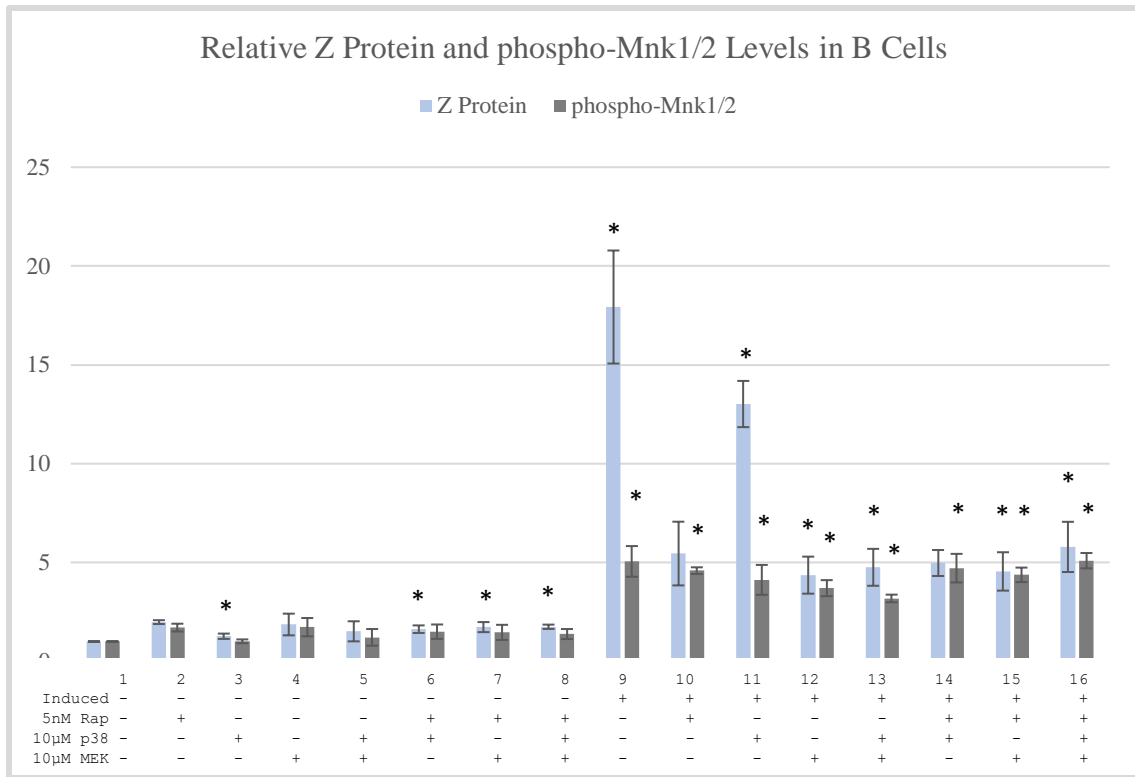


**Figure 35. Levels of Z Protein and phospho-Mnk1/2 in B Cells Across Treatment Conditions for mTORC1, p38, and MEK Inhibition.** B cell Z and phospho-Mnk1/2 levels. Significant increase in Z protein level observed in conditions 9 and 11 relative to condition 1 ( $p < 0.05$ ). Significant decrease in Z protein level observed in condition 3 relative to condition 2, conditions 12, 13, 14, 15, and 16 relative to condition 9, and conditions 12, 13, 14, 15, and 16 relative to condition 11 ( $p < 0.05$ ). Significant increase in Z protein levels observed in conditions 6, 7, 8, 9, and 11 relative to condition 1 ( $p < 0.05$ ). Significant increase in phospho-Mnk1/2 observed in conditions 9, 10, 11, 12, 13, 14, 15, 16 relative to condition 1 ( $p < 0.05$ ). Significant decrease in phospho-Mnk1/2 levels observed in condition 13 relative to condition 10 ( $p < 0.05$ ). All data represent means  $\pm$  SD from biological triplicates.

*Levels of Z Protein and Phosphorylated eIF4E in mTORC1, MEK, and p38 Inhibited Conditions*

Levels of phosphorylated eIF4E and Z protein were measured using flow cytometric analysis. eIF4E is a protein that becomes activated upon phosphorylation via Mnk1/2 and 4EBP1. Upon phosphorylation, eIF4E binds 5' caps of mRNA and aids in translation. Measuring phosphorylated eIF4E levels in relation to Z protein expression provides insight into the pathways being utilized by EBV for protein translation and lytic replication.

In epithelial cell trials for Z protein and phosphorylated eIF4E levels during mTORC1, MEK, and p38 inhibited conditions no significant decreases in Z protein levels were observed amongst conditions. Significant increases in Z protein levels were observed in conditions 4, 7, 9, 10, 11, 12, 13, 14, 15, and 16 relative to condition 1 ( $p < 0.05$ ) (Figure 36). No significant decreases in phosphorylated eIF4E levels were observed. Significant increases in phosphorylated eIF4E were observed in conditions 7, 8, 15, and 16 relative to condition 1 ( $p < 0.05$ ) (Figure 36). The most extensive decrease in Z protein and phosphorylated eIF4E levels was observed in the p38 inhibited condition 11 (Figure 36). This suggests EBV utilizes the p38 MAPK pathways for lytic replication in addition to the mTOR pathway.

In B cell trials for Z protein and phosphorylated eIF4E levels during mTORC1, MEK, and p38 inhibited conditions no significant decreases in Z protein levels were observed. Significant increases in Z protein levels were observed in conditions 9, 10, 11,

12, and, 14 relative to condition 1 ( $p < 0.05$ ) (Figure 37). The same general trends of Z protein decrease with rapamycin treatment of lytic B cells is observed as in other trials. Significant increase in phosphorylated eIF4E levels were observed in conditions 10, 11, 14, 15, and 16 relative to condition 1 ( $p < 0.05$ ) (Figure 37). The most drastic inhibition regarding both Z protein levels and phosphorylated eIF4E was the MEK inhibitor in condition 13. This suggests EBV utilizes MEK in the MAPK pathway in addition to mTORC1 in B cells, and that EBV lytic replication is dependent on phosphorylated eIF4E.

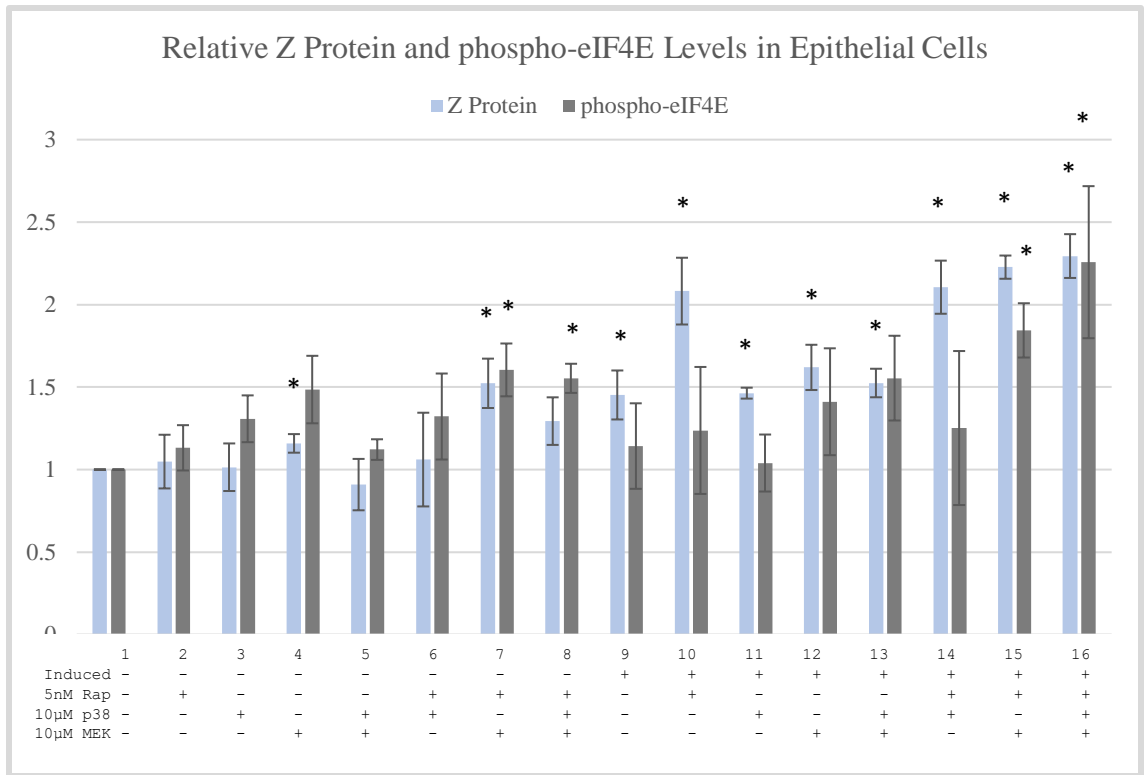


**Figure 36. Levels of Z Protein and phospho-eIF4E in Epithelial Cells Across Treatment Conditions for mTORC1, p38, and MEK Inhibition.** Epithelial cell Z and phospho-eIF4E levels. Significant increase in Z protein levels observed in conditions 4, 7, 9, 10, 11, 12, 13, 14, 15, and 16 relative to condition 1 ( $p < 0.05$ ). Significant increase in phospho-eIF4E observed in conditions 7, 8, 15, and 16 relative to condition 1 ( $p < 0.05$ ). All data represent means  $\pm$  SD from biological triplicates.

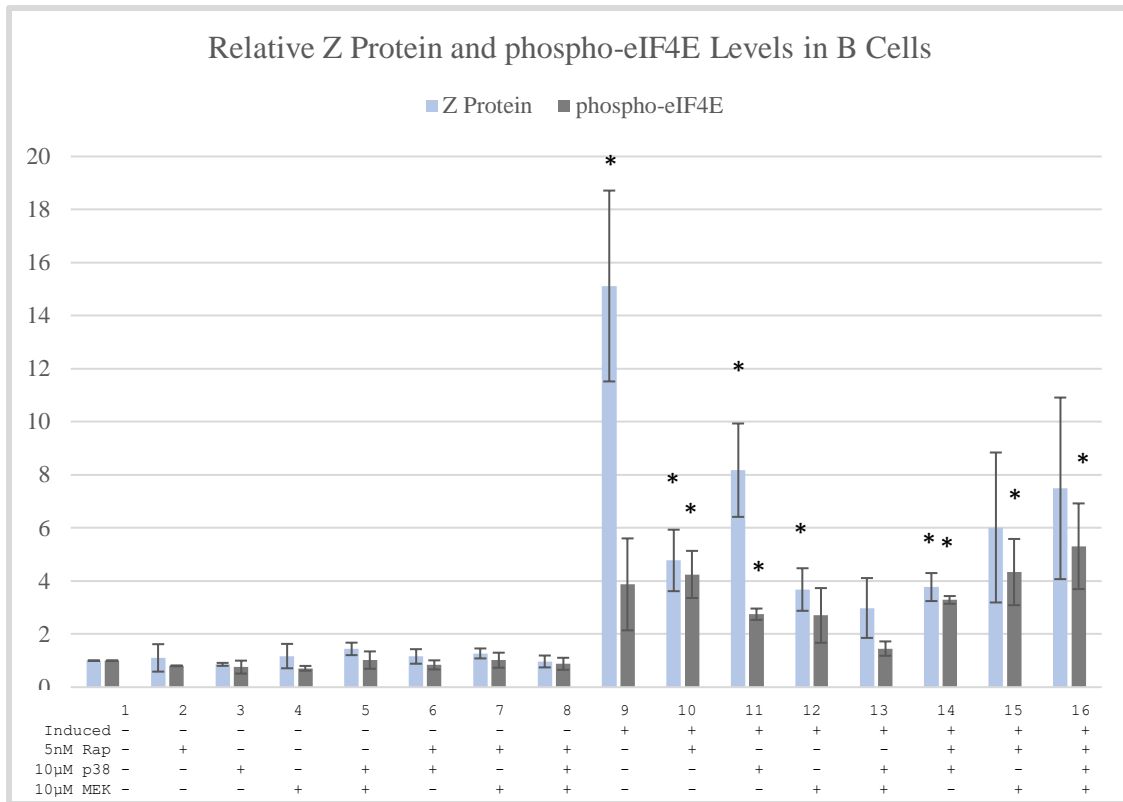


**Figure 37. Levels of Z Protein and phospho-eIF4E in B Cells Across Treatment Conditions for mTORC1, p38, and MEK Inhibition.** B cell Z and phospho-eIF4E levels. Significant increase in Z protein levels observed in conditions 9, 10, 11, 12, and, 14 relative to condition 1 ( $p < 0.05$ ). Significant increase in phospho-eIF4E levels observed in conditions 10, 11, 14, 15, and 16 relative to condition 1 ( $p < 0.05$ ). All data represent means  $\pm$  SD from biological triplicates.

## CHAPTER IV

### DISCUSSION

The PI3K-Akt-mTOR and MAPK pathways are major pathways used by eukaryotic cells to integrate various environmental and nutritional signals for cell growth, metabolism, and protein synthesis. It is well established that EBV, and all other DNA viruses, utilize host cellular cap-dependent translational machinery to produce viral gene products. Based on previous studies, it is known that EBV lytic replication varies amongst B cells and epithelial cells when mTORC1 in the PI3K-Akt-mTOR pathway is inhibited with rapamycin. Levels of Z protein, an immediate early lytic protein, decrease in B cells during rapamycin treatment. Despite rapamycin treatment in epithelial cells, levels of Z protein increase. Based on this knowledge, this study aimed to investigate the cell-type specific responses of EBV protein production during inhibition of the mTORC1 complex. Phosphorylated protein levels within the PI3K-Akt-mTOR and MAPK pathways were analyzed during inhibition of the mTORC1 complex, as well as during inhibition of the MAPK proteins MEK and p38. Flow cytometric and western-blot analyses were conducted to investigate levels of phosphorylated proteins within these pathways in relation to Z protein levels.

Levels of phosphorylated Akt, AMPK, and TSC2 proteins in the PI3K-Akt-mTOR pathways were found to be invariable during EBV lytic replication and rapamycin

treatment in epithelial cells (Figures 6, 8, 10). Levels of phosphorylated 4EBP1 in the PI3K-Akt-mTOR pathway significantly decreased during lytic induction of epithelial cells and remained at low levels during rapamycin treatment, despite increase in Z protein levels (Figure 16). These data suggest that the mechanism by which EBV produces lytic gene product, Z, may not heavily involve phosphorylated Akt, AMPK, TSC2, or 4EBP1 in the PI3K-Akt-mTOR pathway. Activation of these proteins does not appear to be related to the increases in Z protein levels observed during lytic replication and rapamycin treatment in epithelial cells. Levels of phosphorylated mTOR, and p70S6K in the PI3K-Akt-mTOR pathway, as well as p38, ERK, and Mnk1/2 in the MAPK pathways, appear to increase during EBV lytic replication in epithelial cells (Figures 12, 14, 18, 20, and 22). These data suggest that the mechanism by which EBV produces lytic gene product, Z, may involve phosphorylated mTOR, p70S6K, p38, and Mnk1/2 during lytic replication in epithelial cells. Activation of these proteins appears to increase as Z protein levels increase during lytic replication and rapamycin treatment in epithelial cells. These data suggest activation of these proteins may be involved in the cell-type specific response observed with rapamycin treatment in epithelial cells. The common target protein of the PI3K-Akt-mTOR and MAPK pathways, eIF4E, appears to increase in phosphorylation during lytic replication and rapamycin treatment in epithelial cells (Figure 24). This is the protein that binds 5' cap of mRNA, and thus appears to be related to Z protein expression levels during lytic replication. Increase in levels of

phosphorylated eIF4E appear to relate to increases in Z protein levels during rapamycin treatment of lytic epithelial cells.

In the epithelial cell treatments of MEK, p38, and mTORC1 inhibition, it appears the p38 inhibitor provides the most drastic decrease in Z protein levels during lytic replication (Figures 28, 30, 32, 34, and 36). These data suggest p38 may play a role in Z protein levels observed during lytic replication of EBV in epithelial cells. It is possible that EBV in epithelial cells is more heavily reliant on p38 activation for lytic replication and synthesis of viral gene products. Also, it was observed that lytic replication cannot be attenuated with blockage of the pathways that lead to activation of eIF4E and cap-dependent translation. Furthermore, the conditions that included rapamycin treatment showed increases in Z protein levels, despite being treated with MEK and p38 inhibitor combinations. This suggests that lytic replication and synthesis of viral gene products during mTORC1 inhibition can continue, and even increase, despite blockage of alternative MAPK pathways. The underlying mechanism by which this occurs remains to be elucidated.

Figure 38 shows the proposed predominant pathways utilized by EBV in epithelial cells. Based on the experimental data, it appears EBV utilizes the MAPK proteins p38 and MEK during lytic replication. It appears that Z protein level increases during rapamycin treatment in epithelial cells may correspond to levels of phosphorylated proteins in the MAPK pathways; p38, MEK, ERK, and Mnk1/2, to activate the common downstream target of the MAPK and PI3K-Akt-mTOR pathways, eIF4E.

RKIP and phosphorylated RKIP levels do not appear to be drastically influenced by lytic replication and rapamycin treatment in epithelial cells (Figure 26). Levels of these proteins do not appear to correspond to levels of Z protein. In B cells, however, it appears that phosphorylated RKIP levels increase during lytic replication and even during rapamycin treatment in B cells (Figure 27). It is possible that levels of phosphorylated RKIP may play a role in the Z protein levels observed in lytic B cells that remain after rapamycin treatment. A better understanding of the relationship between RKIP and phosphorylated RKIP with Z protein expression could be developed with further experimental investigation. Coimmunoprecipitation studies could assist in identifying how much RKIP is bound to Raf in epithelial cells and B cells during the cell-type specific responses identified during lytic replication and rapamycin treatment. Also, treatment of epithelial cells and B cells with RKIP siRNA could shed light on RKIP's role in EBV lytic replication mechanisms and the observed cell-type specific responses.

It appears that EBV in B cells utilizes a more broad-range approach to activation of eIF4E. Levels of phosphorylated Akt, TSC2, mTOR, p70S6K, and 4EBP1 in the PI3K-Akt-mTOR pathway appear to increase with lytic replication of EBV in B cells. (Figures 7, 11, 13, 15, 17). Despite Z protein level decrease in B cells during rapamycin treatment, the phosphorylated levels of these proteins remain constant or even increase. These data suggest these proteins may play a role in B cells that are still lytic and expressing Z protein despite rapamycin treatment. Levels of phosphorylated AMPK decrease in B cells with rapamycin treatment (Figure 9). Because AMPK is a stress-

responsive negative regulator in the PI3K-Akt-mTOR pathway, these data suggest a role of phosphorylated AMPK in the cell-type specific response of observed decreases in Z protein levels with rapamycin treatment in B cells. In addition to proteins in the PI3K-Akt-mTOR pathway, it appears EBV utilizes MAPK proteins in B cells for lytic replication and synthesis of lytic proteins. Levels of phosphorylated p38, ERK, and Mnk1/2 increase during lytic replication of EBV in B cells (Figures 19, 21, and 23). Levels of these phosphorylated proteins remain constant or even increase during rapamycin treatment, suggesting phosphorylation of these proteins may correspond to levels of Z protein and cells that remain lytic despite rapamycin treatment. The common target protein of the PI3K-Akt-mTOR and MAPK pathways, eIF4E, appears to increase in phosphorylation during lytic replication and rapamycin treatment in B cells (Figure 25). This is the protein that binds 5' cap of mRNA, and thus appears to be related to Z protein expression levels during lytic replication. Increase in levels of phosphorylated eIF4E appear to relate to Z protein levels during lytic replication in B cells, as well as during rapamycin treatment. While rapamycin decreases total lytic Z protein levels in B cells, it does not fully attenuate viral lytic replication. It appears the remaining refractory lytic cells are still producing Z protein due to the abundant activation of these proteins in the PI3K-Akt-mTOR and MAPK pathways.

In the B cell treatments of MEK, p38, and mTORC1 inhibition, it appears the MEK inhibitor provides the most drastic decrease in Z protein levels during lytic replication (Figures 29, 31, 33, 35, and 37). These data suggest MEK may play a role in

Z protein levels observed during lytic replication of EBV in B cells. It was also observed that lytic replication cannot be attenuated with blockage of the pathways that lead to activation of eIF4E and cap-dependent translation. In fact, conditions that combined inhibitors produced increases in Z protein levels during lytic replication. The underlying mechanism by which this occurs remains to be elucidated.

Figure 38 shows the proposed predominant pathways utilized by EBV in B cells. Based on the experimental data, it appears EBV utilizes a very broad range of proteins within the PI3K-Akt-mTOR and MAPK pathways in B cells during lytic replication. It appears that increases in phosphorylated AMPK may play a role in the cell-type specific response of EBV to mTORC1 inhibition in B cells. It also appears that Z protein level increases despite rapamycin treatment in B cells may correspond to levels of phosphorylated proteins in the PI3K-Akt-mTOR and MAPK pathways; Akt, TSC2, mTOR, p70S6K, 4EBP1, p38, MEK, ERK, and Mnk1/2, to activate the common downstream target of the MAPK and PI3K-Akt-mTOR pathways, eIF4E.

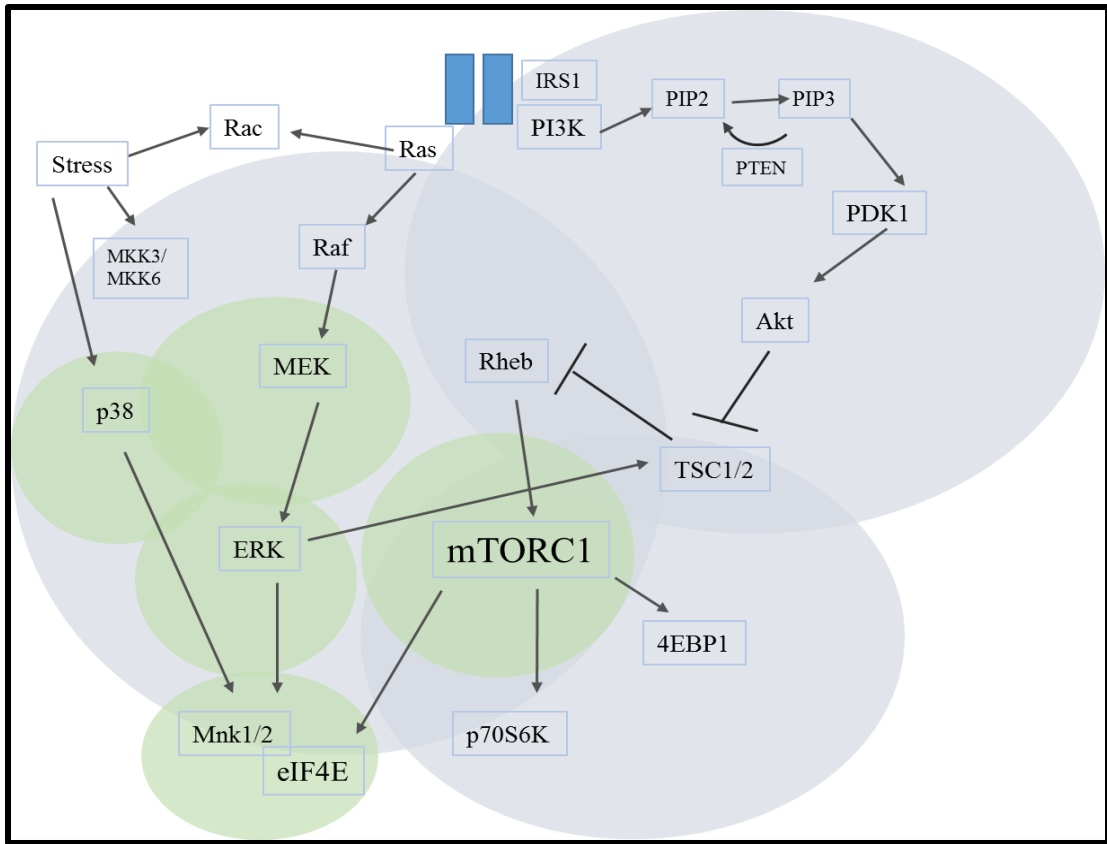


**Figure 38. Proposed Predominant Pathways Utilized by EBV in B Cells and Epithelial Cells.** Epithelial cell EBV network shown in green regions; B cell EBV network shown in blue regions

## REFERENCES

1. Morales-Sánchez A, Fuentes-Pananá EM. Human Viruses and Cancer. Parish J, ed. *Viruses*. 2014;6(10):4047-4079. doi:10.3390/v6104047.
2. Butt, A. Q. and Miggin, S. M. (2012), Cancer and viruses: A double-edged sword. *Proteomics*, 12: 2127–2138. doi:10.1002/pmic.201100526
3. Münz, C. (2015). Epstein Barr Virus Volume 1: One Herpes Virus: Many Diseases.
4. Fields, B. N., Knipe, D. M., & Howley, P. M. (2013). *Fields virology*. Philadelphia: Wolters Kluwer Health/Lippincott Williams & Wilkins.
5. Xiao, J., Palefsky, J. M., Herrera, R., Berline, J., & Tugizov, S. M. (2008). The Epstein–Barr virus BMRF-2 protein facilitates virus attachment to oral epithelial cells. *Virology*, 370(2), 430-442.
6. Li, H., Liu, S., Hu, J., Luo, X., Li, N., Bode, A. M., & Cao, Y. (2016). Epstein-Barr virus lytic reactivation regulation and its pathogenic role in carcinogenesis. *International journal of biological sciences*, 12(11), 1309.
7. Flower, K., Thomas, D., Heather, J., Ramasubramanyan, S., Jones, S., & Sinclair, A. J. (2011). Epigenetic control of viral life-cycle by a DNA-methylation dependent transcription factor. *PloS one*, 6(10), e25922.
8. L. K., & Liu, S. T. (2000). Activation of the BRLF1 promoter and lytic cycle of Epstein–Barr virus by histone acetylation. *Nucleic acids research*, 28(20), 3918-3925.
9. Kenney, S. C., & Mertz, J. E. (2014, June). Regulation of the latent-lytic switch in Epstein–Barr virus. In *Seminars in cancer biology* (Vol. 26, pp. 60-68). Academic Press

10. Li, H., Liu, S., Hu, J., Luo, X., Li, N., Bode, A. M., & Cao, Y. (2016). Epstein-Barr virus lytic reactivation regulation and its pathogenic role in carcinogenesis. *International journal of biological sciences*, 12(11), 1309.
11. Walsh, D., Mathews, M. B., & Mohr, I. (2013). Tinkering with translation: protein synthesis in virus-infected cells. *Cold Spring Harbor perspectives in biology*, 5(1), a012351.
12. Buchkovich, N. J., Yu, Y., Zampieri, C. A., & Alwine, J. C. (2008). The TORrid affairs of viruses: effects of mammalian DNA viruses on the PI3K–Akt–mTOR signalling pathway. *Nature Reviews Microbiology*, 6(4), 266.
13. Laplante, M., & Sabatini, D. M. (2009). mTOR signaling at a glance. *Journal of Cell Science*, 122(20), 3589–3594. <http://doi.org/10.1242/jcs.051011>
14. Hers, I., Vincent, E. E., & Tavaré, J. M. (2011). Akt signalling in health and disease. *Cellular signalling*, 23(10), 1515-1527.
15. DeStefano, M. A., & Jacinto, E. (2013). Regulation of insulin receptor substrate-1 by mTORC2 (mammalian target of rapamycin complex 2).
16. Laplante, M., & Sabatini, D. M. (2012). mTOR signaling in growth control and disease. *Cell*, 149(2), 274–293. <http://doi.org/10.1016/j.cell.2012.03.017>
17. Li, M., Sun, H., Song, L., Gao, X., Chang, W., & Qin, X. (2012). Immunohistochemical expression of mTOR negatively correlates with PTEN expression in gastric carcinoma. *Oncology letters*, 4(6), 1213-1218.
18. Wang, W., Wen, Q., Xu, L., Xie, G., Li, J., Luo, J., ... & Fan, S. (2014). Activation of Akt/mTOR pathway is associated with poor prognosis of nasopharyngeal carcinoma. *PloS one*, 9(8), e106098.
19. Márk, Á., Hajdu, M., Váradi, Z., Sticz, T. B., Nagy, N., Csomor, J., ... & Sebestyén, A. (2013). Characteristic mTOR activity in Hodgkin-lymphomas offers a potential therapeutic target in high risk disease—a combined tissue microarray, in vitro and in vivo study. *BMC cancer*, 13(1), 250.
20. Zhang J., Jia L., Tsang C.M., Tsao S.W. (2017) EBV Infection and Glucose Metabolism in Nasopharyngeal Carcinoma. In: Cai Q., Yuan Z., Lan K. (eds) *Infectious Agents Associated Cancers: Epidemiology and Molecular Biology*. *Advances in Experimental Medicine and Biology*, vol 1018. Springer, Singapore

21. Li, J., Kim, S. G., & Blenis, J. (2014). Rapamycin: one drug, many effects. *Cell metabolism*, 19(3), 373-379
22. Yang, C., Zhang, Y., Zhang, Y., Zhang, Z., Peng, J., Li, Z., ... & Zhu, Y. (2015). Downregulation of cancer stem cell properties via mTOR signaling pathway inhibition by rapamycin in nasopharyngeal carcinoma. *International journal of oncology*, 47(3), 909-917.
23. Wang, D., Gao, L., Liu, X., Yuan, C., & Wang, G. (2017). Improved antitumor effect of ionizing radiation in combination with rapamycin for treating nasopharyngeal carcinoma. *Oncology letters*, 14(1), 1105-1108.
24. Cen, O., & Longnecker, R. (2011). Rapamycin Reverses Splenomegaly and Inhibits Tumor Development in a Transgenic Model of Epstein-Barr Virus-Related Burkitt's Lymphoma. *Molecular cancer therapeutics*, 10(4), 679-686.
25. Adamson, A. L., Le, B. T., & Siedenburg, B. D. (2014). Inhibition of mTORC1 inhibits lytic replication of Epstein-Barr virus in a cell-type specific manner. *Virology Journal*, 11, 110. <http://doi.org/10.1186/1743-422X-11-110>
26. Cargnello, M., & Roux, P. P. (2011). Activation and function of the MAPKs and their substrates, the MAPK-activated protein kinases. *Microbiology and molecular biology reviews*, 75(1), 50-83.
27. Roux, P. P., & Topisirovic, I. (2012). Regulation of mRNA translation by signaling pathways. *Cold Spring Harbor perspectives in biology*, 4(11), a012252.
28. Joshi, S., & Plataniias, L. C. (2014). Mnk kinase pathway: cellular functions and biological outcomes. *World journal of biological chemistry*, 5(3), 321
29. Escara-Wilke, J., Yeung, K., & Keller, E. T. (2012). Raf kinase inhibitor protein (RKIP) in cancer. *Cancer and Metastasis Reviews*, 31(3-4), 615-620.
30. Wottrich, S., Kaufhold, S., Chrysos, E., Zoras, O., Baritaki, S., & Bonavida, B. (2017). Inverse correlation between the metastasis suppressor RKIP and the metastasis inducer YY1: Contrasting roles in the regulation of chemo/immuno-resistance in cancer. *Drug Resistance Updates*, 30, 28-38.
31. Ling, H. H., Mendoza-Viveros, L., Mehta, N., & Cheng, H. Y. M. (2014). Raf kinase inhibitory protein (RKIP): functional pleiotropy in the mammalian brain. *Critical Reviews™ in Oncogenesis*, 19(6).